Telecommunications and Information Technology

Alberto Paradisi
Michel Daoud Yacoub
Fabrício Lira Figueiredo
Tania Regina Tronco *Editors*

Long Term Evolution

4G and Beyond

Springer

Telecommunications and Information Technology

More information about this series at http://www.springer.com/series/14176

Alberto Paradisi · Michel Daoud Yacoub
Fabrício Lira Figueiredo · Tania Regina Tronco
Editors

Long Term Evolution

4G and Beyond

Springer

Editors
Alberto Paradisi
Vice President of Research
and Development
CPqD Foundation
Campinas, SP
Brazil

Michel Daoud Yacoub
School of Electrical and Computer
Engineering
University of Campinas
Campinas, SP
Brazil

Fabrício Lira Figueiredo
Wireless Communications Division
CPqD Foundation
Campinas, SP
Brazil

Tania Regina Tronco
Directory of Innovation Management
CPqD Foundation
Campinas, SP
Brazil

ISSN 2365-564X ISSN 2365-5658 (electronic)
Telecommunications and Information Technology
ISBN 978-3-319-23822-7 ISBN 978-3-319-23823-4 (eBook)
DOI 10.1007/978-3-319-23823-4

Library of Congress Control Number: 2015948767

Springer Cham Heidelberg New York Dordrecht London

Printed on acid-free paper

Springer International Publishing AG Switzerland is part of Springer Science+Business Media
(www.springer.com)

Preface

It has been just over three decades since the brick-size, heavyweight, vehicle-mounted, voice-oriented wireless terminal has been replaced by its lightweight, flexible, wearable, multimedia-oriented version. Whereas in the beginning the use of mobile phone was restricted to those few who could afford to buy equipment and services, today its widespread use has made it unconceivable for anyone to live without it. The number of wireless services subscriptions has long surpassed those of the fixed telephone lines with users eager to make use of and demanding new wireless features. It is now reasonably correct to say that new generations of wireless systems appear in every ten years although equipment and services evolve in a much faster pace.

First-Generation (1G) wireless networks appeared in the late 1970s. The aim was to provide voice services to mobile subscribers. The systems had as their main features voice transmission over analogue frequency modulation (FM) channels and frequency division multiple access (FDMA) as multiple access architecture. They operated over the 800–900 MHz, although one or another could be found in the 450 MHz band. Capacity expansion was rather limited and privacy was inexistent. The best representatives of these systems are: advanced mobile phone service (AMPS) in North America; total access communication system (TACS), European TACS (ETACS), and nordic mobile telephony (NMT) in Europe; Japanese TACS (JTACS) in Japan. Soon, there was the need for more spectrum-efficient and more advanced wireless networks.

As early as in the 1980s, the buzzwords "personal", "anywhere, anytime" permeated talks, speeches, papers, and all things concerning wireless communications. Researchers and engineers alike freed their imagination to conceive a wireless system that would fulfil the requirements of a personal communication, available to anyone, anywhere, anytime. That would constitute the Second-Generation (2G) wireless networks, available in the early 1990s. Of course, the expectations for the predicted services were only partially attained. The 2G systems were indeed able to increase spectral efficiency as well as introduce some kind of privacy but were far from what everyone thought it would really be. They provided robust communications, authentication capability, low-speed data in

addition to voice services. The systems used digital transmission techniques and time division multiple access (TDMA) or code division multiple access (CDMA) as multiple access architectures. The best representatives of these systems were: Global System for Mobile communications (GSM) with its data service aggregate general packet radio service (GPRS)[1], and Digital AMPS—IS-136 (D-AMPS), using TDMA, and CDMA-One (IS-95), using CDMA. In addition to the 800–900 MHz band, GSM inaugurated the use of the 1.8 GHz band. GSM soon became a universally adopted 2G network.

The widespread use of the Internet boosted the development of wireless systems able to provide better data-transmission capability for mobile applications. The Third-Generation (3G) networks were then envisaged by the international mobile telecommunications-2000 (IMT-2000), with standards and specifications developed by several organizations under the auspices of the international telecommunications union (ITU). The aim of a 3G system was to deliver a data rate of 2 Mbps for stationary or walking users and 384 kbps for moving vehicles. In fact, ITU did not clearly specify the minimum required data rate. Hence, different data rates have been sold as 3G and the systems went commercially in the early 2000s. Two major systems are commonly branded 3G: universal mobile telecommunications systems (UMTS) and CDMA2000. UMTS, designed for networks based on GSM, was developed by the 3rd generation partnership project (3GPP). It uses different terrestrial interfaces, named UMTS terrestrial radio access (UTRA), the most popular being wideband CDMA (WCDMA). UMTS networks have been improving their data-transmission capability through high-speed downlink (uplink) packet access (HSD(U)PA) technologies. CDMA2000, designed for networks based on CDMA-One, was developed by 3GPP2. It includes the 1xEV-DO technology for broadband Internet access. A combination of CDMA and TDMA is applied as a means to achieve the desired data-rate transmission. Undoubtedly, UMTS is the predominant 3G system worldwide.

Clearly, communications systems have moved drastically from voice towards data applications. Such applications are increasingly demanding higher data rates, which current wireless systems have not been able to provide. A Fourth-Generation (4G) network was necessary. In this sense, the ITU-radio communication sector (ITU-R) established the requirements for 4G standards, the IMT-Advanced. Some of these requirements include: (i) be an all-IP packet switched network; (ii) provide peak data rates of 100 Mbps for high mobility and 1 Gbps for low mobility; (iii) use scalable channel bandwidths of 5–20 MHz; be able to provide smooth handover through heterogeneous networks; etc. Mobile WiMAX and long term evolution (LTE), already in use (early 2010s), but which did not fully comply with the required standards yet are recognized as 4G systems. In 2009, the LTE-Advanced, standardized by the 3GPP, was formally submitted as a candidate 4G system.

[1]GPRS was known as a 2.5G system.

As usual and ever, a generation is not fully available yet and a vivid discussion on the requirements for the next generation is under way. Fifth-Generation (5G) wireless networks aim: (i) to support tens of Mbps for tens of thousands of users; (ii) to support connections for massive sensor deployments; (iii) to meet new use-cases such as internet of things (IoT); and others. It is predicted that 5G networks should be rolled out by 2020.

It is certain that what is expected for a given wireless generation is only accomplished two or three generations later…

CPqD has been involved with wireless communications since the very beginning. It has been conducting research and development in a wide range of aspects of the system. In addition, it has been actively participating in the Regulatory and Standardization agencies national and internationally. More recently, CPqD has led the move in order to standardize the introduction of the use of 450 MHz in 3GPP, which was officially established in 2013. Also a Radio Access Network, RAN, both in 450 and 700 MHz have been fully developed and tested in laboratory and also in the field with operators.

This book gathers a little of the latest works in the wireless communications field at CPqD. Chapter "LTE and Beyond" traces a thorough overview of the current Long Term Evolution systems and their future. Issues such as fundamentals of LTE (e.g. architecture, control and user plane protocols, physical layer), advanced features (e.g., spectrum usage, efficiency, capacity), interference management, advanced services, and others are nicely covered in the text. Chapter "Brazilian Telecommunications Regulatory Framework and the Impacts on the Development of Broadband Radio Access Systems" the Brazilian Regulatory Framework for telecommunications services is adopted as the basis for an analysis on the impact of introduction of new technological scenarios and the new opportunities that can be envisaged. Chapter "Dual-Polarized Crossed Dipole Antenna Array for LTE Base Station" presents a solution for a dual-polarized antenna array for LTE base station applications operating in the 450 MHz band. In particular, the antenna operates with a $\pm 45°$ slanted polarization diversity with a horizontal beamwidth of 65°. Chapter "Evaluation of the LTE 450 MHz System Performance with Different Terminal Antennas" conducts simulation analysis in order to evaluate the performance of commercial antennas for LTE systems at 450 MHz. The environment, a rural area, is chosen to comply with the ANATEl and 3GPP standards. The results show that the use of directional antennas may improve the cell throughput up to 90 % and terminal throughput up to 10 times as compared to the same scenario using omnidirectional antennas. Chapter "Wavelet-Based Narrowband Interference Suppression in Long Term Evolution Physical Channels" describes a wavelet-approach in order to mitigate narrowband interference in LTE physical channels. Simulations are used that suggest that an optimized a suppression process calls for different wavelet type depending on the physical channel considered. Chapter "Link Adaptation in LTE Systems" details how link adaptation (selection of modulation schemes and code rate) is performed in both downlink and uplink in LTE systems. Chapter "Method and Test Environment for the Validation of Random

Access Channel for Long Term Evolution Systems in 450 MHz" proposes a laboratory method to validate Physical Random Access CHannel (PRACH) procedure implemented in the LTE 450 MHz. The method avoids the costly and time-consuming procedures of field tests. Chapter "Experimental Assessment of Voice Over IP in LTE Systems Under Different Cell Conditions" depicts a measurement-based performance assessment of VoIP in LTE networks for suburban and rural applications when different LTE configurations of QoS and cell conditions are considered. Chapter "Integration Between LTE and Satellite Networks" investigates the viability of introducing satellite-based backhaul connectivity to LTE networks. Both laboratory-simulated link as well as real-world link in a LTE 450 MHz system is tested. The results show that the introduction of a satellite link does not limit the quality of the services provided.

We cordially invite you to enjoy the book.

Alberto Paradisi
Michel Daoud Yacoub
Fabrício Lira Figueiredo
Tania Regina Tronco

Contents

Abbreviations

2G, 3G, 4G	Second, third, and fourth generations
3GPP	Third generation partnership project
ABS	Almost blank subframe
ANATEL	Brazilian National Telecommunications Agency
ARQ	Automatic repeat request
BCCH	Broadcast control channel
BS	Base station
BTS	Base transceiver station
CA	Carrier aggregation
CC	Component carrier
CCCH	Common control channel
CDMA	Code division multiple access
CFTV	Closed-circuit television
CP	Cyclic prefix
CPE	Customer premise equipment
CRS	Cell-specific reference signals
DCCH	Dedicated control channel
DFT	Discrete fourier transform
DTV	Direct-to-video
eICIC	Enhanced inter-cell interference coordination
eMBMS	Evolved multimedia broadcast and multicast service
EMC	Electromagnetic compatibility
eNodeB	Evolved node B
EPC	Evolved packet core
E-UTRAN	Evolved Universal Terrestrial Radio Access Network
FDD	Frequency-division duplexing
FEICIC	Further enhanced inter-cell interference coordination
FM	Frequency modulation
GSM	Global system for mobile communications
HetNets	Heterogeneous networks

HII	High interference indicator
HSDPA	High-speed downlink packet access
HSUPA	High speed uplink packet access
ICIC	Inter-cell interference coordination
IMT	International mobile telecommunications
IP	Internet protocol
IRC	Interference rejection combining
ITU	International Telecommunication Union
ITU-R	ITU radiocommunications
LAA	Licensed-assisted access
LCS	Location services
LTE	Long term evolution
MAC	Medium access control
MBMS	Multimedia broadcast and multicast service
MBSFN	Multimedia broadcast single frequency network
MIMO	Multiple input multiple output
MME	Mobility management entity
MRO	Mobility robustness/handover optimization
MTC	Machine-type communications
NAS	Non-access stratum
OFDM	Orthogonal frequency-division multiplexing
OFDMA	Orthogonal frequency-division multiple access
PAPR	Peak-to-average power ratio
PBCH	Physical broadcast channel
PBTVD	Basic digital TV plan
PCCH	Paging control channel
PCell	Primary cell
PCFICH	Physical control format indicator channel
PCRF	Policy and charging rules function
PDCCH	Physical downlink control channel
PDCP	Packet data convergence protocol
PDSCH	Physical downlink shared channel
PGMQ	Master quality plan
P-GW	Packet-data network gateway
PHICH	Physical hybrid ARQ indicator channel
PM	Pulse modulation
PRB	Physical resource block
PSTN	Public switched telephone network
RACH	Random access channel
RAT	Radio access technology
RF	Radio frequency
RLC	Radio link control
RpTY	Repeater
RRC	Radio resource control

RRM	Radio resource management
RRVSMP	Regulation on operation of personal mobile service through virtual network
SARC	Broadcast auxiliary services and related
SBTVD	Brazilian digital TV system
SCE	Specialized circuit services
SCell	Secondary cell
SC-FDMA	Single-carrier-frequency-division multiple access
SCM	Multimedia communication services
S-GW	Serving gateway
SLD	Dedicated line services
SLE	Special limited services
SLP	Limited private service
Smart Grid	Electric power generation, transmission and distribution sector
SMC	Cellular mobile service
SMP	Personal mobile service
SON	Self-organizing networks
SRB	Signaling radio bearer
SRCC	Circuit switched network services
SRCP	Packet switched network services
SRE	Specialized network services
SRTT	Telecommunications transport network services
STFC	Fixed switched telephone service
STP	Public phone service
TDD	Time-division duplexing
TDMA	Time division multiple access
Telebrás	Telecomunicações Brasileiras S/A
TV	Television
UE	User equipment
UHF	Ultra high frequency
VHF	Very high frequency
WCDMA	Wideband code division multiple access
Wi-Fi	Wireless fidelity
WiGrid	Wireless broadband communications technology optimized for smart grid
WiMAX	Worldwide interoperability for microwave access
WLL	Wireless local loop

Introduction to CPqD Research Series

CPqD Research Series aims to disseminate globally results of research and development projects that are in course in CPqD.

CPqD is the largest R&D Center in Latin America and is located at Campinas, São Paulo, Brazil. Since its creation in 1976, CPqD has excelled as the strengthening bond between the universities and the companies, collaborating to develop and disseminate knowledge (technology) for the industrial sector.

CPqD has built a consistent R&D Program with the purpose of fostering innovation for the telecommunications market, contributing to the industry competitiveness and minimizing the digital divide within Brazilian society. This program is deeply committed to the applicability of their results, achieved by means of projects that generate scientific and technical knowledge, as well as products, processes, systems or services related to telecom and information technologies. It is currently sponsored by FUNTTEL—Fund for Technological Development of Telecommunications of the Brazilian Ministry of Communications, FINEP—Financing Agency for Studies and Projects, of the Brazilian Ministry of Science, Technology and Innovation, Brazilian Development Bank (BNDES) and Brazilian Association for Research and Industrial Innovation (EMBRAPII).

During the last years, CPqD has developed a complete LTE Radio Access Network architecture, comprising Base Stations (eNodeB), user equipment (UEs) and evolved packet core (EPC) elements, targeting macrocell and smallcell applications. In case of macrocells, CPqD has recently led the 450 MHz standardization within 3GPP, now Band 31, together with other companies and with support of Brazilian Communications Ministry. Once operating in Band 31, it has been proven in the field that coverage radius of tens of kilometers is achievable with high performance, even at the cell border.

This first edition is dedicated to CPqD wireless communication research and development on broadband mobile networks, with focus on long term evolution (LTE) technology. It gathers a selection of papers covering key aspects on LTE macrocells for rural and remote area applications, such as system design, functionalities, standardization, performance optimization, system evaluation, and integration with satellite backhaul.

I would like to thank all the authors, and the collaborators Maria Lúcia Herrera, Michael Machado and Tania Regina Tronco, whose valuable contribution turned this book into reality.

Alberto Paradisi

LTE and Beyond

Dick Carrillo, Felipe A.P. de Figueiredo, Fabrício Lira Figueiredo and João Paulo Miranda

Abstract In this chapter, we provide a brief yet comprehensive overview of current Long Term Evolution (LTE) systems and beyond. We begin presenting the baseline technology and the underlying features of network architecture, protocols, and air interface introduced in the first LTE release back in 2008. Having the basics put in place, we move forward to discuss advanced features introduced and further developed throughout subsequent LTE releases. Our discussion takes into consideration even the still under discussion LTE Release 13, which has in March 2016 its estimated freeze date.

1 Introduction

The wireless communications industry has been undergoing great developments since the beginning of this century. The second generation (2G) of cellular technology provided the possibility to increase the number of simultaneous phone calls, while sharing the same radio frequency (RF) spectrum. The third generation

D. Carrillo (✉) · F.A.P. de Figueiredo · F.L. Figueiredo · J.P. Miranda
CPqD Foundation, Campinas, São Paulo, Brazil
e-mail: dickm@cpqd.com.br

F.A.P. de Figueiredo
e-mail: felipep@cpqd.com.br

F. Figueiredo
e-mail: fabricio@cpqd.com.br

J.P. Miranda
e-mail: jmiranda@cpqd.com.br

A. Paradisi et al. (eds.), *Long Term Evolution*, Telecommunications and Information Technology, DOI 10.1007/978-3-319-23823-4_1

(3G) technology, based on wideband code-division multiple access, increased data transmission rates and improved voice services' quality. In recent years, standards such as Long Term Evolution (LTE) advanced by the 3G Partnership Project (3GPP), and IEEE 802.16e/m, also known as Worldwide Interoperability for Microwave Access (WiMAX), have improved the spectral efficiency of wireless channels thanks to the introduction of air interfaces based on orthogonal frequency-division multiplexing (OFDM). LTE has been regarded as the most important candidate to become the leading technology in fourth generation (4G) networks and beyond due to its popularity and continuous development of new features [1].

LTE is a highly flexible radio interface. Its first release defined the fundamental elements of the radio access network (RAN), which is composed of only one base station called evolved node B (eNodeB) providing user- and control-plane terminations toward the user equipment (UE) [2]. eNodeBs are interconnected and directly linked to a core network providing connection to other internet protocol (IP) based networks. This so-called flat architecture simplifies the user data flow and enables flexible, cost-effective capacity scaling [3]. LTE Rel. 8, the first release of the family of LTE standards, provides peak rates of 300 Mbps, latency below 10 ms, and a significant boost in spectrum efficiency as compared to previous cellular systems. It offers a scalable radio bandwidth, ranging from 1.4 to 20 MHz, and supports both frequency-division duplexing (FDD) and time-division duplexing (TDD) operations. Other important features relate to LTE cross-layer mechanisms, such as link adaptation, hybrid automatic repeat request (HARQ), and multiuser diversity through both time- and frequency-adaptive scheduling. The designed system also allows up to four spatial layers for single-user multiple input multiple output (MIMO) transmission [4].

On top of the basic framework put forth along the lines above, 3GPP introduced in LTE Rel. 9 features of location-based services, multimedia services both in broadcast and multicast formats, self-organizing and self-optimizing functionalities, dual layer beamforming, and additional support to new operating bands. Notwithstanding the importance of Releases 8 and 9, they are not intended to meet the requirements issued by the International Telecommunication Union on International Mobile Telecommunications (4G) systems. In contrast, the advanced version of LTE was developed bearing those requirements in mind so as to offer lower latency than the previous releases, peak data rates elevated to up to 3 Gbps in the downlink, operating bandwidth of up to 100 MHz in the downlink, and efficient interference management, just to mention some among a number of other advanced functionalities. The technology evolution continues with LTE Rel. 11 and LTE Rel. 12, which not only improve features already introduced in previous releases, but also introduce entirely new features. LTE Rel. 13 is still ongoing standardization work.

In this chapter, we provide a brief yet comprehensive overview of current LTE systems and beyond. The remainder of the chapter is organized as follows. Section 2 presents the baseline LTE technology and the underlying features of its network architecture, protocols, and air interface. Having these basics in place,

Sect. 3 discusses advanced features that have been introduced and further developed throughout subsequent LTE releases aiming at improving spectrum use, increase network density, and delivering other performance improvements. Two kinds of advanced services are dealt with in Sect. 4, as these have been receiving special attention within 3GPP. Section 5 wraps up the chapter with some concluding remarks.

2 Fundamentals of LTE

This section aims at providing a brief yet comprehensive overview about the LTE technology and its underlying features. The LTE network architecture, protocols, important system features, and air interface are described, putting in place the basic information on top of which the remainder of this chapter develops.

2.1 Architecture

The standardization effort of 3GPP has two primary objectives. The first objective was to create a common packet core network, the evolved packet core (EPC), to support mobile services, not only over 3GPP-defined radio access technology (RAT), but also over other standardized RATs, e.g., Wi-Fi. The second objective was to create a new radio access network, called evolved universal terrestrial radio access network (E-UTRAN), based on OFDM. The next subsection describes these important network elements.

2.1.1 Core Network

The requirements of the EPC are specified in [5]. As seen in Fig. 1, the EPC consists of two control-plane nodes, namely mobility management entity (MME) and home subscriber server, and three user-plane nodes, namely serving gateway (S-GW), packet-data network gateway (P-GW), and policy and charging rules function (PCRF). Also in Fig. 1, it is easily to figure out protocol stack interfaces between every node described in previous lines, for more detailed information refer to [6].

2.1.2 Access Network

The access network for normal user traffic does not have a centralized controller in E-UTRAN, so the architecture is said to be flat [7]. The eNodeB provides the radio interface and performs radio resource management (RRM), including

radio bearer control, radio admission control, and scheduling of uplink and downlink radio resources for every UE. The eNodeB also supports IP header compression and encryption of the user plane data. All eNodeBs are interconnected to one another via an interface X2; which has several uses, e.g., handover.

The other important aspect of LTE is that eNodeBs are connected to the EPC via S1 interface, which is split into user and control planes. The control-plane interface is referred to as S1-MME and terminates in the MME. The S1-U terminates in the S-GW and supports pooling, which is a very important feature establishing a many-to-many relationship between the eNodeBs and the MMEs and the S-GWs. The S1 interface also supports network sharing. This allows operators to share the radio network, which are the eNodeBs, while maintaining their own EPC networks.

The E-UTRAN is responsible for all radio-related functions, which can be summarized as:

- RRM: RRM covers all functions related to the radio bearers, such as radio bearer control, radio admission control, radio mobility control, scheduling, and dynamic allocation of resources to UEs in both uplink and downlink [8];
- Header compression: This helps ensure efficient use of the radio interface by compressing IP packet headers, which could otherwise represent a significant overhead—especially in case of small packets, such as voice over IP [9];
- Security: All data sent over the radio interface is encrypted;
- Connectivity to the EPC: This consists of the signaling toward the MME and the bearer path toward the S-GW.

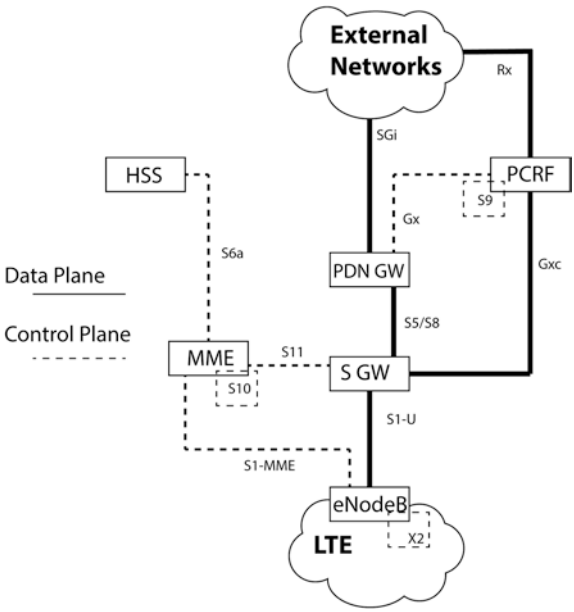

Fig. 1 EPC architecture adapted from [59]. *Dashed lines* represent the control plane, whereas *solid lines* represent the user plane

2.2 Control and User Plane Protocols

Figure 2 shows a general overview of the radio protocol architecture considered in LTE, as well as the use of radio bearers, logical channels, transport channels, and physical channels [10]. This figure provides a big picture of both control and data plane protocols, which are discussed in the sequel.

The dedicated radio resource control (RRC) messages that are transferred across signaling radio bearers (SRBs), which are mapped via the packet-data convergence protocol (PDCP) and radio link control (RLC) layers onto logical channels—either the common control channel (CCCH) during connection establishment or a dedicated control channel (DCCH) in RRC_connected state. Paging messages and system information are mapped directly onto logical channels: the paging control channel (PCCH) and broadcast control channel (BCCH), respectively. SRB 0 is used for RRC messages which use the CCCH, SRB 1 is for RRC messages using DCCH, and SRB 2 is for the (lower-priority) RRC messages using DCCH which only include dedicated non-access stratum (NAS) information. All RRC messages using DCCH are integrity-protected and ciphered by the PDCP layer (after security activation) and use ARQ protocols for reliable delivery through the RLC layer. The RRC messages using CCCH are not integrity protected and do not use ARQ in the RLC layer. It should also be noted that the NAS independently applies integrity protection and ciphering. The RLC supports data segmentation and concatenation [11]. Finally, the medium access control (MAC) sublayer [12] provides hybrid ARQ and is responsible for functionalities required for medium access, e.g., scheduling operation and random access. MAC also performs the mapping between logical channels and transport channels.

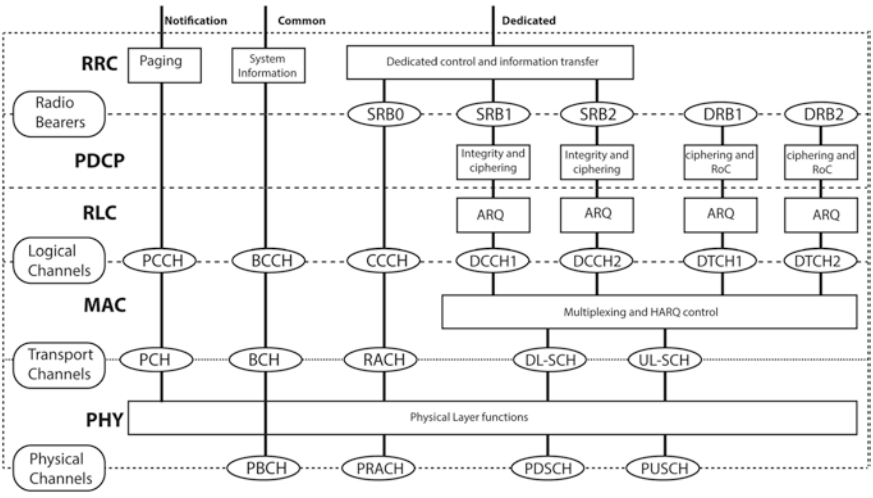

Fig. 2 Overall radio protocol architecture illustrating radio bearer mapping (adapted from [19])

2.3 Physical Layer

Basic concepts of physical layer are described in this subsection. More detailed description can be found in [4, 13].

2.3.1 Frame Structure

The transmitted LTE signal is organized in subframes of duration 1 ms, each consisting of 12 or 14 OFDM symbols, depending on whether normal or extended CP is used. Ten subframes form a radio frame as shown in Fig. 3. The short subframe duration of 1 ms results in small delays, not only for user data, but also for control signaling such as the hybrid ARQ feedback and channel-quality feedback from UEs to eNodeBs.

The main difference between FDD and TDD is that in the latter special subframes provide the required guard time for downlink-to-uplink switching. Each special subframe is divided into three fields, namely the downlink part (DwPTS), the guard period (GP), and the uplink part (UpPTS) shown in the bottom of Fig. 3.

2.3.2 Downlink Air Interface

In the downlink, the LTE air interface uses orthogonal frequency-division multiple access (OFDMA) that is a multiple access technique based on OFDM. OFDMA enables the OFDM transmission to benefit from multiuser diversity, adaptive subcarrier assignment based on feedback information about frequency-selective channel conditions, considerably enhancing the total system spectral efficiency over single-user OFDM systems. OFDM is a technique that mitigates inter-symbol interference, exploits the scarce frequency resource nearly optimally, combines the advantages of broadband and narrowband transmission, while at the same time

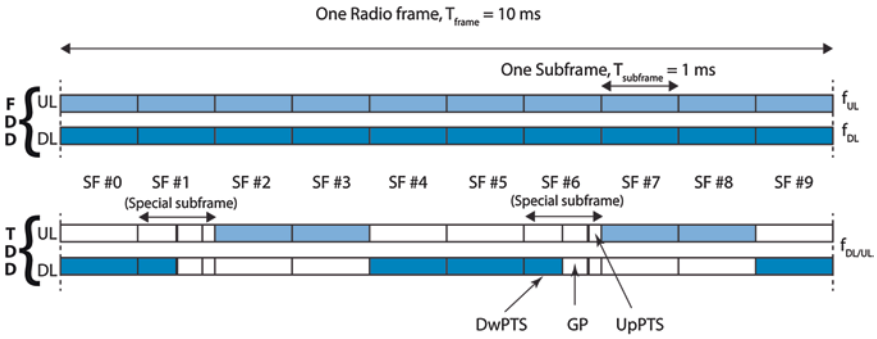

Fig. 3 LTE frame structure (adapted from [11])

avoids their disadvantages. OFDM avoids the guard band between the so-called subcarriers by a modulation of these subcarriers with rectangular pulses.

In the frequency domain, the spectrum of a pulse with duration T_{sym} corresponds to the $\text{sinc}(x) = \sin(x)/x$ function with zero crossings at k/T_{sym}, $k = \ldots, -2, -1, 1, 2, \ldots$ Consequently, if these pulses modulate several subcarriers, the inter-subcarrier interference is zero with a subcarrier spacing of $1/T_{\text{sym}}$ that can be shown to be optimum according to the Nyquist theorem. Furthermore, this optimal value is reached without any filter. The modulation of the equally spaced subcarriers with rectangular pulses corresponds to an inverse discrete Fourier transform (DFT) in the time domain. At the receiver, the original symbols are reconstructed using the opposite function, namely the DFT.

In OFDM systems as LTE, the operation bandwidth can be easily adapted to the needs of the network operator. LTE FDD, for example, offers bandwidths of 1.4, 3, 5, 10, 15, and 20 MHz with a subcarrier spacing of 15 kHz. The total bandwidth includes guard bands at both ends of the spectrum, so that 72, 180, 300, 600, 900, and 1200 subcarriers are conveyed in the respective bandwidth, as outlined in [14]. To support channel estimation for coherent demodulation, as well as for various measurement purposes, including not only measurements for mobility management but also channel-quality measurements, cell-specific reference signals (CRS) are transmitted in the downlink [15].

LTE uses other air interface technologies like MIMO, which is a technique that relies on multiple antennas at the transmitter and receiver to improve the system capacity [16]. LTE also uses code rates close to one when channel quality is excellent and complements this feature using link adaptation algorithms that allow the adjustment of channel quality by choosing the best modulation and coding scheme (MCS). Modulation schemes for quadrature phase shift keying (QPSK) and quadrature amplitude modulation (QAM) (16 and 64 points), which can be combined with multiple code rates, are also provided [17].

2.3.3 Downlink Physical Channels

Physical broadcast channel (PBCH) periodically broadcasts control parameters for initial cell access, such as downlink system bandwidth, the Physical Hybrid ARQ Indicator Channel structure, and the most significant 8 bits of the System Frame Number. These parameters encapsulated in a master information block, which is 14 bits long. PBCH is designed to be detectable without prior knowledge of the system bandwidth and robust enough to be recoverable at the cell edge. Each subframe is self-decodable, aiming at reducing latency and UE battery consumption in case of good signal quality. PBCH is transmitted using space frequency block code, a form of transmit diversity used in case of multiple antennas, thus contributing to increase cell coverage.

Physical downlink shared channel (PDSCH) is the main downlink data bearing channel, which is allocated to users on a dynamic and opportunistic basis. PDSCH carries data over transport blocks, which correspond to a MAC packet-data unit.

They are sent from the MAC layer to the PHY layer once per transmission time interval, which is 1 ms. In order to minimize propagation channel errors, convolutional turbo coder is used for forward error correction. Data is mapped to spatial layers according to the transmission modes in the multiple antenna schemes (e.g., spatial multiplexing, transmit diversity, etc.) and then mapped to a modulation symbol which includes QPSK, 16-QAM, and 64-QAM. PDSCH also conveys broadcast information not transmitted on the PBCH, comprising system information blocks and paging messages.

Physical downlink control channel (PDCCH) purpose is the transmission of the resource assignment for UEs, which are contained in a downlink control information message. Multiple PDCCHs can be transmitted in the same subframe using control channel elements, each of which is a set of four resource elements known as resource element groups. QPSK modulation is used, with four QPSK symbols per group. Furthermore, up to eight groups can be used per UE, depending on channel conditions, in order to increase robustness.

Physical control format indicator channel (PCFICH) is used for the control frame indicator transportation, which includes the number of OFDM symbols used for control channel transmission in each subframe (typically 1, 2, or 3). The 32-bit long CFI is mapped to 16 Resource Elements in the first OFDM symbol of each downlink frame using QPSK modulation.

Physical hybrid ARQ indicator channel (PHICH) is a control channel defined for the HARQ ACK/NAK signaling transmission, which indicates success status of uplink user data carried on PUSCH. BPSK modulation is defined for PHICH with a repetition factor of 3 to increase robustness.

2.3.4 Uplink Air Interface

In its uplink, the LTE standard employs a DFT-spread OFDM also denoted as single-carrier frequency-division multiple access (SC-FDMA). In comparison to conventional OFDM, this OFDM variant provides an improved peak-to-average power ratio (PAPR) that enables more power-efficient terminals [18]. In addition, it is possible to aggregate up to two streams by utilizing MIMO transmissions to increase the data rate.

Both frequency-selective and non-frequency-selective scheduling are supported in the uplink. In the former, the eNodeB exploits available channel knowledge to schedule a UE to transmit using specific physical resource blocks (PRBs) in the frequency domain where the channel response is good. In addition, to transmit data information, the uplink also conveys control information related to scheduling request [11], hybrid ARQ acknowledgments in response to downlink data packets, and channel-quality information for control signaling categorization. The amount of control information a UE can transmit in a subframe depends on the number of SC-FDMA symbols available for transmission of control signaling data [19]. More details about the LTE frame structure are given in the sequel.

2.3.5 Uplink Physical Channels

Physical uplink shared channel (PUSCH) carries user data, based on QPSK and 16-QAM schemes, with 64-QAM modulation being optional. Data bits are first channel-coded with a turbo code of rate of 1/3, followed by a rate matching process for a final code rate. Adjacent data symbols are mapped to adjacent SC-FDMA symbols in the time domain, and then across subcarriers. After this interleaving process, bits are scrambled and submitted to modulation mapping, DFT spreading, subcarrier mapping, and OFDM modulation. Besides user data, PUSCH conveys control signaling for information recovering in the uplink, such as transport format indicators and MIMO parameters. Control data is multiplexed with information data prior to DFT spreading.

Physical uplink control channel (PUCCH) is used for uplink transmission of control information, comprising Hybrid ARQ acknowledgments, channel-quality indicators, MIMO feedback (rank indicator and precoding matrix indicator), and scheduling requests. This channel transmits in a frequency region at the edge of the system bandwidth. It consists of one PRB per transmission, positioned at one channel edge, and another PRB at the opposite channel edge in the following slot, thus making use of frequency diversity.

Physical random access channel (PRACH) is an uplink channel primarily used for initial network access and short message transmission [20]. The main purpose of the random access procedure is to enable UEs to acquire uplink time synchronization and to access to the network. PRACH comprises a preamble composed of a cyclic prefix (CP), of length TCP, and a sequence part, of length T_{PRE}, as shown in Fig. 4.

Prime-length Zadoff–Chu sequences are adopted as random access preambles in LTE systems due to its constant amplitude zero autocorrelation properties [21–23], meaning that all points of the sequence lie on the unit circle and its autocorrelation is zero for all time shifts other than zero. These properties make Zadoff–Chu sequences very useful in channel estimation and time synchronization, and enable improved PRACH preamble detection performance [21].

It is worth mentioning that PRACH plays a key role in the cell coverage performance, since eNodeB must run detection algorithms in order to recover preambles transmitted by UEs, which requires complex statistical real-time processing in the uplink [22].

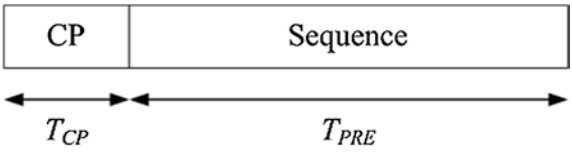

Fig. 4 Random access preamble format

2.4 Other Important Features of LTE

Radio link conditions change in wireless system and there is a necessity to adapt the transmission and reception parameters to the actual link conditions. Therefore, a brief description of link adaptation and handover is presented in next lines.

2.4.1 Link Adaptation

LTE uses code rates close to 1 when the channel quality is excellent and complement this feature using link adaptation algorithms to allow the adjustment of channel quality by choosing the best MCS. LTE provides modulation schemes for QPSK, 16-QAM, and 64-QAM which can be combined with any code rate [17]. As an example, a mapping curve between signal-to-noise ratio (SNR) and MCS is shown in Fig. 5.

2.4.2 Handover

The handover procedure aims at maintaining UEs connections during the migration among neighboring cells. The goal is to minimize the impacts on the services

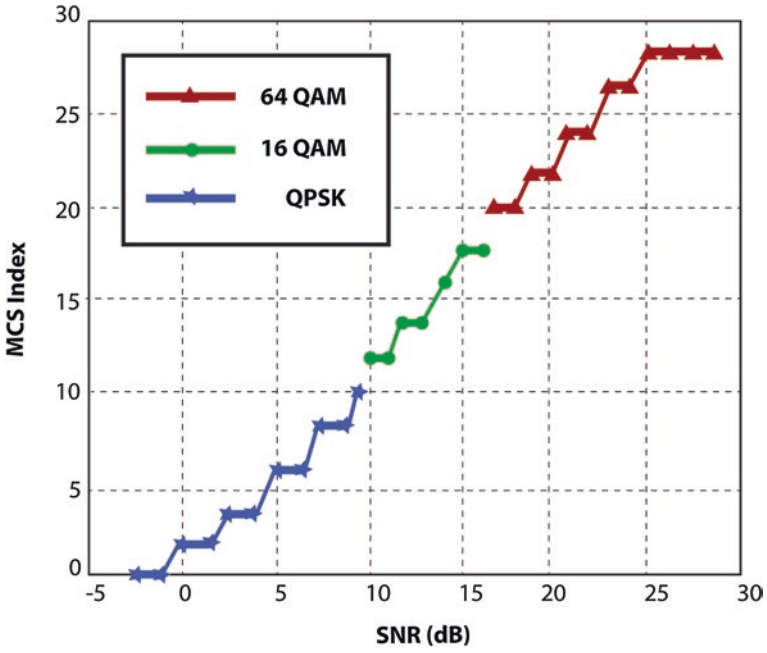

Fig. 5 Modulation and coding scheme (*MCS*) versus signal-to-noise ratio (*SNR*)

continuity, and a variety of mechanisms are defined by 3GPP in order to achieve it. The basic handover procedure mandated by 3GPP for LTE Rel. 8 [24] is illustrated in Fig. 6.

The handover procedure is based on a sequence of key events, detailed in Fig. 7, and starts with the measurement report of a handover event by the UE to its serving eNodeB. The UE periodically performs downlink radio channel measurements based on reference symbols, comprising received power and quality. Once a pre-configured threshold level is met, the UE sends the corresponding measurement report indicating the triggered event. In addition, the measurement report indicates the cell to which the UE has to be handed over, which is named "target" cell.

Based on the received measurement reports, the serving eNodeB starts handover process, with control signaling exchange with target eNodeB and admission control of the new UE. The communication between the serving and the target eNodeBs is performed over X2 interface. Upon successful handover setup, the decision is made and a handover command is sent to the UE. The connection between UE and the serving cell is released and then the UE attempts to

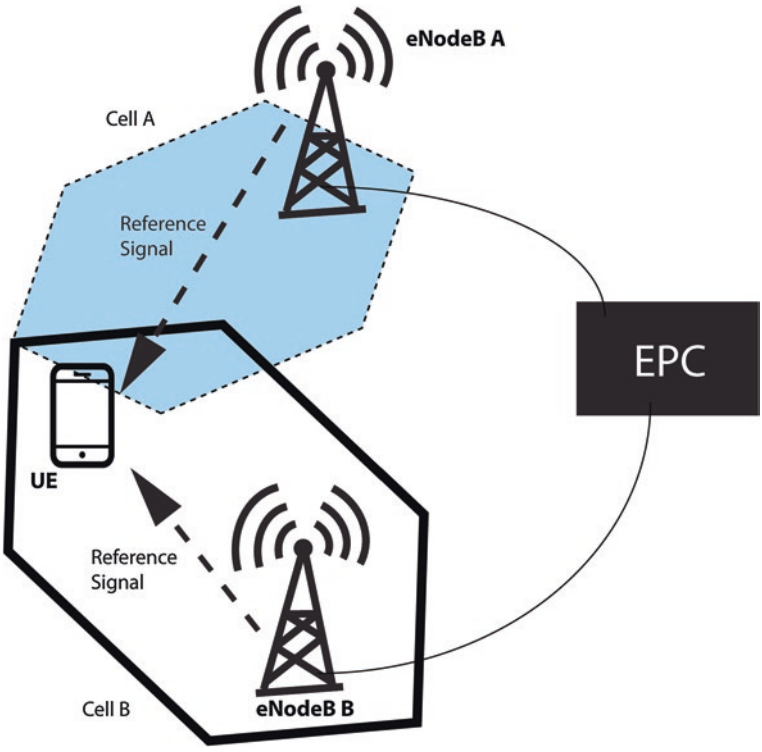

Fig. 6 Basic handover procedure used in LTE

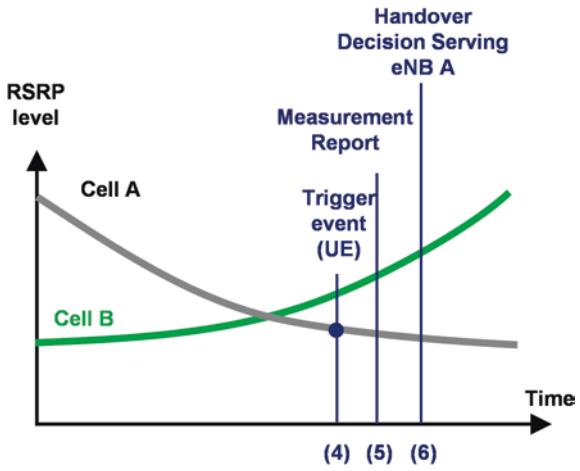

Fig. 7 Handover triggering events

synchronize and access the target eNodeB, by using the PRACH. Upon successful synchronization at the target eNodeB, this last one transmits an uplink scheduling grant to the UE. The UE responds with a handover confirm message, which notifies the completion of the handover procedure at the radio access network part.

3 Advanced Features

Having the basic LTE infrastructure and features discussed in Sect. 2, this section now describes what we shall refer to as advanced features. Such functionalities have been introduced and further developed throughout subsequent LTE releases bearing in mind three goals that are regarded as main requirements for next-generation mobile networks: better spectrum usage (whether by exploiting new bands or improving spectral efficiency), network densification, and performance improvements. This latter requirement will focus solely on features related to interference management, as other improvements, such as air interface modifications for latency reduction in the physical layer and coordinated multipoint, are out of the scope of this chapter.

3.1 Spectrum Usage, Spectrum Efficiency and Capacity

3.1.1 LTE/Wi-Fi Interworking

Mobile operators are known to prioritize the delivery of advanced services and user experience over licensed frequency bands, and this will remain so according

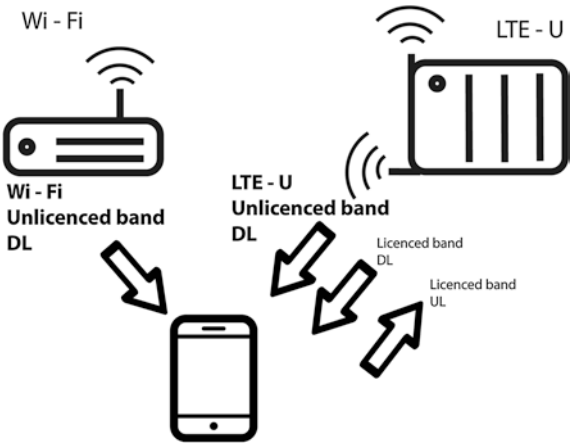

Fig. 8 A typical scenario of licensed-assisted access operating in licensed and unlicensed bands

to a recent assessment from 3GPP [9]. Notwithstanding the unquestionable role played by the licensed spectrum in the quest for more bandwidth, opportunistic use of unlicensed spectrum has been receiving increased attention as complementary means to meet the ever-growing traffic demands. One way to benefit from unlicensed spectrum is through LTE/Wi-Fi Interworking, a framework for traffic offload that is under development since LTE Rel. 8. Interworking forms are getting tighter and tighter throughout subsequent LTE releases, and proposals for Rel. 13 include LTE/Wi-Fi aggregation, mobility control based on UE measurements and network steering capabilities, and an interface to interconnect eNodeBs with Wi-Fi access points [25].

Licensed-assisted access (LAA), sometimes referred to as LTE Unlicensed, is a term used within 3GPP to denote a study item aimed to look into alternative interworking ways for enhancing the operation of LTE in unlicensed bands. The underlying idea of LAA consists of aggregating a primary cell (PCell) with a secondary cell (SCell), respectively, operating in licensed and unlicensed spectra, as it is shown in Fig. 8. The goal of the PCell is to deliver critical information and ascertain the quality of service, whereas that of the SCell is to boost data rates in an opportunistic fashion. The SCell can be set up as downlink-only or both uplink and downlink, although a common view at 3GPP is that the study will begin with the first option and follow with the second one in the future [9]. The core technology under development for LAA targets to be as much frequency agnostic as possible, so initial emphasis will be on unlicensed operation in the 5 GHz bands with other frequencies addressed at later stage.

LAA raises some specific issues that will need to be dealt with, namely effective and "fair"[1] coexistence with Wi-Fi and effective and fair coexistence among

[1]By "fair" it is meant that LAA should not impact Wi-Fi services (data, video, and voice services) more than an additional Wi-Fi network operating on the same carrier would. These metrics could include throughput, latency, and jitter, but will be exactly defined in the coexistence study.

LAA networks operated by different operators. The use of coexistence mechanisms has been deemed required for this to work, including clear channel assessment, discontinuous transmission on carrier with limited maximum transmission duration, dynamic frequency selection in certain bands/regions, carrier selection, and transmit power control [25]. Preliminary simulation results suggest that LTE augmented with appropriate coexistence mechanisms for unlicensed spectrum can effectively coexist with Wi-Fi, and is able to outperform it in terms of spectral efficiency.

3.1.2 Carrier Aggregation

Perhaps the most straightforward way to increase capacity is by making more bandwidth available to a communications system. Since LTE Rel. 10, this is done by simply aggregating more bandwidth through carrier aggregation (CA). Backward compatibility is a mandatory characteristic of the CA technology. Therefore, during the standardization of LTE-Advanced features, 3GPP determined that CA would have to keep backward compatibility with UEs based on Releases 8 and 9. So the larger bandwidths introduced with LTE Rel. 10 are provided through aggregation of standard LTE Rel. 8 and 9 carriers. Other important characteristic of CA, which renders it one of the most remarkable contributions of Rel. 10, is that it can be used for both FDD and TDD deployments of LTE-Advanced systems [26].

CA works with contiguous and non-contiguous spectrum. Each aggregated carrier denotes a component carrier (CC). Each CC can have one of the standardized bandwidths: 1.4, 3, 5, 10, 15, or 20 MHz. A maximum of up to five CCs can be aggregated; hence, the maximum aggregated bandwidth is 100 MHz. As illustrated in Fig. 9, the individual bandwidth of each CC adding up to the aggregated system bandwidth can be different. The number of aggregated carriers can be different in the downlink and uplink for FDD systems. However, the number of uplink CCs must always be lower than or equal to the number of downlink CCs. On the other

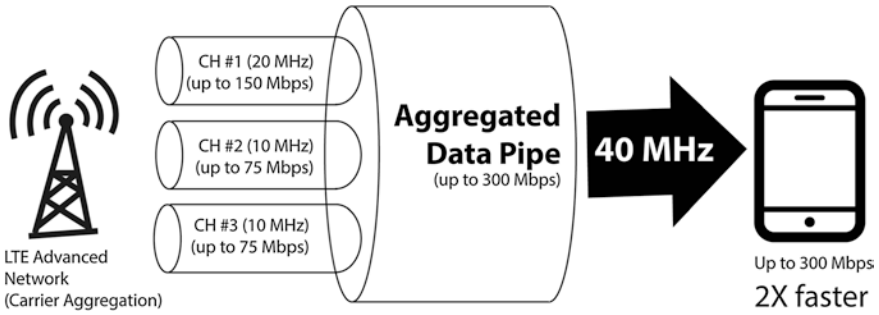

Fig. 9 Exemplary realization of CA where three CCs with individual bandwidths of 20, 10, and 10 MHz are aggregated to yield a wider 40 MHz system bandwidth

hand, for TDD systems, both the number of CCs and their individual bandwidths will be equal for both downlink and uplink [27].

Ongoing work within the scope of LTE Rel. 13 seeks to address the operators' need to expand the CA framework so that it is able to aggregate more than five CCs. The goal is to further boost achievable data rates by aggregating more than five CCs (at least in the downlink). Flexibility will also undergo a major improvement, as the resulting system will be capable of aggregating larger numbers of carriers in different frequency bands. Such enhanced CA framework is also of utmost importance in LAA, explained earlier in this section. However, not all the aspects of CA scale directly with an increased CC number and a number of issues arise when more than three CCs are used [28]:

- PUCCH transmission currently is applied only in the PCell, so increasing the number of CCs will increase the PUCCH payload size per CA UE. Besides the impact on the PCell uplink, which gets worse as the number of CA UEs grows, having all PUCCH transmissions managed by the PCell is believed to impact performance. PCell overload can be alleviated by distributing the UEs PUCCH resources in the network, although this comes at the expense of more involved installation, i.e., simple small cell installation with remote radio heads is no longer possible;
- The dual connectivity concept developed within the scope of LTE Rel. 12 requires UEs capable of uplink CA with simultaneous PUCCH/PUCCH and PUCCH/PUSCH transmissions across cell groups. The introduction of PUCCH in the SCell, known as Dual PUCCH, is seen as essential as it can ease the aforementioned burdens thus allowing for an increased number of aggregated carriers in the downlink. This idea, however, was dropped from the corresponding work item objective due to the tight schedule of LTE Rel-12;
- Finally, and independent of Dual PUCCH mechanisms, CA extension to support up to 32 CCs requires enhancements also when it comes to hybrid ARQ acknowledgment feedback and channel state information feedback carried on a single uplink carrier. This has potential to improve CA in the case of TDD PCells, which faces limitations on PDSCH hybrid ARQ acknowledgment feedback already with three CCs.

3.1.3 Advanced MIMO Techniques

The last relevant features of LTE Rel. 13 discussed in this chapter are elevation beamforming and full-dimension MIMO. In this context, 3GPP seeks a better understanding on how two-dimensional antenna arrays can further improve the spectral efficiency of LTE by exploiting the vertical dimension in addition to the azimuth dimension (the latter has been exploited in isolation since LTE Rel. 10) for beamforming and MIMO operations. A number of strategies are enabled if additional control over the elevation dimension is available, e.g., vertical pattern beamwidth and/or downtilt can be controlled in an adaptive fashion, vertical

domain sectorization, and user-specific elevation beamforming. Besides being a standard-transparent technology, this can improve the average system performance. Elevation beamforming, in contrast, is a UE-specific technique with potential to increase the signal to interference and noise ratio statistics seen by the UEs. This is possible by pointing the vertical antenna pattern in the direction of the intended UE, thus generating less interference to other non-intended UEs operating in adjacent sectors.

The study [28], which is split into two phases, aims to determine the performance benefit of enhancements targeting the operation of two-dimensional antenna arrays (including a single column of cross-poles) with eight or more transceiver units, each having its own, independent amplitude and phase control. Phase 1 will take into account the three-dimensional channel model proposed in [29] to identify antenna settings for two-dimensional arrays with up to 64 antenna ports at the eNodeB, and to evaluate the performance of LTE Rel. 12 downlink MIMO for both single- and multiuser cases. Phase 2 comprises the evaluation of potential enhancements in reference signal design, codebook, and feedback mechanisms for single-user and multiuser MIMO transmission schemes (including support for higher dimension multiuser MIMO settings), channel reciprocity based operation, diversity transmission schemes, methods for common channel coverage, cell/point selection, and/or RRM measurement reliability.

3.2 Network Densification

3GPP began work toward the standardization of self-optimizing and self-organizing capabilities in LTE Releases 8 and 9. These standards provide network intelligence and management features that automate the configuration and optimization of wireless networks as a response to variations in the actual radio channel conditions. A key goal of 3GPP has been the ability to support self-organizing networks (SON) features in multivendor environments, so a significant part of this standardization work has been devoted to defining the appropriate interfaces to allow exchange of common information that can then be used by different SON algorithms [30]. SON specifications have been built over the existing 3GPP network management architecture.

In LTE Rel. 8, the functionality focuses on procedures associated with initial equipment installation and integration to support the commercial deployment of the first LTE networks, also known as “eNodeB self-configuration”. Such procedures include:

- Automatic inventory;
- Automatic software download [31];
- Automatic neighbor relation [32];
- Automatic physical cell ID assignment [33].

In LTE Rel. 9, the SON functionality focuses on operational aspects of commercial networks, particularly on key aspects related to network optimization procedures. The standardization scope includes the following additional use cases [30, 34]:

- Mobility robustness/handover optimization (MRO): in particular, the handover parameter optimization function shall aim at reducing the number of handover-related failures that cause degradation in user experience, such as call drops, radio link failures during or shortly after handovers, and reduced data rates;
- Random access channel (RACH) optimization: an automatic RACH optimization function monitors the prevailing conditions, e.g., a change on RACH load, uplink interference, and determines and updates the appropriate parameters;
- Load balancing optimization: each scenario shall include the load balancing on intra-frequency, inter-frequency, and inter-RAT;
- Inter-cell interference coordination (ICIC): the following scenarios shall be considered in interference control: uplink ICIC, and downlink ICIC;
- Capacity and coverage optimization, in this use case operator shall be able to configure the objectives and targets for the coverage and capacity optimization function.

Other SON-related aspects discussed within the scope of LTE Rel. 9 framework include improvement of the telecom management system so as to increase energy savings, new operations, administration, and maintenance interface to control home eNodeBs, UE reporting functionality to minimize the amount of drive tests, studies on self-testing and self- healing functions, and minimization of drive testing. As will be seen later on in this chapter, SON-related functions continued to expand through the subsequent releases of the LTE standard [35].

In order to maintain network quality with minimum manual intervention on the part of the operator, the concept of SON has been advanced within the scope of the LTE standard since its introduction in Rel. 8. The need for enhanced SON procedures was one of the goals of LTE Rel. 11, as 3GPP identified that previous releases had issues with respect to mobility and inter-RAT operation. The resulting procedures for enhanced SON are found in [36] and encompass:

- MRO test cases were completed in LTE Rel. 10, so that networks based on that release are capable of detecting related issues whenever the UE reconnects to an LTE cell. The event whereby a cell at a different RAT may mistakenly be selected after connection failure was not addressed (no mechanism is currently available to detect nor to correct it). Inter-RAT failure issues related to the deployment of LTE over 2G/3G coverage and connection failure resolution support for some heterogeneous networks (HetNets) deployments were dealt with in LTE Rel. 11;
- Some problems related to mobility were identified since LTE Rel. 9 and have been addressed in LTE Rel. 11. Inter-RAT “ping-pongs”, for instance, are known not to result in a failure but are rather inefficient in that they create unnecessary signaling. Therefore, it was found relevant to exploit UE history data to enhance the existing LTE Rel. 8 mechanism.

3.3 Interference Management

3.3.1 Inter-Cell Interference Coordination

One limiting aspect of system throughput performance in cellular networks is inter-cell interference, especially in the case of cell-edge users. A simple method to improve cell-edge data rates is to statically restrict the use of certain parts of the operation bandwidth. Such static schemes fall into one of three broad categories: traditional (hard) fractional frequency reuse [37], soft frequency reuse [38], and partial frequency reuse [39]. 3GPP addressed this issue through an eNodeB scheduling strategy that includes an ICIC element. This early ICIC mitigates interference on traffic channels only, and operates in both power and frequency domains to mitigate cell-edge interference coming from neighboring cells. Time-domain interference coordination is not used, as it would interfere with the operation of hybrid ARQ processes (especially in the uplink where synchronous hybrid ARQ is used) [40]. In LTE Rel. 8, ICIC is inherently a multicell RRM function that needs to take into account information from multiple cells, e.g., the resource usage status and traffic load situation. The preferred ICIC method may be different in the uplink and downlink [41].

The coordination between LTE cell sites is achieved by exchanging messages between eNodeBs over the X2 interface as shown in Fig. 10. Frequency-domain

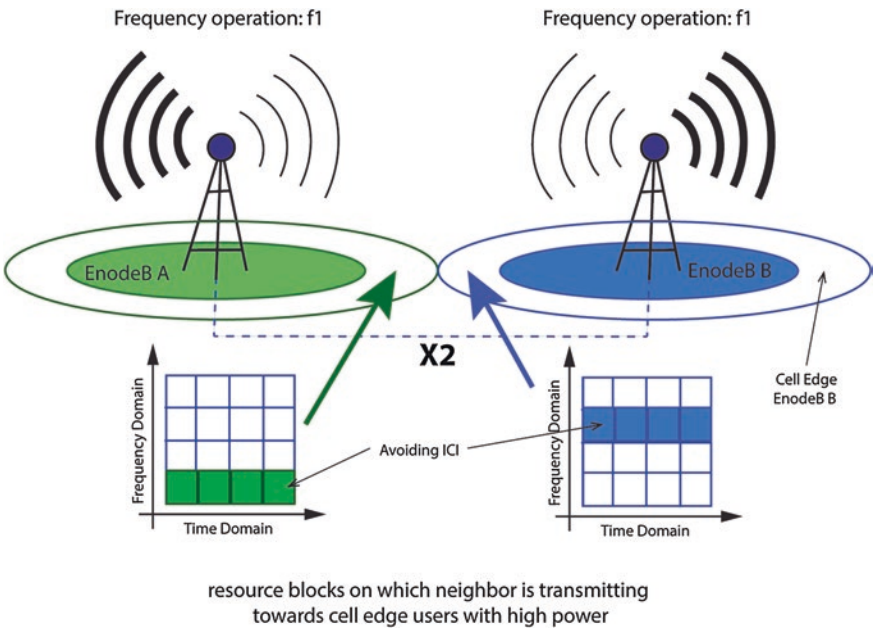

Fig. 10 Pictorial description of the ICIC strategy mandated within the LTE Rel. 8 standard

ICIC in the downlink basically controls the cell power for resources by sending a relative narrowband transmit power message as often as every 200 ms. Such messages contain information about whether a given PRB is limited by transmit power. When a neighboring eNodeB listens to this message, it can avoid scheduling on the indicated PRB. Two messages are defined for uplink interference coordination, namely high interference indicator (HII) and overload indication, and exchanged between eNodeBs as often as every 20 ms. HII is used to communicate on which PRB the eNodeB is going to schedule cell-edge users. By listening to this message, a neighboring eNodeB can avoid scheduling cell-edge users in that same indicated PRB. This results in reduced uplink interference for both cells. The action taken by an eNodeB when it receives an HII message is implementation specific. An eNodeB sends an overload indication to indicate the level of interference (low, mid, or high) experienced in different PRBs to neighboring eNodeBs. Upon receiving such a message, an eNodeB can change its scheduling pattern to free the PRBs indicated in that message, thus reducing the interference for cell-edge users.

We have seen that basic ICIC technology has been in use since LTE Rel. 8. However, in the case of HetNets, where macro cells are complemented with small cells, i.e., femtocells, picocells, and microcells, the interference imposed by small cells on the macro cell and vice versa still lacked a proper strategy. This issue was properly dealt with in LTE Rel. 10 with the introduction of an enhanced ICIC (eICIC) feature, designed bearing the aforementioned interference issues common in HetNets.

eICIC relies on power, frequency, and time domain strategies to mitigate intra-frequency interference. Power and frequency strategies in LTE Rel. 10 are the same for LTE Rel. 8. The strategy used to reduce interference in the time domain is that a serving cell stops transmitting or transmits with very low power at a certain subframe, so that an interfering cell can transmit its signal during that period. The subframe with very low signal power is termed almost blank subframe (ABS). ABSs do not comprise any traffic channels and are mostly control channel frames with very low power. If a macro cell configures ABSs, UEs connected to small cells should then send their data during such subframes, avoiding interference from the macro cell. Therefore, and in contrast to the baseline ICIC, eICIC not only mitigates interference on traffic channels but also on control channels [42].

eICIC strategies proposed in LTE Rel. 10 are, however, not able to address interference caused by CRS transmitted to support legacy deployments, i.e., LTE networks based on Releases 8 and 9. CRS and other mandatory system information are the only signals transmitted during ABS, and it is employed for mobility measurements and demodulation of the downlink control and data channels. Therefore, interference caused by neighboring cells could be detrimental for the measurement of channel quality and demodulation of various data and control channels [43].

In this context, the main enhancement introduced in LTE Rel. 11 is the provision of CRS assistance information of aggressor cells to the UEs. CRS assistance information is provided by the eNodeB to cancel unwanted CRS, thus mitigating

further interference. This information helps UEs improve both CRS-based measurements and demodulation of data/control channels by indicating them the neighbor cells that have ABS configured. This improvement is known as further enhanced ICIC (feICIC). Not only is this technology able to tackle the interference scenarios described from Releases 8 through 10 but it also manages CRS-based interference through coordinated transmitter and receiver actions [44].

As with eICIC, feICIC was also conceived to deal with interference issues in HetNets. The idea is to add a layer of complexity to the receivers, which now must also handle inter-cell interference cancellation. One important benefit introduced thereby is that the mitigation of neighbor CRS interference enables further cell range extension and ensures that weak cells can be detected [45].

3.3.2 Interference Rejection Combining

The LTE technology provides high spectral efficiency within one cell, but it can be shown to be highly vulnerable to inter-cell interference. Interference rejection combining (IRC) is a technology introduced in LTE Rel. 11, which is implemented in the layer 1 of LTE systems, and can be described as an efficient alternative to increase uplink bit rates in areas where cells overlap [46]. Interference caused by adjacent cells restricts throughput in environments where the power of the interference signal is stronger than that of the noise.

The use of IRC receiver technology at the UE was advanced as means to reject and suppress interference, thus mitigating the effects of unwanted signals and increasing user throughput [47]. The main idea behind IRC is the regeneration of the transmitted signal based on the estimation of data from previous receptions, emulation of the distortion introduced by the multipath channels and, finally, the subtraction of all regenerated interfering signals from the uplink received signals in order to obtain a more reliable estimation of the original users' data.

This feature uses the spatial separation and characteristics of inter-cell interference to determine the power of the interfering UE which belongs to another cell. Once the pattern and power level is determined, the victim cell can then remove the interferer from the received signals [48].

4 Advanced Services

This section deals with two services that have been receiving special attention within 3GPP, namely multimedia broadcasting services and machine-centered communication services. The former provides operators with an economical solution for multiuser, high-bandwidth services, while the latter seeks to leverage the LTE technology as competitive option for the multibillion Internet of Things market.

4.1 Multimedia Broadcasting and Multicasting

The term multimedia broadcast and multicast service (MBMS) is not fundamentally new to 3GPP, and so not defined as an LTE-only feature. In fact, this feature was first specified in 3GPP Rel. 6 with the goal of making it possible for network operators to broadcast over their cellular networks. MBMS provides native support for broad- and multi-casting IP packets in wireless networks, thus allowing high bandwidth services to be offered to multiple users in an economical manner, e.g., on-demand video, mobile TV, short news clips, weather reports, match results, and software updates [49]. The evolved MBMS (eMBMS) framework has as its key motivation the integration of broadcast and multicast extensions into mobile communication systems, thus enabling efficient group-related data distribution services—especially over the radio interface. As defined in LTE Releases 8 and 9 [50, 51], eMBMS baseline definition supports adaptive hypertext transfer protocol streaming via broadcast, and a few bugs have been identified and fixed through real implementation.

eMBMS is a unidirectional service, which targets the delivery of multimedia data from a single source entity to multiple recipients, optimizing the use of scarce resources. The main requirements during provisioning of eMBMS services are ensuring efficient overall usage of radio and network resources and reducing the power requirements for the provisioning of such demanding services [52]. Multimedia broadcast single frequency network (MBSFN) operation is a key new feature of LTE that brings about the possibility of exploiting the OFDM radio interface to transmit broadcast or multicast data as a multicell transmission over a synchronized SFN. A pictorial description of the eMBMS service deployed in MBSFN operation is given in Fig. 11.

MBSFN transmission enables a more efficient operation of the MBMS service, allowing over-the-air combination of multicell transmissions toward the UEs. In

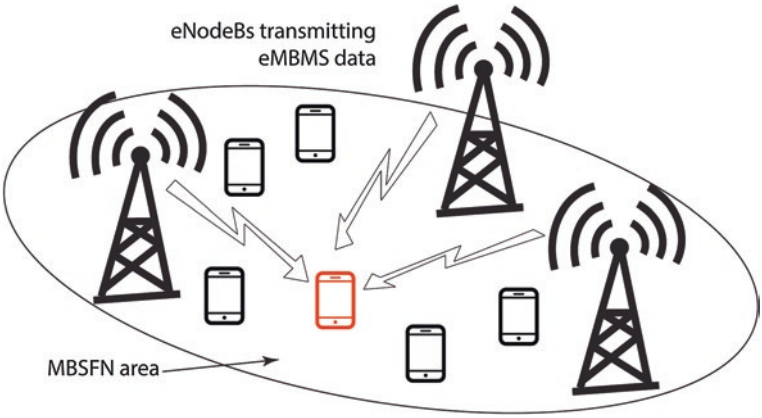

Fig. 11 Pictorial description of the eMBMS service in MBSFN operation

an MBSFN operation, MBMS data is transmitted simultaneously over the air from multiple tightly time-synchronized cells. A UE receiver will therefore observe multiple versions of the signal with different delays due to the multicell transmission. There will be no inter-symbol interference, provided that transmissions from multiple cells are sufficiently synchronized for each to arrive at the UE within the CP at the start of the symbol. In effect, this makes the MBSFN transmission appear to a UE as a transmission from a single large cell, so the UE receiver can treat multicell transmissions in the same way as multipath components of a single-cell transmission without incurring any additional complexity [53–56].

4.2 Machine-Type Communications

Machine-type communications (MTC) have been regarded as such a revenue generation opportunity that mobile operators would not want to let it slide. From the operator perspective, it is clearly more efficient if future MTC devices can be served using already deployed RATs. One crucial question that remains open thus far is whether LTE technology can be competitive enough when it comes to efficient MTC support. MTC devices, often referred to as MTC UEs in the context of LTE, will likely be deployed in large numbers, so individual device cost plays a role of utmost importance for leveraging future LTE-based MTC networks. In such networks, communication will take place in the form of infrequent, short burst transmissions, which in turn call for low operational power consumption on the part of MTC UEs.

Aware of this promising Internet of Things market, 3GPP plans to enhance LTE suitability for MTC-specific applications. Standardization efforts began in Rel. 12 [57] and are expected to continue in Rel. 13 [58]. The goal is to introduce a new, low-complex UE category able to operate with bandwidth and transmit power requirements both reduced for ultra-long battery life. Operation channels 1.4 MHz wide are envisioned, so operators can multiplex reduced bandwidth MTC UEs and regular UEs in their existing LTE deployments. To cater to operation in the presence of poor propagation conditions, e.g., in case of geotechnical sensors deployed under the ground level, delay-tolerant MTC UEs will have a coverage improvement of the order of 15–20 dB.

Assuming multislot class 2 terminals based on enhanced general packet radio service as benchmark for cost comparison and minimum data rate capability, the 3GPP study has put together a list of features and their modifications to reduce cost and improve coverage along with various hardware simplifications. It turns out that the three actions yielding the largest UE cost reduction gains are [57]:

- Reduced bandwidth for both RF and baseband for downlink and uplink: Gain of 39 % at the expense of 1–3 dB degradation to cell coverage;
- Single receive RF: Gains of up to 29 % at the cost of 4 dB degradation to cell coverage;
- Peak rate reduction: Gains of up to 21 % without any degradation to cell coverage.

When jointly implemented, the actions above can cut off UE costs in as much as 59 %. The resulting degradation to cell coverage was found to lie in the range 5–9 dB in this case. Other actions assessed in the study include half-duplex FDD, uplink transmit power reduction, and transmission mode reduction.

5 Concluding Remarks

This brief chapter has presented a comprehensive overview of current LTE systems and beyond. We have presented the baseline technology and the underlying features of network architecture, protocols, and air interface introduced in the first LTE release back in 2008. Having the basics put in place, we moved forward to discuss advanced features introduced and further developed throughout subsequent LTE releases. The discussion found in the present chapter takes into consideration even the still under discussion LTE Release 13, which has in March 2016 its estimated freeze date.

References

1. Al-Kandari A, Al-Nasheet M, Abdulgafer R (2014) WiMAX vs. LTE: an analytic comparison. In: Proceedings of the fourth international conference on digital information and communication technology and it's applications (DICTAP), pp 389–393, May 2014
2. 3GPP TSG RAN (2008) E-UTRA; E-UTRAN; Overall description; Stage 2. In: 3GPP Technical Specifications, version 8.4.0, Mar 2008
3. Osseiran A et al (2009) The road to IMT-advanced communication systems: state-of-the- art and innovation areas addressed by the WINNER + project. IEEE Commun Mag 47(6):38–47
4. Dahlman E et al (2008) 3G evolution: HSPA and LTE for mobile broadband, 2nd edn. Academic Press, Amsterdam
5. 3GPP Technical Specification TS 22.278 (2008) Service requirements for evolution of the 3GPP system, stage (release 8), June 2008
6. Bogineni K et al (2009) LTE part I: core network. IEEE Commun Mag 47(2):40–43
7. 3GPP Technical Specification 36.133 version 8.5.0 (Release 8) (2010) Evolved universal terrestrial radio access (E-UTRA); requirements for support of radio resource management, Jan 2010
8. 3GPP Technical Specification 25.133 version 8.20.0 (2013) Technical specification group radio access network; requirements for support of radio resource management (FDD), Jul 2013
9. 3GPP Technical Specification 36.213 version 8.8.0 (Release 8) (2009) Evolved universal terrestrial radio access (E-UTRA); physical layer procedures, Oct 2009
10. 3GPP Technical Specification TS36.300 version 8.12.0 (Release 8) (2010) Evolved universal terrestrial radio access (E-UTRA) and evolved universal terrestrial radio access network (E-UTRAN): overall description, Apr 2010
11. 3GPP Technical Specification TS 36.321 version 8.12.0 (Release 8) (2012) E-UTRA medium access control (MAC) protocol specification, Mar 2012
12. Meyer M et al (2006) ARQ concept for the UMTS long-term evolution. In: Proceedings of the IEEE VTC, pp 1–5, Sept 2006

13. 3GPP Technical Report TR 25.913 V8.0.0 (2010) Requirements for evolved UTRA (E-UTRA) and evolved UTRAN (E-UTRAN), Feb 2010
14. Rao A, Weber A, Gollamudi S, Robert S (2009) LTE and HSPA + : revolutionary and evolutionary solutions for global mobile broadband. Bell Labs Tech J 13(4):7–34 (Winter 2009)
15. Astely D et al (2009) LTE: the evolution of mobile broadband. IEEE Commun Mag 47(4):44–51
16. Anyi W, Zhaoyang L (2010) The study and analysis of MIMO technology based on LTE physical layer. In Proceedings of the international conference on environmental science and information application technology (ESIAT), pp 306–308, July 2010
17. Ku G, Walsh J (2014) Resource allocation and link adaptation in LTE and LTE advanced: a tutorial. IEEE Commun Surveys Tutorials, vol 99, pp 99, Dec 2014
18. Larmo A et al (2009) The LTE link-layer design. IEEE Commun Mag 47(4):52–59
19. Sesi S, Toufix I, Baker M (2009) LTE: the UMTS long term evolution, from theory to practice, 1st edn. Wiley, Chichester
20. Figueiredo F, Lenzi KG, Bianco Filho JA, Ferreira O, Cardoso F, Figueiredo FL (2013) LTE random access detection based on a CA-CFAR strategy. In: International workshop on telecommunications (IWT2013), Santa Rita do Sapucai, 2013
21. Frank RL, Zadoff SA, Heimiller R (1961) Phase shift pulse codes with good periodic correlation properties. IRE Trans Inf Theor 7:254–257
22. Chu DC (1972) Polyphase codes with good periodic correlation properties. IEEE Trans Inf Theor IT-18:531–532
23. Cardoso F, Figueiredo FL, Lenzi KG, Bianco Filho JA, Figueiredo F, Vilela RM (2013) Multi-stage based cross-correlation peak detection for LTE random access preambles. Revista Telecomunicações do Inatel, pp 21–27
24. 3GPP TS 36.300 (2008) Evolved universal terrestrial radio access (E-UTRA) and evolved universal terrestrial radio access network (E-UTRAN); overall description; stage 2, version 8.7.0, December 2008
25. 3GPP Presentation RWS-140029 (2014) Chairman summary. In: 3GPP Workshop on LTE in Unlicensed Spectrum, June 2014
26. 3GPP Presentation RP-150055 (2015) 3GPP & Unlicensed Spectrum. In: IEEE 802 Interim Session, Jan 2015
27. Carrier Aggregation Explained (June 2013) [Online]. Available: http://www.3gpp.org/technologies/keywords-acronyms/101-carrier-aggregation-explained
28. 3GPP Technical Report TR 36.815 (2010) Further advancements for E-UTRA; LTE-advanced feasibility studies in RAN WG4, July 2010
29. 3GPP Work Item Description RP-141831 (2014) Study on elevation beamforming/full-dimension (FD) MIMO for LTE. In: 3GPP TSG RAN Meeting #66, Dec 2014
30. B. Mondal et al., "3D Channel Model in 3GPP", [Online]. Available: http://arxiv.org/ftp/arxiv/papers/1502/1502.01621.pdf
31. 3GPP Technical Specification TS 36.902 version 9.3.1 (2011) Self-configuring and self-optimizing network (SON) use cases and solutions, May 2011
32. 3GPP Technical Specification TS 32.531 version 9.4.0 (2011) Telecommunication management; software management (SWM); concepts and IRP requirements, Jan 2011
33. 3GPP Technical Specification TS 32.511 version 9.0.0 (2010) Telecommunication management; automatic neighbor relation (ANR) management; concepts and requirements, Feb 2010
34. 3GPP Technical Specification TS 36.300 version 9.1.10.0 (2013) Evolved universal terrestrial radio access network (E-UTRAN); overall description stage 2, Feb 2013
35. 3GPP Technical Specification TS 32.521 version 9.0.0 (2010) Self-organizing networks (SON) policy network resource model (NRM) integration reference point (IRP): requirements, Apr 2010
36. 4G Americas (2014) Self-optimizing networks in 3GPP release 11: the benefits of SON in LTE, Oct 2013
37. Overview of 3GPP Release 11 version 0.2.0 (Sept 2009) [Online]. Available: http://www.3gpp.org/ftp/Information/WORK_PLAN/Description_Releases/Rel-11_description_20140924.zip

38. Boujelben M, Benrejeb S, Tabbane S (2014) Interference coordination schemes for wireless mobile advanced systems: a survey. IOSR J Electron Commun Eng (IOSR-JECE) 9(1):80–90
39. Mills A, Lister D, De Vos M (2011) Understanding static intercell interference coordination mechanisms in LTE. J Commun 6(4):312–318
40. Astely D et al (2009) LTE: the evolution of mobile broadband. IEEE Commun Mag 47(4):44–51
41. Gjendemsj A, Gesbert D, Oien GE, Kiani SG (2008) Binary power control for sum rate maximization over multiple interfering links. IEEE Trans Wireless Commun 7(8):3164–3173
42. Kwan R, Leung C (2010) A survey of scheduling and interference mitigation in LTE. J Electr Comput Eng 2010:10
43. Lopez-Perez D et al (2011) Enhanced inter cell interference coordination challenges in heterogeneous networks. IEEE Wireless Commun 18(3):22–30
44. 3GPP Website. Heterogeneous networks in LTE", [Online]. Available: http://www.3gpp.org/technologies/keywords-acronyms/1576-hetnet
45. 3GPP Technical Report TR 36.913 (2012) Requirements for further advancements for E-UTRA, Sept 2012
46. 3GPP Technical Specification TS 36.300 (2012) Evolved universal terrestrial radio access (E-UTRA) and evolved universal terrestrial radio access network (E-UTRAN); overall description; stage 2 (Release 11), Sept 2012
47. 3GPP Technical Report TR 36.829 (2012) Enhanced performance requirement for LTE user equipment (UE), Mar 2012
48. Nakamura T et al (2010) Overview of LTE advanced and standardization trends. NTT Docomo Tech J 12(2):4–9
49. Léost Y, Abdi M, Richter R, Jeschke M (2012) Interference rejection combining in LTE networks. Bell Lab Tech J 17(1):25–49
50. Rohde & Schwarz, "White paper: LTE Release 9 Technology Introduction", Dec. 2011
51. 3GPP Technical Specification TS 26.346 version 9.15.0 (Release 9) (2014) LTE; multimedia broadcast/multicast service (MBMS); protocols and codecs, Jul 2014
52. 3GPP Technical Specification TS 23.246 version 9.6.0 (Release 9) (2012) Multimedia broadcast/multicast service (MBMS); architecture and functional description, Jan 2012
53. Tata Consultancy Services (2013) Multimedia broadcasting in long term evolution networks
54. 3GPP Technical Specification TS 36.445 (2011) Evolved universal terrestrial radio access network (E-UTRAN): M2 application protocol (M2AP), M1 data transport (release 10), Sept 2011
55. 3GPP Technical Specification TS 22.146 (2011) Multimedia broadcast/multicast service (MBMS); stage 1, Dec 2011
56. 3GPP Technical Specification TS 23.246 (2012) Multimedia broadcast/multicast service (MBMS); architecture and functional description, Mar 2012
57. 3GPP Technical Specification TS 36.331 (2012) Radio resource control (RRC): protocol specification (Release 10), Mar 2012
58. 3GPP Technical Report TR 36.888 (2013) Study on provision of low-cost machine-type communications (MTC) user equipments (UEs) based on LTE, June 2013
59. Ali I et al (2009) Network-based mobility management in the evolved 3GPP core network. IEEE Commun Mag 47(2):58–66

Brazilian Telecommunications Regulatory Framework and the Impacts on the Development of Broadband Radio Access Systems

Carlos Lorena Neto, Edson José Bonon and Fabrício Lira Figueiredo

Abstract The introduction of new radio access technologies into the market has been accelerated in the last years, imposing an equally swift evolution of regulatory instruments aimed at adjusting telecommunication services to the new technological scenarios, e.g., by adequately allocating frequency bands for efficient spectrum utilization, and remodeling normative instruments for product certification. This chapter highlights the impacts of these regulatory sectors on systemic requirements, and points out new opportunities for developing broadband radio access system technologies taking the Brazilian regulatory scenario as a reference.

1 Introduction

The access to voice and data services over a broadband access network is first and foremost a public interest service granted under a public regime, or authorized under a private regime. However, it can also be characterized as the rendering of restricted interest services under a private regime when specific frequency bands are allocated to the different Limited Private Service (SLP). The SLP regime is intended to support the operational activities of companies, such as the electric

C. Lorena Neto (✉) · E.J. Bonon · F.L. Figueiredo
CPqD Foundation, Campinas, SP, Brazil
e-mail: clneto@cpqd.com.br

E.J. Bonon
e-mail: bonon@cpqd.com.br

F.L. Figueiredo
e-mail: fabricio@cpqd.com.br

A. Paradisi et al. (eds.), *Long Term Evolution*, Telecommunications and Information Technology, DOI 10.1007/978-3-319-23823-4_2

power generation, transmission, and distribution sector (Smart Grid), the oil extraction, refinery and distribution sector, the urban and suburban mobility sector, as well as public security and disaster management operations.

In this chapter, the Brazilian Regulatory Framework for telecommunications services is adopted as basis for an analysis, as an effort to assess its impacts and highlight new opportunities for developing Fourth Generation (4G) and beyond broadband radio access system technologies. In order to provide a full understanding of the current scenario, some basic concepts and the evolution of the Brazilian regulatory framework are briefly described within each section.

International demand for a global and uniform distribution of frequency bands for fixed and mobile radio access systems has driven International Mobile Telecommunications (IMT) standardization activities since the 1980s. This broad concept, supported by technical recommendations and requirements, globally defines systemic interoperability issues (for both network and aerial interfaces), and services supported by certified technologies.

Within the IMT scope, and consequently based on a standards set from the National Agency for Telecommunications (Brazilian counterpart of the FCC, hereafter referred to simply as ANATEL) for the Brazilian territory, services supported by broadband radio access system have been defined. These comprise Public Switched Telephone Networks (PSTN), Personal Mobile Service (SMP), Multimedia Communication Services (SCM), for general (collective) interest applications, and SLP, with its different sub-modalities, for private applications.

Furthermore, several frequency bands have been defined, regulated, and allocated to the main collective interest services (fixed/PSTN and mobile/SMP) in the 824 MHz–2.2 GHz portion of the spectrum. The majority of this spectrum has been licensed to SMP service providers and is mainly used for voice services. This segment of the spectrum, although relevant for the sector, is out of the scope of this chapter, as it has already been thoroughly consolidated worldwide, and as such has no significant impact on emerging technologies under development.

The allocation of new frequency bands, for both public and private services, is a topic under constant discussion by ANATEL and the Ministry of Communications. Such frequency bands have a high potential for application in 4G and beyond broadband radio access technology, and are located for the most part in Ultra High Frequency (UHF) bands below 1 GHz, in some segments, in the 1.5 GHz range, and in certain specific bands such as 2.6 and 3.5 GHz. Therefore, special attention must be given to the evolution expected for these new frequency bands, especially regarding the technical requirements of services that occupy that same frequency band, sub-bands, or neighboring sub-bands. These issues pose a direct impact on the requirements for the coexistence of systems and services, and, consequently, on the requirements of new technologies and products under development.

Laboratory tests for ANATEL certification and approval of products are supported by a mixed structure of standards, resolutions, and technical requirements, which have been constantly modified to ensure they are adequate for new technologies and frequency bands. These regulatory standards must be analyzed in terms

of electromagnetic compatibility and electrical protection, and more specifically, in terms of requirements for base transceiver stations, terminals, and antennas.

The remainder of the chapter is organized as follows. In Sect. 2 an overview of the Brazilian Regulatory Framework is presented. In Sect. 3 the use of the radio frequency spectrum and band allocation issues are addressed, while in Sect. 4—products, and in Sect. 5—antennas the matter of product certification is addressed.

2 Regulatory Framework of Telecommunication Services

Telecommunication services are classified as collective interest services or restricted interest services.

2.1 Collective Interest Services

Collective interest services are those that are rendered under a public or private regime, and seek to meet collective needs indiscriminately. The only public service rendered under a federal concession is PSTN. SMP and SCM are authorized private services.

2.1.1 Public Switched Telephone Network

PSTN was first regulated under the name Public Phone Service (STP), by the Ministry of Communications Standard # 05 [1]. In 1998, Resolution # 73 [2] was issued, containing the basic regulations for telecommunication services. A month later, Resolution # 85 [3] was published with the first PSTN regulatory standards, under ANATEL's regulatory administration. The main difference in scope between Standard 05/79 and Resolution 85 is in the way services are provided. The first one regulated telecom services under the state-controlled regime, stipulating that "public phone services are provided nationwide by companies controlled by Telecomunicações Brasileiras S/A (TELEBRÁS) and by other companies and organizations with concession contracts in effect". The second one regulated PSTN, specified that services were to be provided under "contracts or terms of concession, permission and authorization, signed between Service Providers and ANATEL".

Still in 1998, ANATEL published Resolution # 78 [4], laying out guidelines for allocating frequency bands for Fixed Wireless Access Systems to provide PSTN services, a system known at the time as Wireless Local Loop (WLL). In 1999, Resolution # 146 [5] approved regulatory standards for WLL certification, while Resolution # 166 [6], also issued in 1999, regulated WLL system utilization. These were mainly supported by Cellular Mobile Service (SMC) networks,

currently SMP. In 2005, ANATEL published new regulatory standards for PSTN in Resolution # 426 [7]. This resolution increased the scope of PSTN service definitions, especially regarding accessibility, personal services, Significant Market Power, the ability to identify the origins and destinations of calls, the protection or suspension of privacy, the sharing of infrastructure, among other issues. Resolution # 426, issued in 2005, regulates PSTN until today.

2.1.2 Personal Mobile Services

In 1996, Law 9,295 [8], also known as Minimum Law, was passed, defining telecommunication services and their organization, as well as outlining the powers of the regulatory body. This law was the catalyzing element that triggered the beginning of competition in the mobile services sector, as the first private service providers began operating in Band B, while state-owned providers continued their Band A operations.

During this period, Land Mobile Services were known as SMC. The first regulatory standard for SMP, now supported by the General Communications Law (Law 9,472) [9], approved the guidelines for SMP deployment in Resolution # 235 [10]. Still in 2000, Resolution # 245 [11] and Resolution # 248 [12] were issued, establishing the SMP Master Authorization Plan. This set of three resolutions composed the initial framework for migrating SMC to SMP and increasing the number of authorized SMP service providers.

A relevant evolution took place in 2010, with the publication of Resolution # 550 [13], regulating Virtual Network SMP exploration (RRVSMP). Additionally, service quality was defined by the Master Quality Plan (PGMQ), published in Resolution # 317 [14] gauged by the quality indicators established in Resolution # 335 and measured in compliance with Resolution # 443 [15]. SMP is currently regulated by Resolution # 477 [16], supported by the Master Authorization Plan defined in Resolution # 321 [17] and gauged by PGMQ-SMP.

2.1.3 Multimedia Communication Services

Until August 2001, the transmission of multimedia communication data was supported by Special Limited Services (SLE), using the sub-modalities Specialized Network Services (SRE) and Specialized Circuit Services (SCE), as well as the Telecommunications Transport Network Services (SRTT), comprising Dedicated Line Services (SLD), Packet Switched Network Services (SRCP), and Circuit Switched Network Services (SRCC), all general (collective) interest services. In 2001, ANATEL published Resolution # 272 [18], defining SCM regulatory standards.

In 2003, ANATEL published Resolution # 328 [19], approving models for the Term of Authorization for SCM exploration, which could also be adapted for SLE and SRTT authorizations. Resolution # 614 [20], besides improving several

features used on an experimental basis during the first years of authorization, established the milestones for increasing widespread use of the SCM services.

2.2 Restricted Interest Services—Limited Private Services

The SLP regulatory framework has its origin in Law 4,117 [21], which established the Brazilian Telecommunications Code. Chapter 6 of this law defines limited services: "a limited service is that provided by stations not open to public correspondence to be utilized by Brazilian private citizens or companies. Such limited services include, security, regularity, orientation, and administration of transportation services in general, multiple destinations, rural services, and private services, to name some". Not long after that, the first limited service and the SLP submodality were assigned.

Standard 13 [22] defines the characteristics of SLP and SLE and their submodalities: Private Mobile Services, Private Radio Call Services, Private Network Services and Private Radio-Taxi Services, Specialized Mobile Services, Specialized Circuit Services, Specialized Network Services, and Specialized Radio-Taxi Services.

In 2013, ANATEL published Resolution # 617 [23], which consolidated in a single regulatory standard the following definition: "SLP is a restricted interest telecommunications service, explored nationwide or worldwide under a private regime, taken by users themselves or rendered to a given group of users, selected according to criteria defined by the service provider, comprising multiple applications, including the data communication, audio and video signal communication, and voice and text communication, as well as capturing and transmitting Scientific Data related with the Exploration of the Earth by Satellite, Meteorology Assistance, Satellite Meteorology, Space Operations and Space Research". This resolution revoked a large number of regulatory standards that had become enacted over the years.

3 Regulatory Framework for Frequency Band Allocation

This topic focuses on regulatory standards regarding the allocation of certain bands specifically strategic for the development of broadband radio access systems.

3.1 225–470 MHz Sub-Bands

Until recently, the sub-bands located in the 225–470 MHz UHF range had been used by several narrowband voice and telemetry services, especially

SLP and Private Mobile Limited Services (SLMP). In 2010, ANATEL published Resolutions # 555 [24], 556 [25], 557 [26], and 558 [27], reassigning frequency bands from 225 to 270 MHz, 360 to 380 MHz, 380 to 400 MHz, and 450 to 470 MHz, respectively. Resolutions # 555 and 558 stand out from the other regulatory standards since they assign sub-bands in the 250 and 450 MHz range, with wide channels able to handle broadband radio access systems operations. These resolutions partially replace the standards enacted by the Ministry of Communications in Decree 623 [28].

ANATEL launched Resolution # 558, which allocates the sub-bands from 451.5875 to 454 MHz, from 456.5875 to 459 MHz for airport SLP, and of Resolution # 446 [29], which regulates this service specifically. These sub-bands occupy part of the uplink sub-band allocated to PSTN, SMP, and SCM for broadband network access. The conditions for the coexistence of these services and airport SLP are defined in Resolution # 446, which defines a 10 km protected perimeter around all national airports identified in the resolution.

3.2 698–806 MHz Sub-Bands

The digitalization brought about by the deployment of the Brazilian Digital TV System (SBTVD) opened up the possibility for a more efficient use of the spectrum assigned to TV services. Moreover, the fact that the chosen digital transmission standard allows signals to be repeated isofrequentially (on the same channel), optimizing spectrum use. For a proper analysis of the current and future allocation of the 700 MHz frequency band, it is important to bear in mind the following issues:

(a) The frequency band known as the 700 MHz band is located between the 698 and 806 MHz frequencies. Today, this band is allocated to Sound and Image Broadcasting Services (TV), occupying UHF channels 52–69;
(b) The Basic Digital TV Plan (PBTVD) proposes allocating channels 14–59 (470–746 MHz) for DTV in Brazil;
(c) Channels 60–68 (746–800 MHz) have been earmarked for Television and Public Digital Television Retransmission Services.

Figure 1 illustrates this issue within the scope of the digital divide to be obtained once the migration from analog-to-digital TV has been completed, scheduled for 2016.

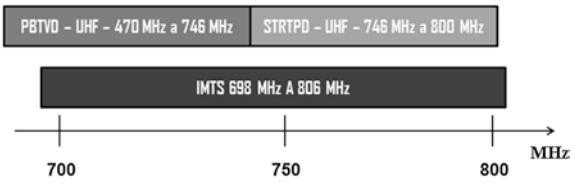

Fig. 1 Analogue-to-digital TV migration

In their 2008 Radio Regulations edition [30], ITU-R allocated the 698–806 MHz range to IMT (mobile services). In 2009, Decree # 24 [31] approved the General Standard for Executing Public Digital Television Services, defining channels 60–68 (746–800 MHz) for this. In 2010, Decree # 276 [32] approved the Technical Standard for Executing Sound and Images Broadcasting Services and Television Retransmission with digital technology. According to the standard, the allocation of the 54–88 MHz sub-bands in Very High Frequency (VHF), channels 2–6, no longer existed; the allocation of sub-bands 174–216 MHz (VHF channels 7–13) and 470–800 MHz (UHF channels 14–68) was maintained; the 608–614 MHz sub-band, corresponding to channel 37, is internationally allocated to radioastronomy services on a primary basis; and 60–68 are exclusively for Television and Public Digital Television Retransmission Services.

ANATEL Resolution # 584 [33], in 2012, changed the Regulations for Channeling and Terms of Radio Frequency Use for SARC, RpTV, and CFTV, besides enacting other measures. Among these measures, Chap. 17 called for studies to be carried out until December 2012 to define future use of the radio frequency spectrum, especially the 698–806 MHz range. Decree # 681 [34], in 2012, established a Work Group to study conditions for using the radio frequency range of 698–806 MHz. Recommendation ITU-R M.1036-4 [35] reinforced the allocation of the 698–806 MHz range, indicated by WRC-2007, to IMT, as shown in Fig. 2.

The 1.5 GHz band was first assigned to fixed services in Resolution # 198 [36], which revoked Standard # 15, from 1994. This resolution established the frequency channeling and terms of use of the 1427–1452 MHz and 1492–1517 MHz bands for fixed service digital systems, with transmission capacity

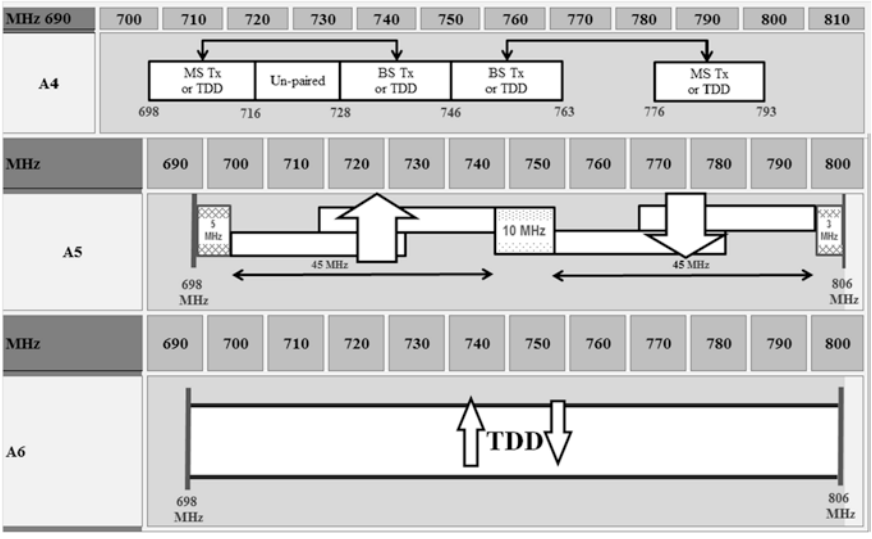

Fig. 2 Allocation of the 698–806 MHz range for IMT

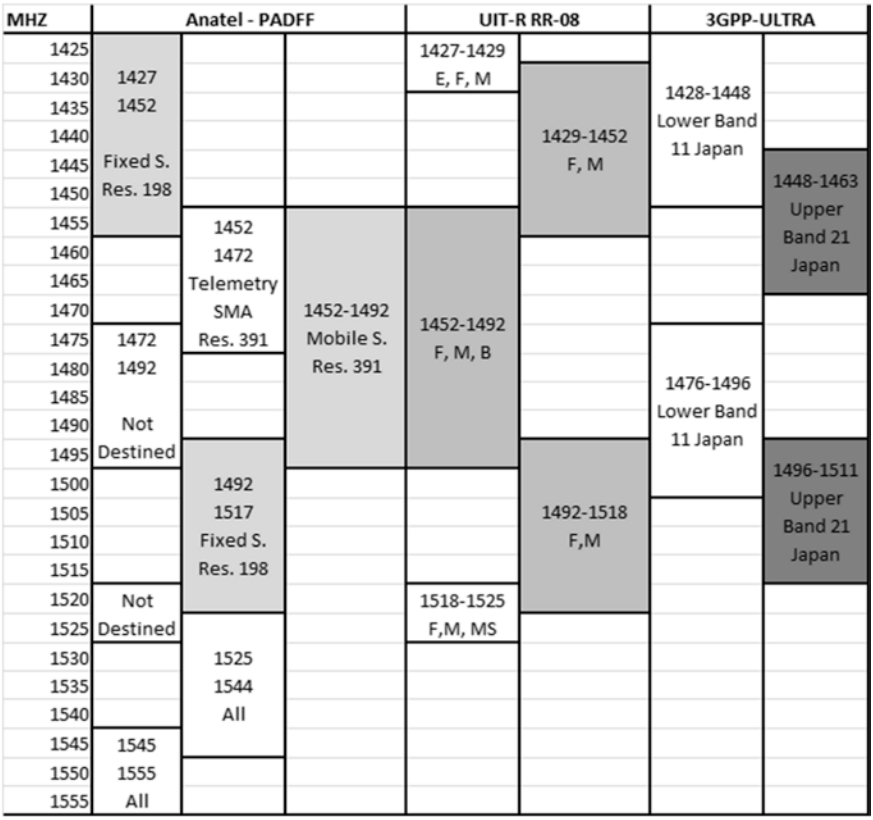

Fig. 3 Definition of frequency bands for the E-UTRA aerial interface

of 2 × 2 Mbps for point-to-point and point-to-multipoint applications. Later, Resolution # 391 [37], published in January 24, 2005, approved Regulations for the Terms of Radiofrequency Use in the 1452–1472 MHz range, assigned to air force mobile services, for Telemetry applications, on a primary basis, the 1452–1466 MHz radio frequency range, and on a secondary basis, the 1466–1472 MHz range, and assigned the 1452–1492 MHz radio frequency range additionally to mobile service, on a primary basis.

Figure 3 is a diagram portraying ANATEL's allocation based on the two above-mentioned resolutions, on the ITU-R Radio Regulations 2008 issue, and on the 3GPP Forum's definition of frequency bands for their E-UTRA aerial interface.

Based on this scenario, one can deduce that fixed services, PSTN and SCM in the case of Brazil, could use the two 25 + 25 MHz segments from 1427 to 1452 MHz and from 1492 to 1517 MHz ranges for point-to-point and point-to-multipoint applications, while mobile services could use the 6 MHz segment between 1466 and 1472 MHz for TDD applications, where SMA-Telemetry would be allocated on a

Table 1 ANATEL SitarWeb system data

Service	MIN	MAX	ENL	%
12-Radio for Private Mobile Service	1429	1515	28	1.00
9-Limited Private Service	1429	1582	1127	24.00
46-Radio for Multimedia Communication Service	1429	1519	70	2.00
53-Radio for Personal Mobile Service	1429	1522.5	346	7.00
175-PSTN	1429	1526	3044	66.00
			4615	

secondary basis. However, 3GPP's definition of bands 11 and 21 compromises the utilization of the above-mentioned bands. That leaves only the 1518 and 1555 MHz sub-bands as possibilities for broadband access system allocation.

Several equipment manufacturers supply products for operation in this frequency range, called WiGrid, used by the WiMAX Forum. The technical specifications of these products indicate they are for use in the 1330–1530 MHz or 1350–1517 MHz frequency range. This segment of the spectrum is currently allocated to several services and according to the ANATEL SitarWeb [38] system's directory of granted licenses, 4,615 licenses have been distributed among PSTN, SLP, and point-to-point radio link licenses for SCM and SMP support (Table 1).

4 Regulatory Framework for Certification and Approval of Telecommunication Products

This section presents an overview of the context and the current stage of product certification in Brazil.

4.1 Classification of Telecommunication Products

For certification and approval purposes, telecommunication products are segregated in three categories, according to their applications and use:

(a) Category I: Terminal equipment for use by the general public to access collective interest telecommunication services;
(b) Category II: Equipment not included in the Category I definition, but that uses the radio electric spectrum to transmit signals, including antennas and all equipment characterized under specific regulations as restricted radiation radio-communication equipment;
(c) Category III: Products that do not fit the definitions of Categories I and II, and need to be regulated to ensure the interoperability and reliability of the telecommunication support networks.

4.2 Magnetic Compatibility and Electrical Safety Requirements

In 2000, ANATEL published Resolution # 237 [39] and Resolution # 238 [40], approving Regulatory Standards for the Certification of Telecommunication Equipment regarding Electromagnetic Compatibility Aspects and regarding Electrical Safety Aspects, respectively. These resolutions were revised and updated in 2006 and 2009. In 2006, ANATEL published Resolution # 442 [41] approving Regulatory Standards for the Certification of Telecommunication Equipment regarding Electromagnetic Compatibility Aspects and revoked Resolution # 237. In 2009, ANATEL published Resolution # 529 [42], approving Regulatory Standard for the Certification of Telecommunication Equipment regarding Electrical Safety Aspects and revoked Resolution # 238. In general, all telecommunication equipment must meet the compatibility and safety requirements defined in Resolutions # 442 and 529, respectively.

Another caveat to be made to EMC and Safety requirements is on its applicability on the respective Resolutions' (BS and Terminal) Previous regulations—Technical Requirements and Test Procedures Applicable to Telecommunication Products Certification in Category I and II, respectively, from April 16 and 17, 2013 [43, 44]. It was a directive from ANATEL to protect the public in general, not including certain regulatory tests in the framework of the equipment intended for Operators' Companies, being more strict for Category I equipment (Terminals—Estação Terminal de Acesso and Telefone Móvel Celular) when compared to the equipment classified as Category II (Base Stations—Transceptores para Estação Rádio Base). Until 2015 the mandatory tests for Terminals included the full execution of the Amendments to the Resolutions # 442 (EMC) and # 529 (Safety), while Base Stations were tested only for Emission aspects (Title II of Annex to Resolution # 442), not including Immunity tests and three paragraphs in the Annex to Resolution # 529, when applicable.

This understanding was recently changed and in the new issue—Technical Requirements and Test Procedures Applicable to Telecommunication Products Certification in Category I and II, respectively, from June 1 and April, 2015 [45, 46]—the EMC and Safety tests (Annexes to the Resolutions # 442 and # 529) are demanded in the full, both for Terminals and Base Stations.

4.3 Base Transceiver Stations and Terminal Requirements

In April 2004, ANATEL published Resolution # 361 [47], approving the Standard for the Certification and Approval of Analogue FM and PM Mono-channel Transmitters and Transceivers Operating in the Under-1 GHz Frequency Range. This resolution replaced Standard 01/89—Technical Specifications Standard for Mono-channel Radio Equipment in the 30–470 MHz range with Angular

Modulation—and Standard 02/89—Measurement Method Standard for Monochannel Radio Equipment in the 30–470 MHz range with Angular Modulation. For lack of specific regulatory standards for the certification and approval of under-1 GHz digital transceivers, this standard was adapted to delineate the technical requirements for radio access equipment in process of development, production, and commercialization.

Still in the same year, ANATEL published Resolution # 368 [48] to attend to the demand for the certification of WLL products for PSTN services. This resolution defined the general and specific technical requirements to be demonstrated in the evaluation of the conformance of digital transmitters and transceivers (CDMA and TDMA, including GSM) for fixed services in point–multipoint applications operating in over-1 GHz frequency ranges. In 2006, ANATEL published Resolution # 433 [49], approving the Standard for the Certification and Approval of Transmitters and Transceivers in Base Transceiver Stations (BTS) and PSTN Repeater Stations. This resolution affects BTS equipment operating in the 400, 1900, and 3500 MHz ranges, with CDMA or TDMA technology, including GSM.

No specific regulatory standards were found to support the process of testing and certifying OFDM/OFDMA equipment for base transceiver stations and terminals. However, the document describing the technical requirements and test procedures for category I telecommunication products, updated on April 16, 2013, and available on ANATEL's web site does indicate a sub-set of technical requirements defined by the 3GPP Forum for the E-UTRA (Long Term Evolution—LTE) aerial interface, applicable for a SMP Access Terminal with this technology, that is: 3GPP TS 36.521-1 V9.5.0 (2011-06) 3GPP; Technical Specification Group Radio Access Network; Evolved Universal Terrestrial Radio Access (E-UTRA); User Equipment (UE) conformance specification Radio transmission and reception Part 1: Conformance Testing; (Release 9), in items 6.2.2–6.6.3.1.

The current regulatory scenario for product certification can be summarized as follows, according to the major globally standardized wireless technologies:

(1) WiMAX (IEEE 802.16) equipment are classified as Digital Transceptor (Transceptor Digital), fitting into Category II. This understanding is valid for both Base Stations and Customer Premises Equipment.
(2) Wi-Fi (IEEE 802.11) equipment are classified as Restricted Radiation Equipment (Equipamento de Radiação Restrita), also in Category II.
(3) 4G (LTE) equipment, as well as the legacy mobile technology (2G, 3G), are classified as:
    (a) BS—BTS—Category II.
    (b) Customer Premises Equipment (CPE)—Access Terminal Station (ETA), Category I.
    (c) Handsets and Tablets—Cellular Mobile Telephone (Telefone Móvel Celular), Category I.

Additionally new resolutions have been issued for different technologies and frequency bands, as well as the addition of more recent 3GPP standards references for LTE equipment in the regulatory framework, focusing essentially on the

protection of the electromagnetic spectrum (the tests demanded usually focus on the Transmission characteristics, not covering the reception).

Within this scenario, the new Technical Requirements and Test Procedures Applicable to Telecommunication Products Certification in Category I and II for Base Station and Terminal operating on 4G technology are the following:

Base Station

Category: II

Product: Base Station Transceiver

(1) Annex to Resolution # 554 [50]—December 20, 2010—Standard for Certification and Homologation of Transmitters and Transceivers for Base Stations and Repeaters, applicable in full;
(2) Annex to Resolution # 359 [51]—April 1, 2004—Standard for Certification and Homologation of Digital Transmitters and Transceivers for the STFC in Point-to-Multipoint Applications under 1 GHz, applicable in full;
(3) Annex to Resolution # 492 [52]—February 19, 2008—Standard for Certification and Homologation of Digital Transmitters and Transceivers for the STFC in Point-to-Multipoint Applications above 1 GHz, applicable in full;
(4) LTE Technology: 3GPP TS 36.141 V9.8.0 (2011-06) 3rd Generation Partnership Project; Technical Specification Group Radio Access Network; Evolved Universal Terrestrial Radio Access (EUTRA); Base Station (BS) conformance testing (Release 9) [53], items 6.2, 6.4, 6.6.1, 6.6.2, 6.6.3.5.2, 6.6.4.5.2, and 7.7, the last one, although referring to a Transmitter test on the issue of Spurious Emission from the Receptor.

Access Terminal—CPE

Category: I

Product: Access Terminal Station

(1) Technology LTE: 3GPP TS 36.521-1 V9.5.0 (2011-06) 3rd Generation Partnership Project; Technical Specification Group Radio Access Network; Evolved Universal Terrestrial Radio Access (E-UTRA); User Equipment (UE) conformance specification Radio transmission and reception Part 1: Conformance Testing; (Release 9) [54], items 6.2.2, 6.2.3, 6.2.5, 6.3.2, 6.3.4.1, 6.5.1, 6.5.2.1, 6.5.2.2, 6.5.2.3, 6.6.1, 6.6.2.1, 6.6.2.3, 6.6.3.1;
(2) Annex to Resolution # 359—April 1, 2004—Standard for Certification and Homologation of Digital Transmitters and Transceivers for the STFC in Point-to-Multipoint Applications under 1 GHz, applicable in full;
(3) Annex to Resolution # 492—February 19, 2008—Standard for Certification and Homologation of Digital Transmitters and Transceivers for the STFC in Point-to-Multipoint Applications above 1 GHz, applicable in full.

For both cases, CPEs and Base Stations, there are requirements specific for legacy technology such as GSM, TDMA, CDMA, WCDMA/HSDPA/HSUPA, etc.. not covered in this chapter, applicable when necessary.

EMC and Safety regulatory framework covered in item 3.2.

5 Antenna Requirements

In 2004, ANATEL published Resolution # 366 [55], approving the Standard for the Certification and Approval of Linear Antennas and replaced Standard # 08/95—Minimum Linear Antenna Radiation Characteristics. In 2004, ANATEL also published Resolution # 372 [56], which approved the Standard for the Certification and Approval of Directional and Omnidirectional Antennas. In 2013, ANATEL published Resolution # 609 [57], approving the Standard for the Certification and Approval of Antennas for Use in Point-to-Point Applications and Resolution # 610 [58], approving the Standard for the Certification and Approval of Antennas for Use in Bidirectional Point-to-Area Applications. This standard applies to antennas in operation in bidirectional point-to-area systems for fixed and mobile terrestrial services, for the 138 MHz to 40.5 GHz bands, with gain equal to or above 8.5 dBi for omnidirectional antennas and above or equal to 9.5 dBi for all other antennas. Furthermore, the standard rules that telecommunication terminals equipped with gain antennas lower than 8.5 dBi, in the case of omnidirectional antennas, and 9.5 dBi, in the case of all others, must meet the requirements of the certification standards and of the services they are designated for.

6 Conclusions

Based on what has been set forth throughout this chapter, it can be observed that, regarding telecommunication services, PSTN had its moment of wireless technology application when WLL systems were deployed. This initiative occurred in a specific scenario, when PSTN and SMP service providers, during the SMC period, were separate companies and even competitors. Today, the vast majority of service providers own licenses for PSTN, SMP, and more often than not, for SCM as well.

SCM, in turn, is an important tool for the operation of public policies aiming to universalize broadband access through small- and medium-sized private carriers. Another publication, Resolution # 617/2013, consolidated SLP definitions in a single regulatory standard, causing a major impact on services rendered by public and private organizations.

Thus, if we take into consideration the strategies for the development of 4G and beyond broadband radio access technology systems in Brazil, the following impacts and opportunities can be highlighted:

(a) PSTN: Wireless broadband access system represents an important competitive tool for PSTN service providers, allowing them to launch new market strategies. However, the systemic requirement must ensure the exclusive requirements of these public general (collective) interest services, that is, the universality and continuity of such services;
(b) SMP: Mobile broadband access technology is naturally applicable to the SMP access networks of SMP service providers. Regarding its systemic requirements,

special attention must be paid to the issues of network sharing and virtualization, essential tools for compliance with recent regulatory standards and for supporting the exponential growth of users and traffic, especially data;

(c) SCM: As with PSTN, a network access platform with 4G technology is an important market entry tool, giving small- and medium-sized service providers a strategic competitive edge. Regarding its systemic requirements, special attention must be paid to the issue of network scalability and total cost of ownership, critical for the feasibility of small- and medium-sized companies' business plans when attempting to penetrate competitive markets;

(d) SLP: The need for applications to support the various SLP operation modalities opens up an entire universe of niche opportunities for 4G and beyond technologies. In this case, special attention must be given to the regulatory trends triggered by Resolution # 617, which consolidated the various limited services under a unified regime, and to the impacts of future termination of the allocation and assignment of frequency bands to the different SLP modalities. This refarming began with the 4.9 GHz band and with the VHF and UHF sub-bands located between 215 and 470 MHz. Thus, future specifications are expected to define modular and flexible requirements for aerial interfaces currently under development, allowing them to be quickly adjusted to the new SLP applications.

As for the assignment of frequency bands in Brazil, one can observe from the contents of this chapter that the coordination of the radio frequency spectrum usage by services operating on a primary basis is not a simple task. To make things worse, the radio electric spectrum is a scarce public natural resource, that historically has been inefficiently provisioned. Due to the current state of spectrum saturation, several complex issues of coexistence among neighboring systems have begun to sprout up, usually caused by new co-channel systems, or systems operating in adjacent channels, with existing systems, that fail to meet the requirements needed for coexistence. For the frequency bands and systems analyzed in this chapter, the following conditions are critical for coexistence:

(a) 250 MHz band: The 225–270 MHz frequency range is prone to suffer and generate interference in narrow-band limited services operating in neighboring sub-bands, and in the sound and image broadcasting services (TV), operating in the high VHF segment, between 174 and 216 MHz (channels 7–13);

(b) 450 MHz band: The 451–458 MHz and 461–468 MHz frequency range are prone to suffer and generate interference in narrow-band limited services and auxiliary broadcasting services operating in neighboring sub-bands, and in the sound and image broadcasting services (TV), operating in the UHF segment, above 470 MHz (channels 14–59);

(c) 700 MHz band: The 698–806 MHz frequency range is prone to suffer and generate interference in narrow-band limited services and auxiliary broadcasting services operating in neighboring sub-bands, and in the sound and image broadcasting services (TV), operating in the UHF segment, between 470 and 746 MHz (channels 14–59);

(d) 1500 MHz band: New point-to-area systems using part of the 1427–1555 MHz range are not likely to suffer or generate interference in the point-to-point and point-to-area systems currently licensed for these frequencies. However, it has been proven that the new point-to-area systems operating in these segments of the spectrum and GPS systems cause strong interference between themselves.

Several opportunities exist for developing 4G and beyond technologies for radio access systems, especially for niche applications in frequency bands whose provisions have been reformulated to meet the needs of these new applications. In such cases, special attention must be paid to the air interface specifications, in order to mitigate coexistence issues with pre-established neighboring systems.

Finally, regarding the requirements for certification and approval, it can be observed that the set of standards regulating telecommunication products for their certification and approval can be grouped into three categories in terms of their compliance with new technology and the frequency bands assigned to 4G and beyond radio access systems, as follows:

(a) The requirements for electromagnetic compatibility and electrical protection are the same for all telecommunication equipment and are consolidated and consistent;
(b) The requirements for antenna approval have been updated recently and are compliant with the latest international standards and adequate for the newest broadband radio access systems;
(c) The regulatory standards for the certification and approval of base transceiver stations and access terminals, on the other hand, still need to be updated, or even created, to meet the needs of 4G systems and coexistence among systems.

References

1. Brasil (1979) Ministério das Comunicações. Norma nº 5, de 1979. Da prestação do Serviço Telefônico Público, 1979
2. Agência Nacional de Telecomunicações (ANATEL) (1998) Resolução nº 73, de 1998. Regulamento dos Serviços de Telecomunicações, nov. 1998
3. Agência Nacional de Telecomunicações (ANATEL) (1998) Resolução nº 85, de 1998. Regulamento do Serviço Telefônico Fixo Comutado, dez. 1998
4. Agência Nacional de Telecomunicações (ANATEL) (1998) Resolução nº 78, de 1998. Regulamento sobre Diretrizes para Destinação de Faixas de Freqüências para Sistemas de Acesso Fixo sem Fio, para a Prestação do STFC, dez. 1998
5. Agência Nacional de Telecomunicações (ANATEL) (1999) Resolução nº 146, de 1999. Regulamento para Certificação de Sistemas de Acesso Fixo sem Fio para a Prestação do Serviço Telefônico Fixo Comutado Destinado ao Uso do Público em Geral—STFC, jul. 1999
6. Agência Nacional de Telecomunicações (ANATEL) (1999) Resolução nº 166, de 1999. Regulamento para Utilização de Sistemas de Acesso Fixo sem Fio para a Prestação do Serviço Telefônico Fixo Comutado Destinado ao Uso do Público em Geral—STFC, jul. 1999
7. Agência Nacional de Telecomunicações (ANATEL) (2005) Resolução nº 426, de 2005. Regulamento do Serviço Telefônico Fixo Comutado—STFC, dez. 2005

8. Brasil (1996) Lei nº 9.295, de 19 de julho de 1996. Dispõe sobre os serviços de telecomunicações e sua organização, sobre o órgão regulador e dá outras providências, jul. 1996
9. Brasil (1997) Lei nº 9.472, de 16 de julho de 1997. Dispõe sobre a organização dos serviços de telecomunicações, a criação e funcionamento de um órgão regulador e outros aspectos institucionais, nos termos da Emenda Constitucional nº 8, de 1995, jul. 1997
10. Agência Nacional de Telecomunicações (ANATEL) (2000) Resolução nº 235, de 2000. Diretrizes para Implementação do Serviço Móvel Pessoal—SMP, jul. 2000
11. Agência Nacional de Telecomunicações (ANATEL) (2000) Resolução nº 245, de 2000. Regulamento do Serviço Móvel Pessoal—SMP, dez. 2000
12. Agência Nacional de Telecomunicações (ANATEL) (2000) Resolução nº 248, de 2000. Plano Geral de Autorizações do Serviço Móvel Pessoal—SMP, dez. 2000
13. Agência Nacional de Telecomunicações (ANATEL) (2010) Resolução nº 550, de 2010. Regulamento sobre Exploração de Serviço Móvel Pessoal—SMP por meio de Rede Virtual (RRVSMP), nov. 2010
14. Agência Nacional de Telecomunicações (ANATEL) (2002) Resolução nº 317, de 2002. Plano Geral de Metas de Qualidade para o Serviço Móvel Pessoal—PGMQSMP, set. 2002
15. Agência Nacional de Telecomunicações (ANATEL) (2006) Resolução nº 443, de 2006. Norma do Processo de Aferição do Grau de Satisfação da Sociedade com Relação ao Serviço Telefônico Fixo Comutado (STFC), ao Serviço Móvel Pessoal (SMP) e aos serviços de televisão por assinatura, ago. 2006
16. Agência Nacional de Telecomunicações (ANATEL) (2007) Resolução nº 477, de 2007. Regulamento do Serviço Móvel Pessoal—SMP, ago. 2007
17. Agência Nacional de Telecomunicações (ANATEL) (2002) Resolução nº 321, de 2002. Plano Geral de Autorizações do Serviço Móvel Pessoal—PGA-SMP, set. 2002
18. Agência Nacional de Telecomunicações (ANATEL) (2001) Resolução nº 272, de 2001. Regulamento do Serviço de Comunicação Multimídia, ago. 2001
19. Agência Nacional de Telecomunicações (ANATEL) (2003) Resolução nº 328, de 2003. Modelos de Termo de Autorização para Exploração do Serviço de Comunicação Multimídia, de interesse coletivo, jan. 2003
20. Agência Nacional de Telecomunicações (ANATEL) (2013) Resolução nº 614, de 2013. Regulamento do Serviço de Comunicação Multimídia e altera os Anexos I e III do Regulamento de Cobrança de Preço Público pelo Direito de Exploração de Serviços de Telecomunicações e pelo Direito de Exploração de Satélite, maio. 2013
21. Brasil (1962) Lei nº 4.117, de 27 de agosto de 1962. Institui o Código Brasileiro de Telecomunicações, ago. 1962
22. Brasil (1997) Ministério das Comunicações. Norma nº 13, de 1997. Serviço Limitado, 1997
23. Agência Nacional de Telecomunicações (ANATEL) (2013) Resolução nº 617, de 2013. Regulamento do Serviço Limitado Privado, jun. 2013
24. Agência Nacional de Telecomunicações (ANATEL) (2010) Resolução nº 555, de 2010. Regulamento sobre Canalização e Condições de Uso de Radiofrequências na Faixa de 225 MHz a 270 MHz, dez. 2010
25. Agência Nacional de Telecomunicações (ANATEL) (2010) Resolução nº 556, de 2010. Regulamento sobre Canalização e Condições de Uso de Radiofrequências na Faixa de 360 MHz a 380 MHz, dez. 2010
26. Agência Nacional de Telecomunicações (ANATEL) (2010) Resolução nº 557, de 2010. Regulamento sobre Canalização e Condições de Uso de Radiofrequências na Faixa de 380 MHz a 400 MHz, dez. 2010
27. Agência Nacional de Telecomunicações (ANATEL) (2010) Resolução nº 558, de 2010. Regulamento sobre Canalização e Condições de Uso de Radiofrequências na Faixa de 450 MHz a 470 MHz, dez. 2010
28. Brasil (1973) Ministério das Comunicações. Portaria nº 623, de 6 de setembro de 1973. Norma de canalização e condições de utilização das subfaixas entre 225 MHz e 470 MHz atribuídas aos Serviços Fixo e Móvel, Ministério das Comunicações, set. 1973

29. Agência Nacional de Telecomunicações (ANATEL) (2006) Resolução nº 446, de 2006. Regulamento sobre Condições de Uso de Radiofrequências, na Faixa de 450 MHz, pelo Serviço Limitado Privado, no Âmbito dos Aeroportos Nacionais, out. 2006
30. International Telecommunication Union—Radiocommunication Sector (ITU-R) (2008) Radio Regulations. ITU, 2008. 4v
31. Brasil (2009) Ministério das Comunicações. Portaria nº 24, de 11 de fevereiro de 2009. Norma Geral para Execução dos Serviços de Televisão Pública Digital, nº 01/2009, fev. 2009
32. Brasil (2010) Ministério das Comunicações. Portaria nº 276, de 29 de março de 2010. Norma Técnica para Execução dos Serviços de Radiodifusão de Sons e Imagens e de Retransmissão de Televisão com utilização da tecnologia digital, nº 01/2010, mar. 2010
33. Agência Nacional de Telecomunicações (ANATEL) (2012) Resolução nº 584, de 2012. Regulamento sobre Canalização e Condições de Uso de Radiofrequências para os Serviços Auxiliar de Radiodifusão e Correlatos—SARC, de Repetição de Televisão—RpTV e de Televisão em Circuito Fechado com Utilização de Radioenlace—CFTV, mar. 2012
34. Brasil (2012) Ministério das Comunicações. Portaria nº 681, de 6 de agosto de 2012. Institui o Grupo de Trabalho para estudar as condições de uso da faixa de radiofrequências de 698 MHz a 806 MHz, na forma do art. 17 da Resolução 584/12, ago. 2012
35. International Telecommunication Union—Radiocommunication Sector (ITU-R) (2012) Recommendation ITU-R M.1036-4 – Frequency arrangements for implementation of the terrestrial component of International Mobile Telecommunications (IMT) in the bands identified for IMT in the Radio Regulations (RR). ITU-R, mar. 2012
36. Agência Nacional de Telecomunicações (ANATEL) (1999) Resolução nº 198, de 1999. Regulamento sobre canalização e condições de uso da faixa de 1,5 GHz, dez. 1999
37. Agência Nacional de Telecomunicações (ANATEL) (2005) Resolução nº 391, de 2005. Regulamento sobre Condições de Uso de Radiofrequências na Faixa de 1452 MHz a 1472 MHz, jan. 2005
38. Agência Nacional de Telecomunicações (ANATEL) The SITAR System [online]. Available: http://sistemas.anatel.gov.br/apoio_sitarweb/
39. Agência Nacional de Telecomunicações (ANATEL) (2000) Resolução nº 237, de 2000. Regulamento para certificação de equipamentos de telecomunicações quanto aos aspectos de compatibilidade eletromagnética, nov. 2000
40. Agência Nacional de Telecomunicações (ANATEL) (2000) Resolução nº 238, de 2000. Regulamento para certificação de equipamentos de telecomunicações quanto aos aspectos de proteção elétrica, nov. 2000
41. Agência Nacional de Telecomunicações (ANATEL) (2006) Resolução nº 442, de 2006. Regulamento para a Certificação de Equipamentos de Telecomunicações quanto aos Aspectos de Compatibilidade Eletromagnética, jul. 2006
42. Agência Nacional de Telecomunicações (ANATEL) (2009) Resolução nº 529, de 2009. Regulamento para Certificação de Equipamentos de Telecomunicações quanto aos Aspectos de Segurança Elétrica, jun. 2009
43. Agência Nacional de Telecomunicações (ANATEL) (2013) Requisitos Técnicos e Procedimentos de Ensaios Aplicáveis à Certificação de Produtos para Telecomunicação de Categoria I, 16 de abril de 2013
44. Agência Nacional de Telecomunicações (ANATEL) (2013) Requisitos Técnicos e Procedimentos de Ensaios Aplicáveis à Certificação de Produtos para Telecomunicação de Categoria II, 17 de abril de 2013
45. Agência Nacional de Telecomunicações (ANATEL) (2015) Requisitos Técnicos e Procedimentos de Ensaios Aplicáveis à Certificação de Produtos para Telecomunicação de Categoria I, 1 de junho de 2015
46. Agência Nacional de Telecomunicações (ANATEL) (2015) Requisitos Técnicos e Procedimentos de Ensaios Aplicáveis à Certificação de Produtos para Telecomunicação de Categoria II, 17 de abril de 2015

47. Agência Nacional de Telecomunicações (ANATEL) (2004) Resolução nº 361, de 2004. Norma para Certificação e Homologação de Transmissores e Transceptores Monocanais Analógicos FM e PM para Operação nas Faixas de Frequências Abaixo de 1 GHz, abr. 2004
48. Agência Nacional de Telecomunicações (ANATEL) (2004) Resolução nº 368, de 2004. Norma para certificação e homologação de transmissores e transceptores digitais para o serviço fixo em aplicações ponto-multiponto nas faixas de frequências acima de 1 GHz, mai. 2004
49. Agência Nacional de Telecomunicações (ANATEL) (2006) Resolução nº 433, de 2006. Norma para certificação e homologação de transmissores e transceptores de estações rádio base e de estações repetidoras do serviço telefônico fixo comutado (STFC), mar. 2006
50. Agência Nacional de Telecomunicações (ANATEL) (2010) Resolução nº 554, de 2010. Norma para Certificação e Homologação de Transmissores e Transceptores de Estações Rádio Base e de Estações Repetidoras., dez. 2010
51. Agência Nacional de Telecomunicações (ANATEL) (2004) Resolução nº 359, de 2004. Norma para Certificação e Homologação de Transmissores e Transceptores Digitais para o Serviço Fixo em Aplicações Ponto-Multiponto nas Faixas de Frequências abaixo de 1 GHz., abr. 2004
52. Agência Nacional de Telecomunicações (ANATEL) (2008) Resolução nº 492, de 2008. Norma para Certificação e Homologação de Transmissores e Transceptores Digitais para o Serviço Fixo em Aplicações Ponto-Multiponto nas Faixas de Frequências acima de 1 GHz., fev. 2008
53. 3GPP TS 36.141 V9.8.0 (2011-06) (2011) 3rd Generation Partnership Project; Technical Specification Group Radio Access Network; Evolved Universal Terrestrial Radio Access (EUTRA); Base Station (BS) conformance testing (Release 9), jun. 2011
54. 3GPP TS 36.521-1 V9.5.0 (2011-06) (2011) 3rd Generation Partnership Project; Technical Specification Group Radio Access Network; Evolved Universal Terrestrial Radio Access (E-UTRA); User Equipment (UE) conformance specification Radio transmission and reception Part 1: Conformance Testing; (Release 9)., jun. 2011
55. Agência Nacional de Telecomunicações (ANATEL) (2004) Resolução nº 366, de 2004. Norma para Certificação e Homologação de Antenas Lineares, mai. 2004
56. Agência Nacional de Telecomunicações (ANATEL) (2004) Resolução nº 372, de 2004. Norma para certificação e homologação de antenas setoriais e omnidirecionais, mai. 2004
57. Agência Nacional de Telecomunicações (ANATEL) (2013) Resolução nº 609, de 2013. Norma para Certificação e Homologação de Antenas para Uso em Aplicações Ponto-a-Ponto, abr. 2013
58. Agência Nacional de Telecomunicações (ANATEL) (2013) Resolução nº 609, 610, de 2013. Norma para Certificação e Homologação de Antenas para Uso em Aplicações Ponto-Área Bidirecionais, abr. 2013

Dual-Polarized Crossed Dipole Antenna Array for LTE Base Station

Diogo Carvalho de Souza e Silva and Cristiano Borges de Paula

Abstract This chapter presents a dual-polarized antenna array solution for LTE base station applications. The antenna array operates in the frequency band of 450 MHz and it is intended to provide broadband access to suburban, rural, and remote areas. The proposed array is composed of four dual-polarized crossed dipoles placed a quarter-wavelength above a reflector. The antenna operates with ±45° slanted polarization diversity with a horizontal beamwidth of 65°. The main advantages are the use of expanded metal in the reflector and individual radomes per element, which reduces the weight and wind load of the antenna. These advantages, aligned with fully integrated solutions for the structure and low-cost materials, make it an attractive solution for base station antennas.

1 Introduction

From 2012 to 2015, CPqD Foundation was responsible for the project of an integrated solution to provide broadband access to suburban, rural, and remote areas [1]. The proposed solution is based on Long Term Evolution (LTE) technology and operates in the frequency range of 450–470 MHz, which was recently added to LTE Standard with the technical support of CPqD and other companies [2]. The project comprises the development of an Evolved Node B (eNodeB), a User

D.C. de Souza e Silva (✉) · C.B. de Paula
CPqD Foundation, Campinas, SP, Brazil
e-mail: diogos@cpqd.com.br

C.B. de Paula
e-mail: cborges@cpqd.com.br

A. Paradisi et al. (eds.), *Long Term Evolution*, Telecommunications and Information Technology, DOI 10.1007/978-3-319-23823-4_3

Equipment (UE), an Evolved Packet Core (EPC), and directive antennas for LTE network infrastructure. In the context of this project, a directional antenna was developed for installation in the eNodeB. The most suitable antenna for this application is the sector panel antenna, which presents directive radiation pattern in the vertical plane and sectorial radiation pattern in the horizontal plane. This characteristic allows to divide the cell site coverage into sectors, depending on the horizontal beamwidth of the antenna, in which the most used beamwidth sector in a three-sector cell is 65° as shown in [3].

In this chapter, a ±45º slant-polarized antenna array operating at 450 MHz band is proposed, which has as main differentials low values of weight, cost, and wind load. Low weight and wind load reduce the structural requirements of the tower and have a significant impact on the overall installation cost. The ±45º slanted polarization is used as antenna diversity to mitigate the multipath effects on radio channel. Polarization diversity is widely used nowadays due to the possibility of reducing the space and installation cost as compared to spatial diversity [4]. The ±45º slanted polarization offers some benefits due to the symmetry of the antenna that result in equal radiation patterns for each polarization. Furthermore, the results of field trials are slightly better for ±45º than H/V polarization as shown in [5, 6].

The chapter is organized as follows. Sect. 2 describes the proposed radiating element, the employed materials, and the main results. In this section the simplification adopted in the model of the radiating element that ensures faster simulations and lower memory consumption is also included. Sect. 3 shows the proposed four-element array, including the corporate feed network that provides the necessary current for each element to synthesize the desired radiation pattern in the broadside direction. The radiation pattern in the main planes and the scattering parameters for each port are also shown in this section. Finally, the conclusions and considerations of the antenna array are offered in Sect. 4. The main requirements of this project are summarized in Table 1.

Table 1 Antenna specifications

Parameter	Value
Frequency range	450–470 MHz
VSWR	<2:1
Port-to-port isolation	>20 dB
Impedance	50 Ω
Gain	14 dBi
Polarization	±45°
Half power beamwidth in H-plane[a]	65°
Half power beamwidth in V-plane[a]	<25°
Front-to-back ratio	>25°dB

[a]The radiation pattern must be in accordance with Anatel Resolution 610/2013 [7]

2 Radiating Elements

The radiating elements of a ±45º slant-polarized antenna array are usually made of patch antennas, crossed dipoles, or square dipole arrays. The crossed dipole structure is the most used and sometimes approximates to bow-tie dipoles or corner-driven square loops. The elements are usually composed of printed circuits or metallic pieces, e.g., wires, tubes, or planar sheets [4]. The proposed element is a crossed half-wavelength dipole constructed with aluminum round tubes. The crossed dipole consists of two dipoles placed perpendicular to each other. Additionally, the crossed dipole is placed a quarter-wavelength above the reflector and their arms are supported by tubular posts. The junction between the arm and the post defines a unique tubular structure and it can be obtained by soldering the extremities of two tubes cut in 45º angle. In addition, each one of the dipoles is fed by a quarter-wave coaxial balun.

The balun has two functions: (1) convert unbalanced signal into balanced signal at the terminals of the dipole; (2) transform the dipole input impedance into a desired impedance. The proposed λ/4 coaxial balun is divided into two parts and it integrates fully to the tubular structure. The first part is the coaxial structure formed by supporting posts and their inner conductor. The second part is the Γ-shaped probe formed by an aluminum sheet bent and two screws. Since the structure has two dipoles placed perpendicularly, the two probes must be mirrored to each other, in order to avoid mechanical intersections. The probe width is a half diameter of the tubular structure. One post has in its interior a copper wire creating a coaxial line and it is called main post. The other post has no inner conductor and it is called stub post. The Γ-shaped probe is supported slightly above the dipoles and provides electrical contact between the inner conductor of the main post and the stub post. Connections between the main post and the probe are prohibited. For this reason, it requires a non-metallic piece to support the probe and isolate the inner conductor. In contrast, it is necessary to fix a metal piece to the stub post. The short circuit among posts, at the reflector plane, completes the λ/4 balun topology. The input N-type connector is placed at the base of the main post. The center pin is connected to the inner conductor and the connector body is attached to the reflector structure. An individual radome, covering the balun structure, is utilized to avoid accumulation of water, which would results in changes in the material properties and, consequently, impedance mismatch. For the same reason, the extremities of the dipoles are covered and sealed. The proposed dipole structure is detailed in Fig. 1 in a cut view. In this representation, only one of the dipoles is shown, while the other one is omitted in order to clarify the visualization of the structure. In Fig. 2 it is shown a closely viewed of the crossed dipole, where it is possible to see the two Γ-shaped probes mirrored.

To implement the coaxial balun, the height of the supporting posts assumes values equal to λ/4 and it was optimized to be 171.27 mm. The separation among these posts is defined as the shortest distance between the outer diameter of them and it was designed to be approximately λ/20, which results in 30 mm. The dipole

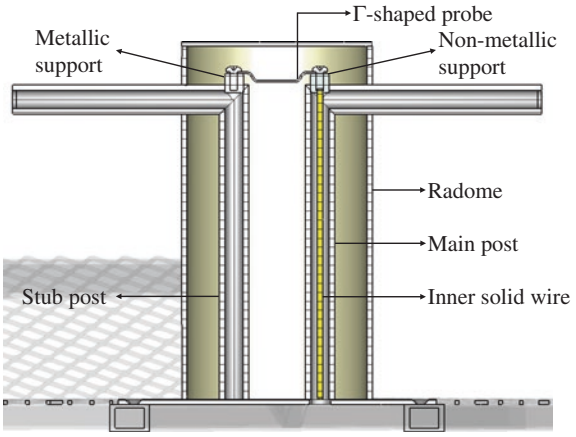

Fig. 1 Cut view of the dipole structure

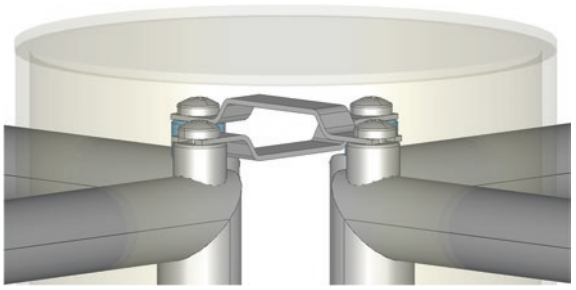

Fig. 2 Close view of the Γ-shaped probes

length is designed to be λ/2 and optimized to get a real impedance at their input terminals. Therefore, each arm has the length optimized for 126.06 mm. Note that one of the extremities is cut in 45° angle and the length is measured on the larger side. All dimensions mentioned above are designed for the center frequency of 460 MHz. The completely tubular structure was designed with a 5/8″ aluminum round tube. This tube has the inner diameter of 9.87 mm and outer diameter of 15.87 mm. It is known that the outer diameter is related to the input impedance stability of the dipole [8]. Accordingly, the outer diameter is proportional to the frequency bandwidth and it was selected to ensure the impedance matching at the frequency range of 450–470 MHz. Besides, the wall thickness was chosen to facilitate junction among the tubes.

The optimized length of the dipole provides a real impedance of around 110 Ω at a reference plane on the top of balun structure. The desired impedance at the input connector is equal to 50 Ω. The impedance matching can be achieved by adjusting the characteristic impedance of the coaxial line. This characteristic impedance is obtained from the square root of the product of these impedances and results in approximately 74 Ω. The characteristic impedance of a coax line depends on the diameter of the conductors and the dielectric permittivity of the

medium. The diameter of the outer conductor is equal to 9.87 mm and it is delimited by the inner diameter of the tube. Considering that the structure is filled with air, the diameter of the inner conductor is determined as being 2.87 mm [9]. This diameter can be approximated to 2.9 mm (AWG 9) and it is possible to use a solid bare copper wire. The individual radome intended to protect the feed structure from the weather conditions is a plastic PVC pipe covered on the top with a cap of the same material. The arms of the dipoles are exteriorized from the radome through four holes punched on the plastic body. The pipe has an inner diameter equal to 96 mm and an outer diameter equal to 101.6 mm. The height of the radome is equal to 190 mm measured from the base of the reflector. The dimensions of the crossed dipoles are shown in Fig. 3.

A crossed dipole above a plane reflector provides a horizontal beamwidth of around 90°. The beamwidth of 65º can be obtained using bent reflectors. The bent reflector is divided into three parts: one plane part and two side tabs bent in angle. Thus, there are three different variables to adjust the beamwidth: the width of the plane part, the width of the bent parts, and the angle among them. Considering the angle among the parts as 135º, the widths are optimized to be equal to 455 and 110 mm, for the plane part and the bent parts, respectively. It results in a reflector with an overall width of 610 mm and depth of 77 mm. The reflector height of the one-element antenna is designed to be approximately 3λ/4, which results in 500 mm. To provide mechanical resistance to structure, the reflector is mounted on a frame built with square tubes. The reflector was designed using an expanded metal instead of a sheet metal, with the purpose to reduce the weight and the wind load of the structure. As a reference, Part Number F25X12A of the manufacturer Telas Nova Era® was selected in this project [10]. The expanded metal is made of

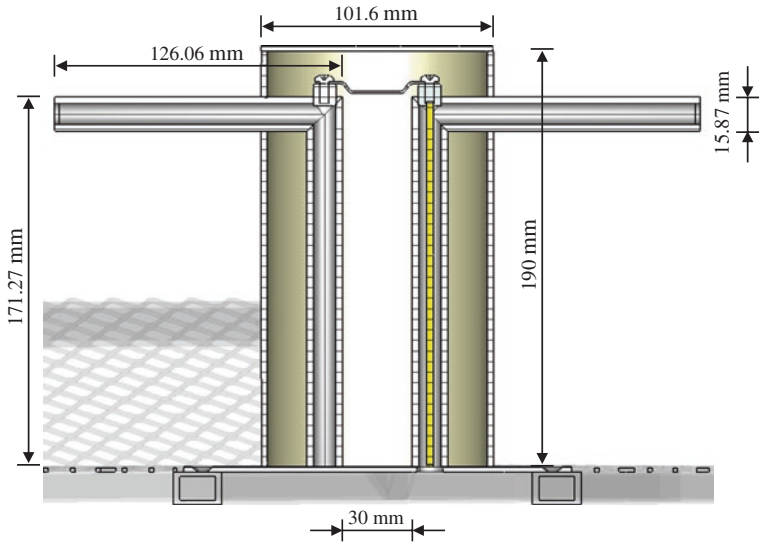

Fig. 3 Crossed dipole dimensions

aluminum and it has a nominal open area around of 77 %. This open area reduces the reflector weight to 23 %, as compared to the sheet metal of the same material. The dimensions of the reflector are shown in Fig. 4.

The radiating elements described above were analyzed by full-wave commercial software MWS CST® [11]. The frequency range of analysis was from 370 to 570 MHz and the simulations were performed using the frequency domain solver. The antenna ports were excited by waveguide ports and the ports #1 and #2 are related to the −45° and +45° polarization, respectively. Besides, it was observed that the complexity of the expanded metal employed on the reflector has a great impact on the simulation time and the memory usage of the workstation. For comparison purposes, the simulation time was 35 min for sheet and 66 min for the expanded metal. Furthermore, the memory usage was 4.5 GB for the sheet and 8.5 GB for the expanded metal. The hardware setup for the simulation consisted of a Dell workstation with an Intel® Xeon® CPU X5650 2.67 GHz; 48 GB of RAM; operational system MS Windows7 Professional. In a worst case, considering the four-element array and the reflector built with expanded metal, the memory usage reaches the total available memory on the workstation, making the analysis impossible. Thus, it was necessary to simplify the electromagnetic model to render the array

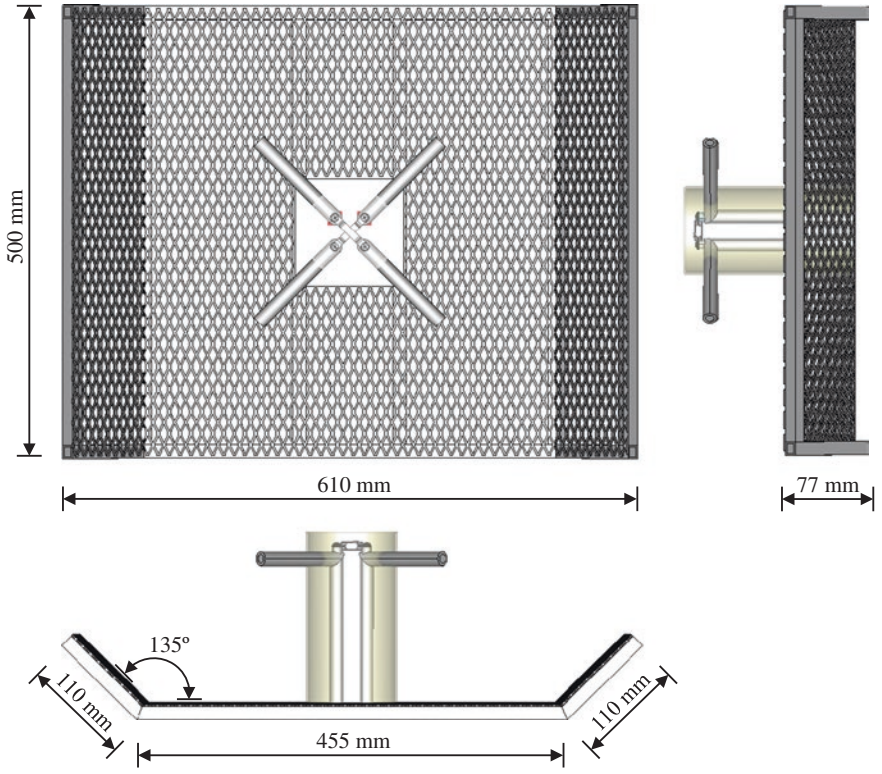

Fig. 4 Reflector dimensions

analysis feasible. To evaluate the impact of the usage of a sheet metal instead of expanded metal on the electrical characteristics of the antenna array, the results were compared against each other. Despite this, it is important to note that it is just a simplification of the electromagnetic model and does not change the proposed structure.

The simulated results of the magnitude of the scattering parameters at the input of the antennas are shown in Fig. 5. From the reflection coefficients, S11 and S22, it is possible to note that the elements can operate in a frequency range from 410 to 540 MHz, considering the threshold of −10 dB. The slight difference between S11 and S22 is due to the fact of that the Γ-shaped probes were mirrored in the dipoles. In addition, the isolation between the port #1 and #2 is higher than 30 dB in all the frequency range. All scattering parameters are normalized to 50 Ω. In Fig. 6 the radiation pattern for the main and cross polarizations, calculated in the horizontal plane and at the center frequency of 460 MHz, is shown. In the same way, the radiation pattern in the vertical plane is shown in Fig. 7. The half power beamwidth is equal to 65° and 77° for the horizontal and vertical planes, respectively. The gain is 8.15 dBi on the broadside direction. According to what is observed, there is an excellent agreement between the simulated results given for the reflector using a sheet and expanded metal. This result was expected since, a solid ground plane can be simulated, especially at low frequencies, by a metal mesh with openings lower than 1/10 of the wavelength [8]. In comparison, the larger opening of the expanded metal is equal to 25 mm that represents only 4/100 of the wavelength at the center frequency of 460 MHz. The major difference is noted for the front-to-back ratio that is equal to −44 and −40 dB for the sheet and expanded metal reflectors, respectively. This difference can be disregarded since that both scenarios meet the requirements of front-to-back ratio higher than 25 dB.

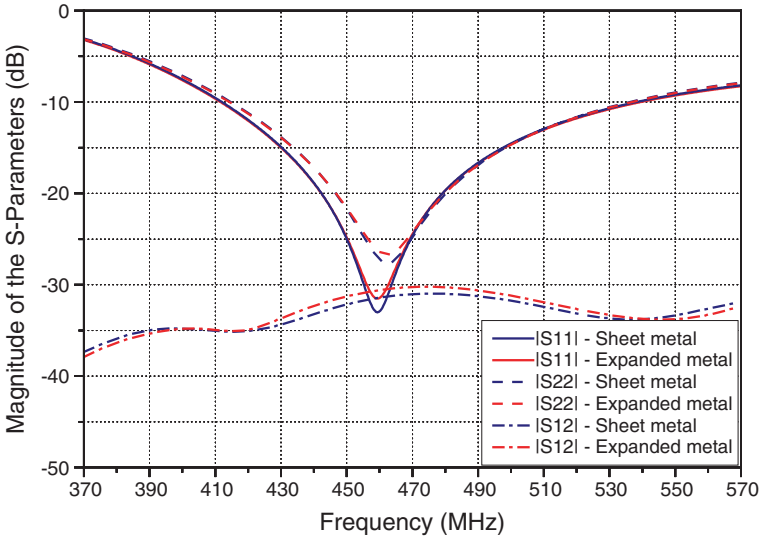

Fig. 5 Magnitude of the S-parameters, in logarithmic scale, of the radiating element

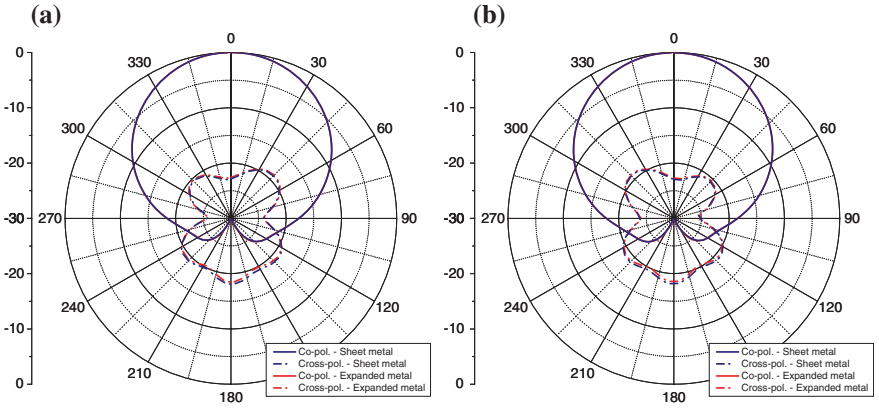

Fig. 6 Co-polar and cross-polar radiation pattern in the horizontal plane at 460 MHz. **a** Port #1/−45° polarization. **b** Port #2/+45° polarization

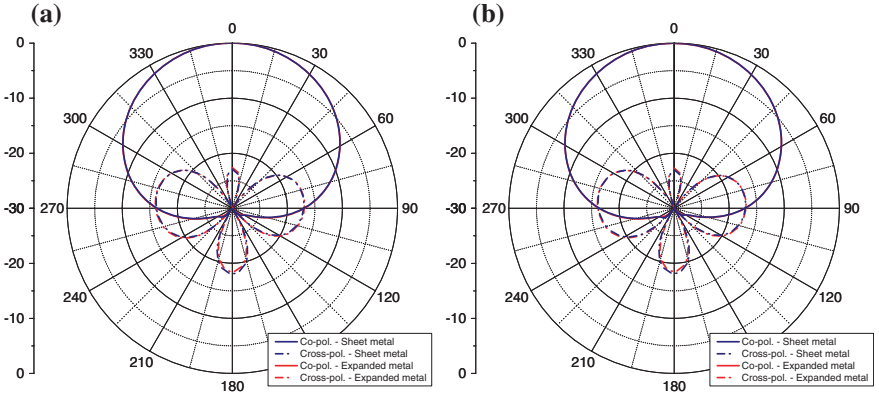

Fig. 7 Co-polar and cross-polar radiation pattern in the vertical plane at 460 MHz. **a** Port #1/−45° polarization. **b** Port #2/+45° polarization

3 Antenna Array

The radiating elements are vertically arranged, forming a linear array, in order to provide the required gain. The vertical arrangement is the most suitable because it increases the gain and does not change the horizontal beamwidth, which defines the cell sector. This gain is achieved by focusing the energy in the vertical plane, i.e., narrowing the vertical beamwidth [4]. The array is composed of four radiating elements spaced from $3\lambda/4$, what represents 490 mm at the center frequency of 460 MHz. To assess the impact of the simplified model on the final electric characteristics of the array, a preliminary analysis of the array considering just two radiating elements was performed. The major purpose of this analysis is to

evaluate the behavior of the port-to-port isolation, and in a special way, the isolation between ports that operates at the same polarization. The isolation between elements that operate at same polarization could not be performed in Sect. 2, and it is fundamental to validate the simplified model for the electromagnetic analysis of the array. The ports related to the $-45°$ polarization are numbered with odd numbers. The ports related to the $+45°$ polarization are numbered with even numbers. Thus, the first radiating element is composed of the ports #1 and #2 and the second radiating element is composed of the ports #3 and #4.

The simulated results from the magnitude of the port-to-port isolation at the input of the antennas are shown in Fig. 8. To clarify the visualization of the results, the port #1 was taken as the reference and the isolations were computed from it. Due to the reciprocity of the structure, the other results were omitted from this graph. The isolation between the ports at same polarization is defined as the negative of the magnitude of |S13| and it is higher than 20 dB in all the frequency range. The magnitude of |S14| relates to the isolation between ports with different polarizations and spaced from $3\lambda/4$. Finally, the magnitude of |S12| relates to the isolation between ports of the same radiating element. Once again, there is an excellent agreement between the simulated results, which demonstrates that the simplified model is suitable for analysis of the four-element array. For comparison purposes, the simulation time was 60 min for the sheet and 135 min for the expanded metal. Furthermore, the memory usage was 8.5 GB for the sheet and 17.5 GB for the expanded metal.

The final model of the antenna array, composed of four radiating elements, is shown in Fig. 9. Due to the limited capacity of memory, the analysis of this array built with expanded metal was not feasible. Thus, it was needed to adopt the

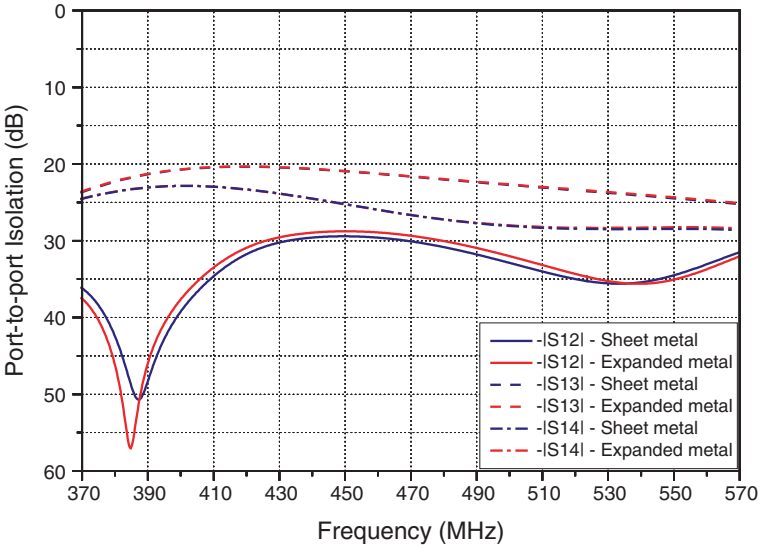

Fig. 8 Magnitude of the port-to-port isolation in logarithmic scale

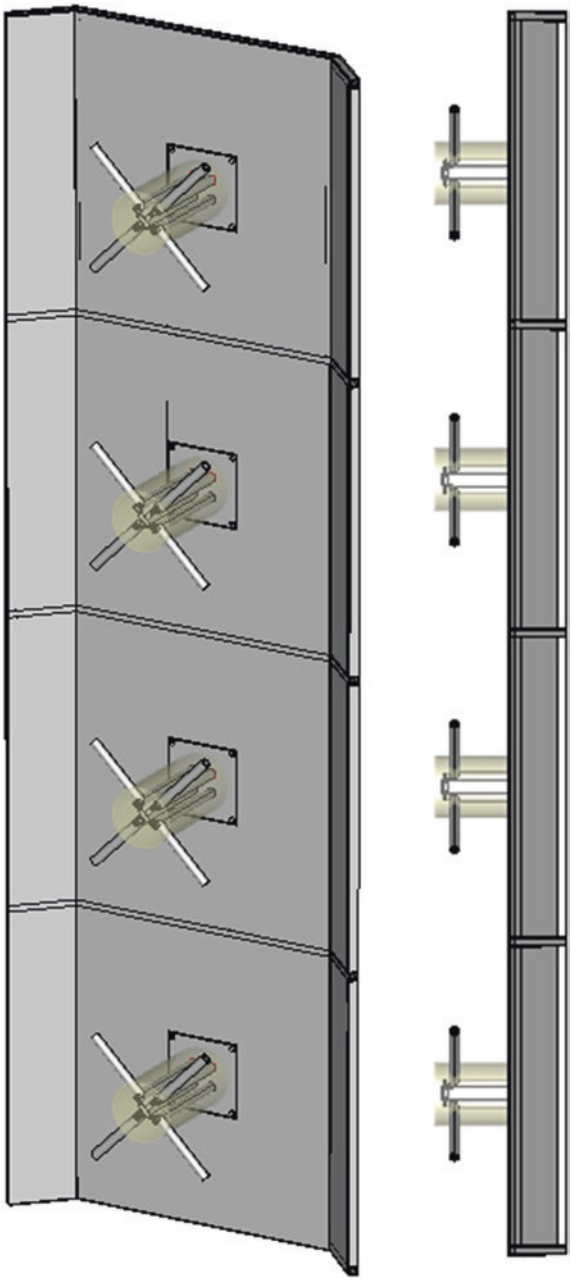

Fig. 9 Antenna array composed of four radiating elements

simplified model, which replaces the expanded metal by a sheet metal. The reflector of the four-element array has 610 mm in width, 1960 mm in height, and 77 mm in depth. As the radome height is higher than the reflector depth, the overall depth of the antenna array is equal to radome height, i.e., 190 mm. The ports of same

polarization are combined into a single connector by a corporate feed network constructed with coaxial cables. Thereby, the connector #1 relates to the −45º polarization and the connector #2 relates to the +45° polarization. The corporate network feeds the radiating elements in parallel, splitting the power among them. To get the maximum gain oriented to broadside direction, it is needed that all the radiating elements excited with equal amplitude and phase [8].

The corporate feed network is used to feed $N = 2^n$ radiating elements, where n is the number of levels of the feed network. In this project, the number of radiating elements is four, so that the corporate feed network must have two levels. The first level divides the input power of the array into two branches. At the second level, the power in each one of these two branches is divided again into two branches, which results in four branches and each one of these branches feeds one radiating element. In the design of this network feed, it is necessary to consider both physical aspects, as the distance between the elements, and the electrical aspects, as the desired impedance at the input of the array.

The first consideration to be done is that the input of the network feed is located in the middle of the array structure. Thus, the total physical length of the corporate feed, composed of two branches, must be, at least, equal to the distance from the middle of the structure to the radiating elements. Given that the distance between elements is 490 mm, the total physical length must be, at least, 245 and 735 mm, for the nearest and farthest elements, respectively. The second consideration is that the radiating elements are matched to 50 Ω, as well as the desired input impedance of the feed network matched to 50 Ω. Thereby, it is necessary to use quarter-wavelength impedance transformers on both levels of the network, in order to match all radiating elements to a single connector. In contrast, the electrical length of each level given as λ/4 does not meet the minimum physical length of the feed. Thus, λ is added to the length to repeat the impedance of the elements, before the impedance transformation. The resulting electrical length for each level is equal to 450°.

In this quarter-wavelength transformers coaxial lines with a characteristic impedance of 75 Ω were employed. Ideally, at the second level of the network, each of the four branches transforms the impedance of the elements, 50 Ω, into an impedance equal to 112.5 Ω. The 112.5-Ω impedances are connected in parallel, two by two, which results in two impedances of 56.25 Ω. At the first level of the network, each of the two branches transforms the 56.25 Ω impedance into an impedance equal to 100 Ω. The 100-Ω impedances are connected in parallel, which results in 50 Ω at the input of the corporate feed network. Additionally, a 50-Ω coaxial line can be connected to the input of the feed to relocate the array input connector.

To analyze and optimize the proposed feed network, the Keysight ADS® circuit simulator was employed [12]. The simulated results from the scattering parameters were exported from the CST® to ADS® by a Touchstone file. The optimized electrical lengths of the branches are 439° and 422°, for the first and second levels, respectively. In addition, Part Number C291 360 000, from the manufacturer Radiall® [13], for the 75-Ω coaxial lines was selected. This part number relates to an RG59 coaxial cable and has a velocity of propagation equal to 66 %. Thereby,

the physical lengths of the cables are 525 and 504 mm, for the first and second levels, respectively. The simulated corporate feed network, using coaxial line models from the ADS, is shown in Fig. 10. In this simulation a 50-Ω coaxial cable with 100 mm in length to relocate the array input connector was considered. As a reference, Part Number C291 305 000, from the manufacturer Radiall®, can be used for the 50-Ω coaxial cable. The results from this analysis are shown in Fig. 11. From the reflection coefficients, S11 and S22, it is possible to note that both polarization systems can operate in a frequency range from 420 to 520 MHz, considering the threshold of −10 dB. Once again, the slight difference between S11 and S22 is due to the fact that the Γ-shaped probes were mirrored in the dipoles. Also, the isolation between the systems is 20 dB in all the frequency range. It is also

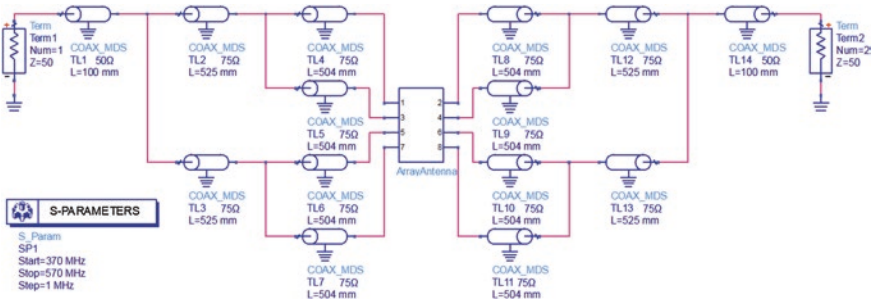

Fig. 10 Corporate feed network simulation on ADS

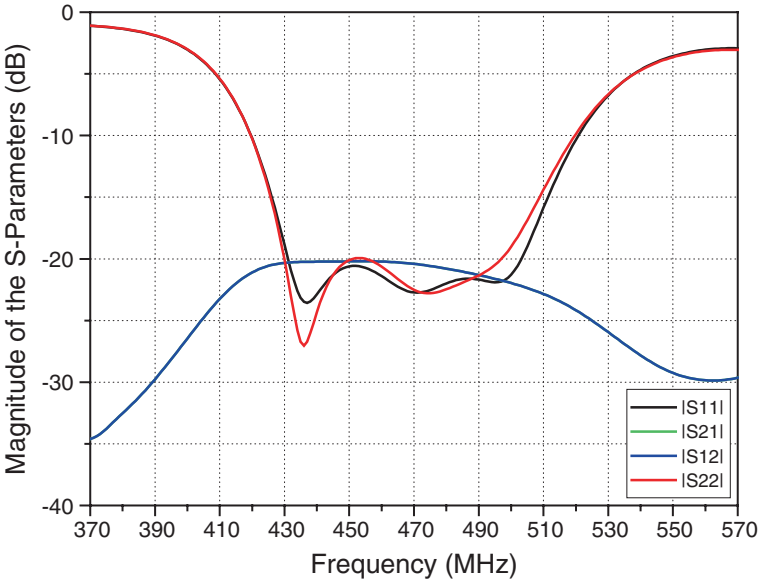

Fig. 11 Magnitude of the S-parameters, in logarithmic scale, of the antenna array

important to point out that the attenuation of the cables is 0.47 and 0.3 dB/m for the RG58 and RG59, respectively. These attenuations result in an insertion loss of around 0.35 dB for the feed network. Considering possible losses in the coaxial junctions, the insertion loss can be approximated to 0.5 dB.

The simulated results from the radiation pattern of the array are calculated using a post-processing tool that combines the far-field results, given weighted excitation for each element. For the −45° polarization, the radiation pattern is obtained by exciting the elements #1, #3, #5, and #7 with equal amplitude and phase. For the +45° polarization, the radiation pattern is obtained by exciting the elements #2, #4, #6, and #8 with equal amplitude and phase. In Fig. 12 the radiation pattern for the main and cross polarizations, calculated in the horizontal plane and at the center frequency of 460 MHz, is shown. In the same way, the radiation pattern in the vertical plane is shown in Fig. 13. The half power beamwidth is equal to 68° and 17° for the horizontal and vertical planes, respectively. The gain of the radiating elements, disregarding the feed network losses, is 14.5 dBi on the broadside direction and the front-to-back ratio higher than 38 dB. Since the insertion loss of the feed network is estimated as 0.5 dB, the total gain can be approximated to 14 dBi. Besides, the calculated gain deviates less than ±0.1 dB in all 450 MHz bands. The horizontal half power beamwidth deviates less than ±0.8° in the same band. These variations are in accordance with Anatel Resolution 610/2013, which specifies a tolerance of ±1 dB for the gain and ±10 % for the beamwidth [7]. To assess if the antenna array meets the specification of the normalized radiation pattern envelope, the radiation pattern of the −45° polarization is shown in Fig. 14, in Cartesian coordinates, for both horizontal and vertical planes.

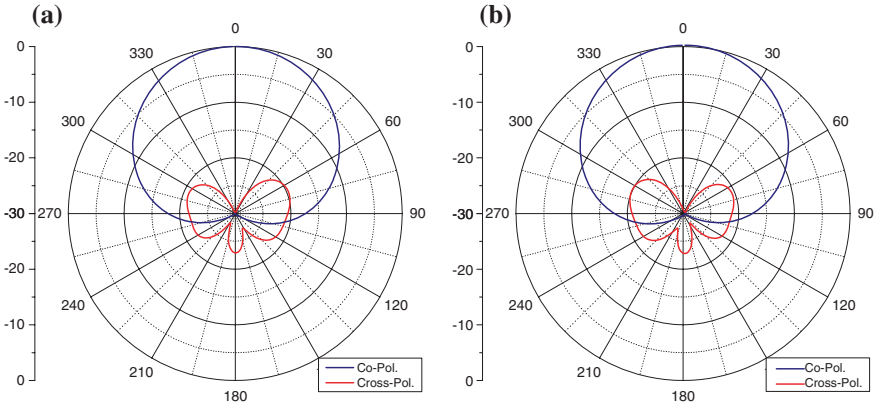

Fig. 12 Co-polar and cross-polar radiation pattern in the horizontal plane at 460 MHz. **a** Port #1/−45° polarization. **b** Port #2/+45° polarization

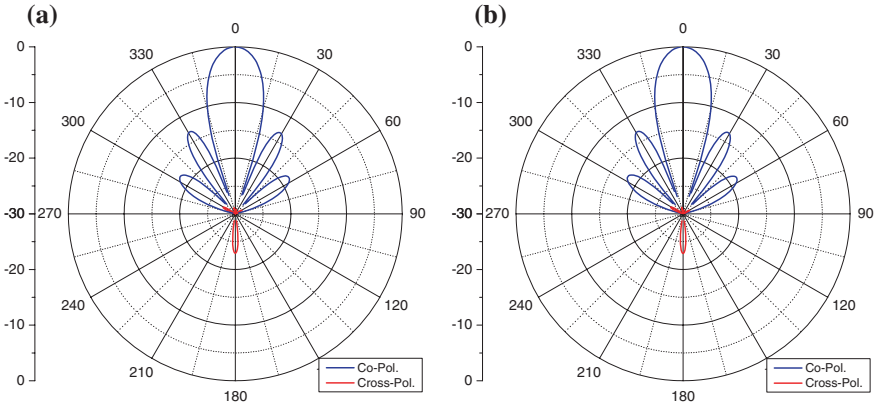

Fig. 13 Co-polar and cross-polar radiation pattern in the vertical plane at 460 MHz. **a** Port #1/−45° polarization. **b** Port #2/+45° polarization

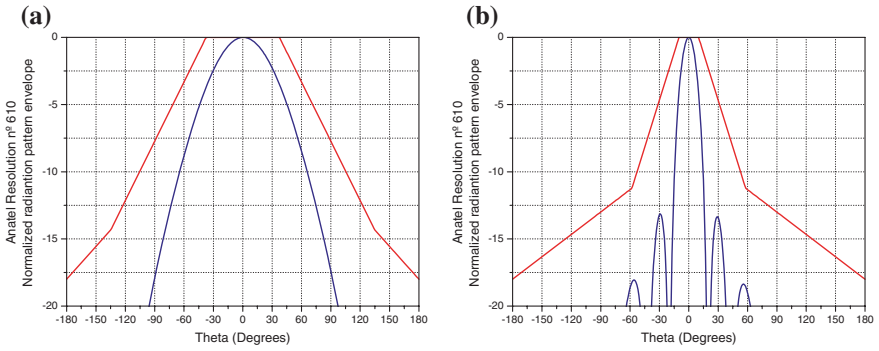

Fig. 14 Anatel Resolution N° 610—Normalized radiation pattern envelope at 460 MHz—Port #1. **a** Horizontal plane. **b** Vertical plane [7]

4 Conclusions

In summary, a dual-polarized antenna array solution for base station applications was presented. The use of round tubes, combined with a fully integrated quarter-wavelength balun, in the structure of the crossed dipoles demonstrated to be a suitable choice for the radiating elements, providing a fractional bandwidth of around 27 % for a single radiating element. The usage of coaxial cables of standard impedances in the feed network proved to be a cheap and easy-mount solution, allowing the antenna array to operate in the frequency range from 420 to 520 MHz with VSWR lower than 2:1 for both polarizations. Furthermore, the port-to-port isolation obtained for this array is equal to 20 dB in all the bandwidth. The desired

beamwidth was achieved through the usage of a bent reflector, which provides a horizontal beamwidth of around 68° for both polarizations. The antenna gain of 14 dBi in the broadside direction was possible due to the vertical arrangement of radiating elements on the array. Moreover, the employment of the expanded metal in the reflector proved to be a solution to reduce the weight and wind load of the antenna, providing a front-to-back ratio higher than 38 dB without disturbing the synthesized radiation pattern of the array. Finally, the antenna array is in accordance with the Anatel standard for certification and homologation, which make it a possible solution for a further commercial product.

Acknowledgments This material is based upon work supported by FUNTTEL/FINEP under Grants 01.12.0481.00. The author would like to thank Gustavo M. Contin for the support with the mechanical modeling of the antenna.

References

1. CPqD (2015) LTE 450 MHz: a solution for universalizing broadband access in rural and suburban areas (Online). Available http://www.cpqd.com.br/cpqd_en/index323f.html?option=com_content&view=article&id=4280:lte-450-mhz-a-solution-for-universalizing-broadband-access-in-rural-and-suburban-areas&catid=70:rad-e-inovation-&Itemid=118. Accessed 27 May 2015
2. Itunews.itu.int (2015) LTE 450 MHz technology for broadband services in rural and remote areas case study of Brazil—Academia—Innovating for society (Online). Available https://itunews.itu.int/en/4618-LTE-450MHz-technology-for-broadband-services-in-rural-and-remote-areas-BR-Case-study-of-Brazil.note.aspx. Accessed 27 May 2015
3. 3GPP TR 36.942 (2014) Technical specification, radio frequency (RF) system scenarios (release 9), 3rd Generation Partnership Project Std., 12.0.0, (2014/10/03)
4. Chen Z, Luk K (2009) Antennas for base stations in wireless communications. McGraw-Hill, New York
5. Laiho-Steffens J, Lempiainen J (1997) Impact of the mobile antenna inclination on the polarisation diversity gain in a DCS 1800 network. In: Proceedings of 8th international symposium on personal, indoor and mobile radio communications—PIMRC '97
6. Laiho-Steffens J, Lempiainen J, Salmenkaita M, Siltaniemi J, Jukarainen O (1998) Experimental evaluation of polarisation diversity gain at the base station end in a GSM900 network. In: 48th IEEE vehicular technology conference, VTC '98. Pathway to global wireless revolution (Cat. No. 98CH36151)
7. Anatel Resolution 610/2013 Standard for certification and homologation of antennas for bidirectional point-to-multipoint applications (2013-04-18) (in Portuguese)
8. Balanis C (2005) Antenna theory. Wiley Interscience, Hoboken
9. Wadell B (1991) Transmission line design handbook. Artech House, Boston
10. Telasnovaera.com.br (2015) Telas Nova Era (Online). Available http://www.telasnovaera.com.br/chapas.php. Accessed 27 May 2015 (in Portuguese)
11. CST (2015) CST—computer simulation technology (Online). Available http://www.cst.com/. Accessed 27 May 2015
12. Keysight Technologies (2015) Advanced design system (ADS) (Online). Available http://www.keysight.com/pt/pc-1297113/advanced-design-system-ads?nid=-34346.0.00&cc=BR&lc=por&cmpid=zzfindeesof-ads. Accessed 27 May 2015
13. Radiall.com, Radiall—Innovator of interconnect components and more. Disponível em http://www.radiall.com/. Acesso em: 27 maio. 2015

Evaluation of the LTE 450 MHz System Performance with Different Terminal Antennas

Juliano João Bazzo and Paulo Cardieri

Abstract The proper choice of the radiation characteristics of antennas used in LTE terminal is of vital importance, requiring a judicious analysis with appropriate tools to evaluate system performance. This chapter evaluates the 450 MHz LTE system performance with different terminal antennas. The evaluation environment is carefully configured in a system-based simulator, which takes into account the ANATEL and 3GPP standards, and the characteristics of commercial antennas and the geographical distribution of terminals in rural areas. Results show that the use of directional antennas can improve cell throughput from 14 % to 90 % compared to the use of omnidirectional antennas. Moreover, terminal throughput at the edge of the cell is improved by up to 10 times using directional antennas with the same gain as that of omnidirectional antennas.

1 Introduction

Long Term Evolution (LTE) technology has been intensely developed and standardized in several different versions, with the intention of substituting the 2G and 3G cell systems currently deployed worldwide. In densely populated areas,

J.J. Bazzo (✉) · P. Cardieri
CPqD Foundation, State University of Campinas—UNICAMP, Campinas/SP, Brazil
e-mail: jbazzo@cpqd.com.br

P. Cardieri
e-mail: cardieri@decom.fee.unicamp.br

A. Paradisi et al. (eds.), *Long Term Evolution*, Telecommunications and Information Technology, DOI 10.1007/978-3-319-23823-4_4

the 700 MHz and 2.5 GHz frequency ranges are the most common choice. The last one, auctioned in Brazil in 2012, is already in use in Europe. 3GPP (Third Generation Partnership Project) standardization of LTE for the 450 MHz range is already in an advanced stage, and band 31 has been part of this standard since July 2013, with the ratification of the proposal presented in May of the same year [1].

The success of this system, in any of the frequency ranges mentioned, is based on the access network's planning capability and the availability of simulation tools to evaluate network performance—particularly in the case of the 450 MHz frequency range, where the ability to service extensive areas is one of the main challenges. Such capability is particularly critical when it comes to the wireless interface, in which performance-limiting factors, like propagation and the characteristics of the technology employed, constitute the greatest bottlenecks for the access network's capacity. It is therefore necessary to create an appropriate evaluation methodology that allows variation of the system parameters and generates statistical results for diverse scenarios.

Relevant factors for the construction of these scenarios include density and type of distribution of the terminals in the coverage area, the characteristics of the traffic associated with the services, and how available user plan data transmission resources are allocated in the aerial interface. The results presented in this chapter are based on evaluation scenarios built to take into account such factors.

Unlike other publications that present results focusing on the urban scenario, characterized by user mobility or high building density, [2–4], this chapter explores the preferred scenario for LTE technology operating in the 450 MHz range in Brazil. This scenario is typically characterized by the absence of mobility, low building density, extensive coverage areas and, because of current frequency spectrum regulations, scarce opportunities for frequency reuse.

Because of the requirement to provide coverage in the range of dozens of kilometers, described in the next section, it is expected that, based on the propagation characteristics of Ultra High Frequency (UHF) range frequencies in rural environments, especially in the case of terminals located toward the edge of the cell be connected by directive antennas with a gain superior to that of antennas incorporated in mobile terminals. Therefore, as will be demonstrated throughout the text, the adequate selection of the radiation characteristics for antennas used in the terminals is of vital importance, which creates the need for a thorough analysis, using the appropriate tools, and fed by a set of parameters able to represent the rural broadband scenario.

This chapter is structured as follows: Sect. 2 presents a summary of the introduction of the 450 MHz range in the LTE standard, its regulations and forms of utilization in Brazil. Sect. 3 describes the evaluation scenarios and the parameters characterizing them. The results achieved for these scenarios are presented and discussed in Sect. 4. Finally, the most important results are consolidated and highlighted in the Conclusion.

2 LTE 450 MHz in Brazil

2.1 Motivation

The LTE 450 MHz technological proposal aimed at bringing broadband Internet to areas served precariously or without any kind of telecommunication services at all, as in the case of rural or isolated areas. For LTE systems, this is a new application profile, operating in the 450–470 MHz band, providing more favorable propagation conditions resulting in coverage ranges typically superior to the currently standardized 3GPP profiles.

The effort to specify and develop LTE 450 MHz began with the focus on the Brazilian scenario, where the deployment of this system is expected to help fulfill the goal of providing universal broadband access to all regions of the country. These services in rural areas will be made available in expressive portions of the Brazilian territory, benefiting more than 30 million inhabitants who currently have no access to broadband services [5].

Recent initiatives of the Brazilian government to promote the National Broadband Plan (PNBL) [6] have been stimulating LTE 450 MHz as a viable alternative to meet the goals of this program in areas neglected up to this time. According to the PNBL, the application scenario of the highest priority is that of sparsely populated rural areas, since they present the lowest percentages of homes with broadband Internet access. Data from the National Home Sample Research (PNAD), conducted by Brazilian National Geographic Statistics Bureau (IBGE), in 2008, and by Applied Economic Research Bureau (IPEA), in 2010, discloses that only 5.5 % of homes located in the Brazilian southeastern rural region have broadband access. Still according to IBGE, the average number of homes per km^2 in rural areas is 3.75.

In rural areas without access to any kind of service, the advent of LTE 450 MHz is most likely the only alternative for providing data and voice services to their inhabitants.

With this purpose in mind, the Brazilian government recently created policies to make viable the use of the 450 MHz spectrum, prioritizing rural area services, as described below.

2.2 Regulatory Aspects

In 2012, the government auctioned the operating licenses, based on ANATEL Resolution 558 [7]. This resolution, besides defining frequency ranges and sub-ranges, established the attributions for Personal Mobile Services (PMS) and other services, including Multimedia Communication Services (MCS) and Public Switched Telephone Network (PSTN) in the same sub-ranges, creating room for the use of mobile, fixed, or nomadic user terminals.

Table 1 Requirements of the 4G auction notice for systems operating in the 450 MHz range in Brazil [8]

Time frame	% of counties covered	Rate (download)	Rate (upload) (kbps)
6/30/2014	30	256 kbps	128
12/31/2014	60	256 kbps	128
12/31/2015	100	256 kbps	128
12/31/2017	100	1 Mbps	256

The auction laid a number of obligations on the winning operators, linking the 2.5 GHz range, 3GPP band 7, acquisitions those in the 450 MHz range, 3GPP band 31. Besides providing voice services to the cities, goals were defined for the rendering of retail data services, and services to rural schools (data) and cities with less than 30,000 inhabitants prioritized. Table 1 shows the minimum transmission rates and the percentage of cities to be covered by 2017, as required by the government auction notice, which also established as criteria the coverage of at least 80 % of the area comprised within a 30 km radius, measured out from the boundary of the county seat.

Based on this information, on IBGE statistics, as well as on the results of a study carried out in Brazil [9] calculating broadband Internet occupancy rate at 4 %, a plausible estimate is that at least 21 terminals with simultaneous access will be needed in the area defined according to county coverage criteria. Due to the available information regarding rural population distribution, it is important to point out that this estimate is expected to suffer significant variations: 1– 41 terminals in a 30 km radius.

The study of the LTE access networks in this scenario, especially as data service providers, takes on an unprecedented relevance, as only until recently telecommunication service providers preferred rendering voice services via existing 2G and 3G technologies. Data traffic is at the mercy of the limitations imposed by the transmission technology used by these generations of cell systems.

Therefore, LTE expansion, in this scenario, is strongly supported by regulatory initiatives and government policies, aligned with the progress reached globally with 3GPP standardization of the 450 MHz range as described in the next Section.

2.3 3GPP Standardization

Besides the specific scenario of application in Brazil, 3GPP believes LTE 450 MHz has the potential to establish itself as a global system and the most adequate option for the deployment of 4G networks in sparsely populated regions around the world. One of the greatest challenges to reach this goal consists in the definition of economically sustainable models, particularly when considering the difficulties related to the deployment, operation, and maintenance of such networks.

The process for standardizing the 450 MHz band for LTE began in September 2012 [10], in the form of an unprecedented proposal from a Brazilian delegation.

Several challenges related to the channelization of the spectrum, the coexistence of adjacent services, the transmission and reception performance parameters, and the standardization of test methodologies and procedures had to be overcome. The process took into account the Brazilian scenario, characterized by particularities regarding the regulation of the spectrum, not only that allocated for LTE use, but for adjacent services as well. However, the approach used in the specification did not limit itself to a specific scenario, but considered, for example, terminal mobility. In these conditions, band 31 became part of the standard in mid-2013 [1], becoming a decisive and motivating factor to encourage Brazilian service providers and manufacturers to invest in products and solutions based on LTE systems operating in the 450 MHz range.

Based on this scenario, a system-based analysis of the performance for different terminal antennas types is presented below.

3 Evaluation Scenario

The scenario in question was evaluated by simulation, based on the LTE-Sim simulator [11], available as open source on the Internet. This simulator has been used in diverse situations, with results considered significant, as attested by Boggia et al. [12], Camarda et al. [13], Capozzi et al. [14], Grieco et al. [15], and Piro et al. [16]. The software simulates the transmission of resource blocks (RB), in compliance with LTE technology. It additionally offers the following features: direct and reverse link transmission, several types of schedulers and traffic generators, multiple cell treatment, interference calculation, customization of propagation models, generation of random cell terminal distribution, and mobility model selection.

However, the software does not provide the resources needed to evaluate conditions compatible with the preferred scenario for 450 MHz range utilization. The authors therefore decided to include the following functionalities in the simulator:

(a) treatment for interference for directional antennas, with equations described in Sect. 3.1;
(b) a propagation model, mentioned in Sect. 3.2;
(c) the generation of random coordinates of terminal locations, according to the distribution, either Uniform or Gaussian, as described in Sect. 3.3.

This section also presents the disposition of cells and base transceiver stations, as well as the simulator configuration parameters.

3.1 Terminal Antennas

In the priority scenario, proposed for analyzing the LTE 450 MHz system performance, the terminals (User Equipment—UE) are considered fixed equipment. In this context, configurations with omnidirectional and directional antennas are

Table 2 Electrical characteristics of the antennas

Antenna	Gain (dBi)	Φ_{-3dB} (degree)	FTBR (dB)
#1	8	80	15
#2	12	55	15
#3	8	Omnidirectional	

evaluated alternatively. The gain and front-to-back ratio (FTBR), when applicable, of these antennas varies and certain metrics for system performance measurement are calculated, to single out the antennas settings with the best performance.

In Table 2, the electrical characteristics of the antennas are presented. In particular, the gain, the −3 dB beam width in the horizontal plane (azimuth plane $\boldsymbol{\Phi}_{-3dB}$ and the front-to-back ratio of the radiators are specified. These characteristics are based on commercial Yagi–Uda antenna performance specifications [17]; in other words, the analyzed scenarios depicted real conditions. Furthermore, gain variations are linked to variations in the −3 dB beam width in the horizontal plane.

To represent the gain radiation pattern in the horizontal plane of the terminal, the following expression was used (3GPP, 2013a):

$$G_H(\phi) = G - \min\left[12\left(\frac{\phi}{\phi_{-3dB}}\right)^2, \text{FTBR}\right] \text{(dBi)}, \tag{1}$$

where G indicates the antenna gain in dBi, $\boldsymbol{\Phi}_{-3dB}$ its −3 dB beam width in the horizontal plane in degrees, FTBR its front-to-back ratio in dB, and $-180° \leq \boldsymbol{\Phi} < 180°$. This equation is widely used in studies to assess system-based performance [18], since it is a faithful representation of the azimuth pattern in directional antennas.

Figures 1, 2, and 3 below present the radiation patterns related with antennas #1, #2, and #3, described in Table 2.

Still on the subject of the antennas used to evaluate performance, the existence of polarization mismatch was not taken into consideration, due to the propagation environment and the antenna mounting alignment, nor was the impedance mismatch with feeder system, since commercial antennas dedicated for use in terminals display return loss better than 10 dB in the operating band.

Having defined the antennas, the next section will evaluate the suitable propagation model, taking into account the frequency, climate, antenna height, and other parameters.

3.2 Propagation Model

The UHF band propagation model was derived from the method recommended for point-to-area coverage prediction in the 30–3000 MHz range by the International Telecommunication Union [19]. Based on the propagation over soil charts and the

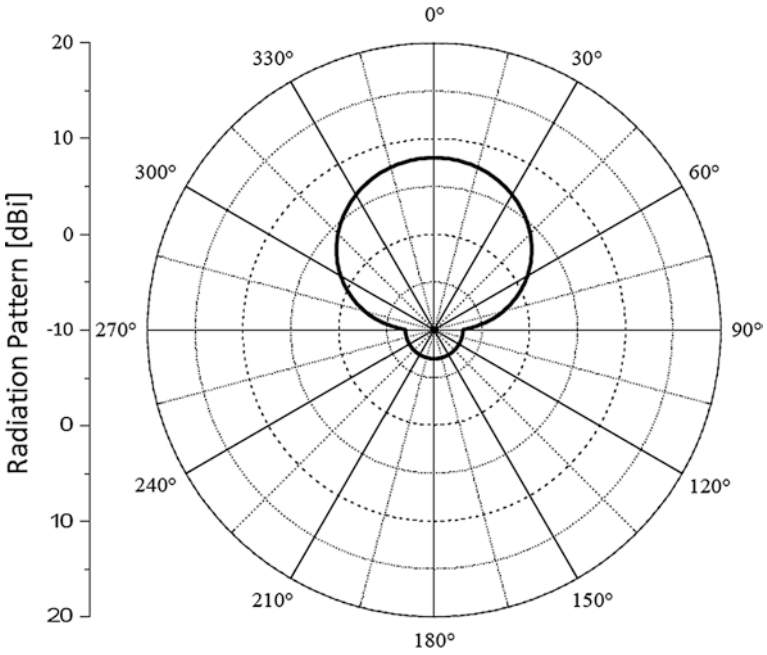

Fig. 1 Azimuth radiation pattern for antenna #1

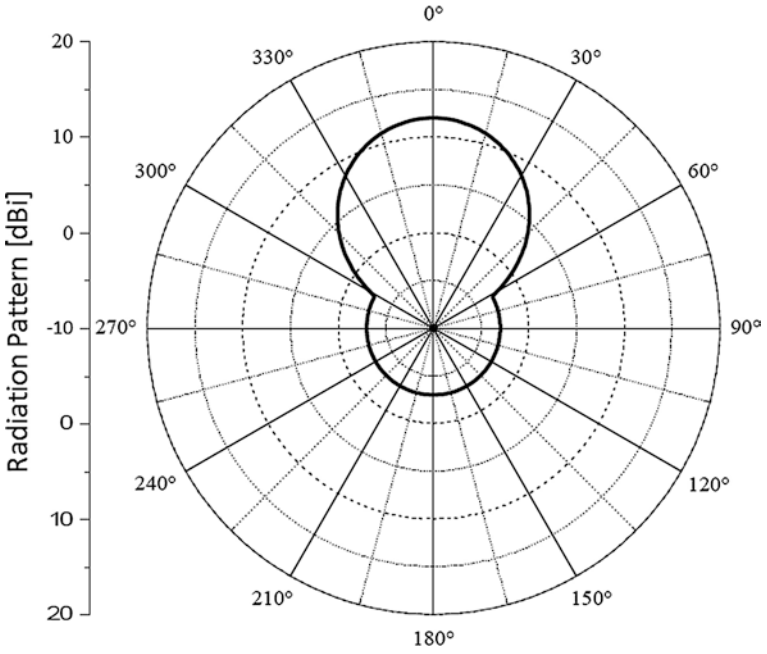

Fig. 2 Azimuth radiation pattern for antenna #2

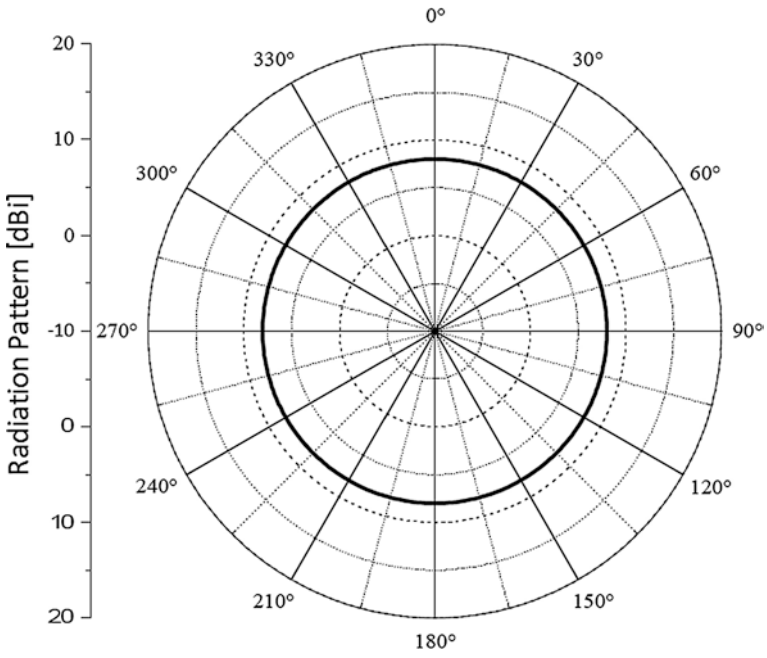

Fig. 3 Azimuth radiation pattern for antenna #3

average signal level (50 % of the time in 50 % of the locations) and as recommended, the field level received in dBμV/m, was interpolated between the data presented for 100 and 600 MHz, in order to determine the field level received at 460 MHz, which is the average value between the central frequencies of the direct link (465 MHz) and reverse link (455 MHz).

However, the field value received informed in the ITU document was obtained from the measurement of a half-wave dipole in a transmitting station with effective radiated power of 1 kW. Thus, the effectively isotropic radiated power (EIRP) corresponds to 62.15 dBm.

To calculate loss by propagation, the power received by a matched load coupled with the receiving antenna must first be determined. Considering that the power level P_r, delivered to the matched load connected to the receiving antenna with gain G_r, matched in polarization with an incident wave with electric field intensity $E_{\mu V/m}$ and frequency f_{MHz}, is expressed by:

$$P_r = -77,2 + E_{\mu V/m} - 20\log(f_{MHz}) + G_r \text{ (dBm)}, \tag{2}$$

then, based on the data [19], the power received at distances between 1 and 50 km from the transmitting antenna was determined.

Once the received power had been established and knowing the transmission power, the loss by propagation between the antennas was calculated. The equation expressing the propagation loss was determined by non-linear regression, as presented in Fig. 4, with a coefficient of 98.5 %.

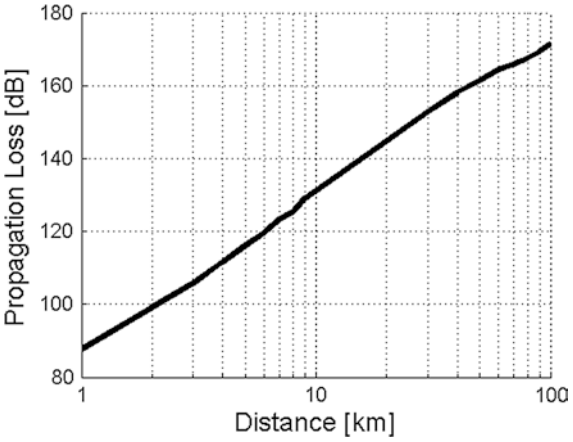

Fig. 4 Propagation loss between the transmitter and receiver for a transmitting antenna with 75 m height

The adjusted propagation loss is then used in the performance evaluation scenario of the different terminal antennas.

The terminals' geography distribution for a rural area can follow different patterns as discussed in the next section.

3.3 Distribution of the Terminals

The terminals were distributed in seven cells, as shown in Fig. 5. In this configuration, the base stations are located in the center of the cells.

The terminal stations were laid out in each cell according to the following distributions:

- Uniform: this distribution is commonly used in urban environment simulation, but is not the most adequate for rural environments.
- Gaussian: although there are no references indicating that rural homes are laid out according to this distribution, it was adopted with the assumption that it is the most adequate for evaluating system performance in a rural environment. In fact, this application scenario typically features a greater concentration of terminals in the central region of the cell, where the radio base station is usually installed. In this project, a standard deviation of $\sigma = 12$ was considered, implying that 95.2 % of the terminals are located between 1 and 24 km from the radio base station. This interval encompasses a small county with a population under 100,000 and large extensions of land, such as those typically found in the north and middle-western regions of Brazil. There is no reference of an adequate value for this standard deviation, thanks to the great diversity of the 5000-plus Brazilian counties in terms of population, territory, and housing characteristics (rural and urban). A study of the different configurations of this distribution can be carried out in future projects.

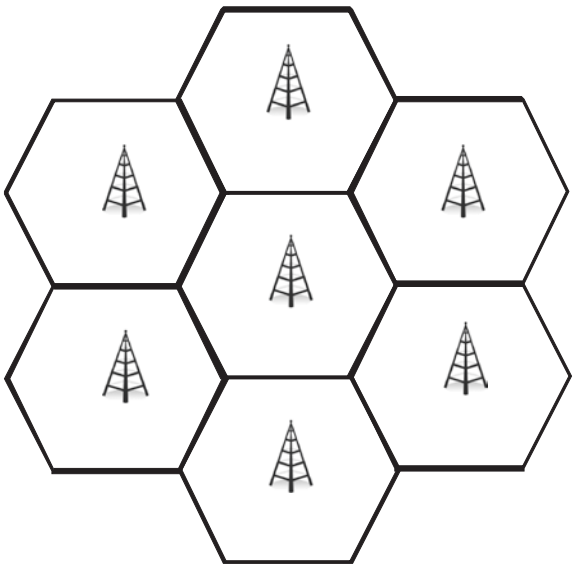

Fig. 5 Simulation scenario with seven cells

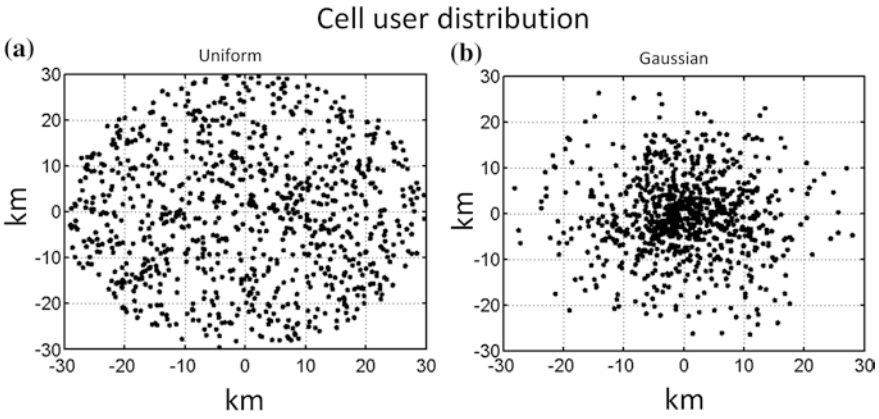

Fig. 6 Terminals laid out in: **a** Uniform distribution; **b** Gaussian distribution

Figure 6 illustrates the layout of the terminals, in Uniform and Gaussian distribution. In each figure, the locations of the 900 terminals are marked. The total number of locations is the result of 30 terminals considered in each one of the 30 simulation runs used to achieve the results.

The possibility of using terminals with mobility was not considered, since the long distances defined by the coverage requirements to be met by the service providers and the power limits imposed by the ANATEL resolution [7] do not favor the use of this kind of terminal.

The transmission power and base transceiver station antenna gain considered are compliant with the maximum values allowed by ANATEL Resolution 558/2010 (2010).

The simulation settings are detailed below based on the considerations exposed in the previous sections.

3.4 Simulator Settings

The basic configuration of the simulator used to characterize the analyzed scenarios is described in Table 3.

The adopted operation mode is Single-Input Single-Output (SISO), since the simulator only supports such transmission mode. The data rate can be adjusted according to a multiplexing gain in order to estimate the performance with Multi-Input Multi-Output (MIMO).

As stated previously, the simulations were run for the direct link and, to this end, terminal reception noise was determined and used to evaluate signal to interference plus noise ratio (SINR) throughout the cell.

Thermal noise per resource block (RB) was calculated at −121.4 dBm. Using a noise figure (NF) of 9 dB in the terminal receiver and 10 dB white noise in the cell, above thermal noise, terminal reception noise was determined to be −109 dBm per RB.

These SINR values are used as input parameters for the adaptive modulation mechanism implemented in the simulator.

It was presumed that all terminal antennas were correctly installed, so that the radiation pattern would be pointed toward the Base Station (BS) in the direction ensuring the highest gain.

Losses by penetration were not taken into consideration, based on the assumption that the antennas were installed in outdoor environments, several meters above the ground.

The cell radius was set at 30 km, covered by the service associated with the respective authorization for the use of radio frequency in the sub-range, in accordance with Decree No. 7512 [20], regulating the 450 MHz range, which establishes this coverage radius as a reference for minimum geographical range commitments to be met by service providers acquiring the rights to use this range.

It was presumed that the terminals were located farther than 1 km from the BS, since even in small cities, the central cell region is considered urban area, and will very likely be serviced by systems operating in higher frequencies. A best effort traffic generator was used, that is, non-stop transmission in the direct link for all active terminals (Radio Resource Control—RRC).

The following section lists the performance results for all scenarios defined according to the premises presented in this section, with varied terminal antenna types, parameters, and layouts.

Table 3 Simulation parameters

Parameter	Value
System	
Number of eNodeBs	7
Number of sectors	1
Cell radius	30 km
Minimum user distance	1 km
Frequency	450 MHz
Band	5 MHz
Noise caused by RB	−109 dBm
Shadowing	Lognormal $\sigma = 6$ dB
Loss by penetration	0 dB
Scheduler	Round robin
Adaptive modulation	Yes
CQi period	1 ms
Traffic generator	*Best effort*
Simulated channel	Downlink
Operation mode	SISO
# of users/cell	30
Scenario	fixed-nomadic
Simulation runs per scenario	30
eNodeB	
Antenna type	Omni
Antenna gain	10 dBi
Antenna height	75 m
Transmission power	40 dBm
Sensitivity /RB	−115.5 dBm
Terminal	
Antenna type	Omni or directive
Antenna gain	See scenario
Antenna height	10 m
Transmission power	23 dBm
Sensitivity/RB	−111 dBm
Mobility	No

4 Results

The results presented below refer to the average throughput of the direct link in the central cell of the cell cluster in the scheme represented in Fig. 5. This throughput is the chosen parameter for validating the influence of using antennas with different characteristics on the terminals distributed in the analyzed cell.

Figure 7 shows the average throughput simulations in different positions in the central cell for the various scenarios indicated in the figure (scenarios #1–#4).

The antennas used are those described in Table 2 and identified in the captions of Fig. 7. The legends use T (N, G) to mean the following:

- T: "D" or "O" for directional or omnidirectional antennas, respectively.
- N: Number of cells.
- G: Antenna gain.

In cases of distance of 2.5 km and lower, although they are not presented in the chart, the resulting throughput is the same for all scenarios, even for those with interference and an omnidirectional antenna O(N, G) = 7.8. This is because the SINR in this region favors the selection of the highest level modulation, even if the least robust, for all scenarios, thus resulting in a greater throughput.

The purpose of the comparison between scenarios #1 and #4 is to assess the gain resulting from the use of directional antennas instead of an omnidirectional antenna with the same gain, assuming that the number of cells in the system is the same. Results prove that the absolute advantage achieved by using a directional antenna is practically constant throughout the cell. This is explained by the fact that this antenna is able to minimize interfering signals originating from neighboring cells because of the width of its beam in the horizontal plane and its front–back ratio.

The purpose of the comparison between scenarios #3 and #4 is to assess how interference affects throughput. As expected, the greatest degradation occurs at the edge of the cell, where, as indicated in Fig. 8, the terminal is located in the least favorable position, resulting in a reduction in performance by a factor of 10. This reduction becomes smaller as the terminal approaches the BS.

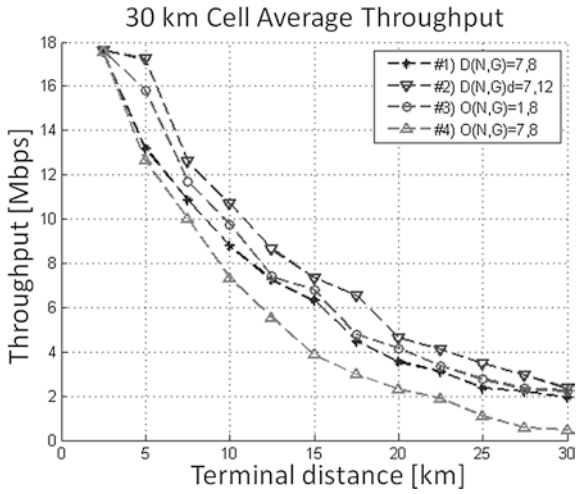

Fig. 7 Average central cell throughput for different distances from the base transceiver station

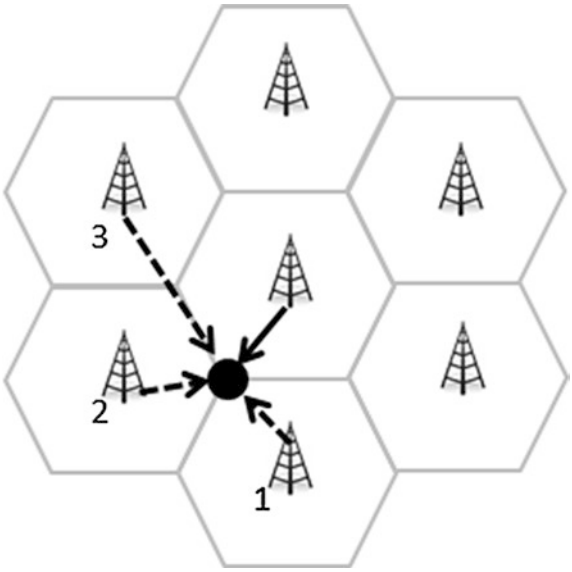

Fig. 8 Three greatest interfering signals affecting a terminal located at the edge of the central cell

The purpose of the comparison between scenarios #1 and #2 was to evaluate the performance for the same number of interfering BSs, however, with different antennas' gains. The front–back ratio in both scenarios is the same. The achieved results quantify the improvement of system performance based on parameters assembled from real antennas; the authors thus avoided extreme variations of the parameters, which would result in assessments diverging from reality. It was determined that the greatest gain in performance was achieved at the edge of the cell, since in this region, the antenna suffers discrimination regarding the directions associated with the two greatest interfering signals.

The achieved results quantify the improvement of system performance based on parameters assembled from real antennas; the authors thus avoided extreme variations of the parameters, which would result in assessments diverging from reality. It was determined that the greatest gain in performance was achieved at the edge of the cell, since in this region, the antenna suffers discrimination regarding the directions associated with the two greatest interfering signals.

This discrimination is associated with the front–back ratio, with a value of 15 dB for both antennas, as shown in Table 2. In this case, the antenna aperture, different than that used for scenarios #1 and #4, does not contribute to minimize the interference, leaving the task of increasing antenna gain to SINR improvement, which causes the resulting gain in throughput.

The comparison of scenario #1 with scenario #4, considering the use of Gaussian distribution, produced a 14 % gain in performance, thanks to the use of a directional antenna with the same gain as that of an omnidirectional antenna.

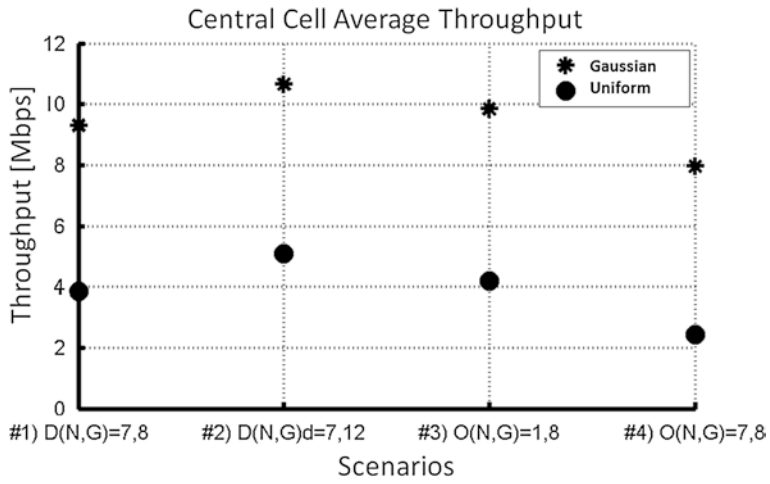

Fig. 9 Average cell throughput for different user distributions and antenna characteristics

Since most terminals are located in the central region of the cell, the loss of performance caused by interferences and by the use of an omnidirectional antenna becomes less relevant when using Gaussian distribution and comparing it with Uniform distribution. In the latter case, loss is approximately 90 %. Figure 9 shows absolute average central cell throughput.

The comparison of scenario #3 with scenario #4 revealed a 25 % gain in throughput when using Gaussian distribution, and approximately 100 % for Uniform distribution. This is due to the fact that when using Uniform distribution, there are a greater number of terminals at the edge of the cell, which are more susceptible to interference originating from neighboring cells. This explains the greater degradation in the scenario with Uniform distribution compared to that observed with Gaussian distribution.

For scenarios #1 and #2, with Gaussian distribution, a relative gain of approximately 20 % is achieved when using an antenna with more gain. In this case, average terminal throughput increases from 300 to 360 kbps for a 30-km radius cell.

Based on the results presented, the conclusions are described as follows.

5 Conclusion

This chapter evaluated the scenario for using LTE technology for the 450 MHz frequency based on ANATEL resolutions, 4G auction requirements in Brazil, 3GPP norms, and the characteristics of commercial terminal antennas, as well as the geographic distribution of homes in the rural area.

Cell throughput was evaluated in the direct link for both omnidirectional and directional antennas, using a system-based simulator, configured for operation in the rural scenario, with and without the presence of other interfering cells.

In scenarios with interference, there was a 14–19 % increase in the throughput of terminals operating with directional antennas, compared with a directional antenna of the same gain with Gaussian and Uniform distribution of the terminal in the cell's geographic area.

The 4 dB increase of gain of the directional antenna and the resulting narrowing of the beam caused a 20 and 25 % increase in throughput for the Gaussian and Uniform terminal layouts, respectively.

The absence of interfering factors improved throughput between 25 and 92 % when using the same omnidirectional antenna and different terminal layouts.

It was also determined that when using an omnidirectional antenna, the performance of terminals located at the edge of the cell was severely damaged, almost ten times worse than when using a directional antenna with the same gain. The disparity in the terminal throughput over the cell increases with the use of omnidirectional antenna.

This work will help the operators to choose the best terminal antenna, improving system performance and meeting the 450 MHz spectrum auction requirements. Terminal manufacturers can create product segments with varied antenna characteristics to bring service providers the appropriate solution for the different cell regions.

The next section presents suggestions for future research projects that will bring improvements to this area.

6 Future projects

The evolution of this project must assess performance in other scenarios and configurations that were not broached in this chapter—for example, the evaluation of performance in the reverse channel, especially for terminals located in the edge of the cell, the assessment of the level of equity of performance between terminals and the configuration of scenarios with frequency reuse and sector coverage.

Acknowledgments The authors would like to thank the Ministry of Communication for financing the CPqD LTE 450 Project with FUNTTEL resources. They also would like to thank researcher João Paulo Miranda, Ph.D., who reviewed this chapter and contributed to improve it.

References

1. 3rd Generation Partnership Project (3GPPa) (2013b) TSG-RAN WG4 Meeting #67, RP-133076: TP on frequency band arrangement. Fukuoka, Japão
2. Basit A (2009) Dimensioning of LTE network: description of models and tool, coverage and capacity estimation of 3gpp long term evolution radio interface. Universidade de Tecnologia, Helsinki

3. Jaafar A et al (2013) On coverage analysis for LTE-A cellular networks. Int J Eng Technol (IJET), Singapura
4. Mathar R, Reyer M, Schemeink M (2007) A cub oriented ray launching algorithm for 3D urban for field strength prediction. In: International conference on communications (ICC), Glasgow. Proceedings… IEEE: Glasgow, Scotland, UK
5. Brazil (2009) Ministry of communications PNBL—A national broadband plan: Brazil at high speed. 2009. Available at: http://www.mc.gov.br/images/pnbl/o-brasil-em-alta-velocidade1.pdf. Accessed on 21 September 2013
6. Brazil (2010) Casa civil. Decree 7175, 2010. National Broadband Program (PNBL)
7. Brazilian Telecommunication Regulatory Agency (ANATEL) (2010) Resolution No. 558, 2010: Approves the regulation of the channelization and conditions of use for radiofrequencies in the 450 MHz to 470 MHz Range Brasília
8. Brazilian Telecommunication Regulatory Agency (ANATEL) (2012) Radiofrequencies in the 2500 MHz to 2690 MHz sub-range and/or in the 451 MHz to 458 MHz and 461 MHz to 468 MHz sub-ranges, Bid Notice 004/2012/PVCP/SPV. Brasília
9. Silva J, Costa R (2013) Field application scenarios—LTE 450 MHz. CPqD Technical report
10. 3rd Generation Partnership Project (3GPPa) (2012) TSG-RAN WG4 Meeting #57, RP-121414: New work item proposal: introduction of LTE 450 in Brazil. Chicago, EUA
11. Piro G et al (2011b) Simulating LTE cellular systems: an open-source framework. In: IEEE transactions on vehicular technology
12. Boggia G. et al (2012) On accurate simulations of LTE femtocells using an open source simulator. EURASIP Journal on Wireless Communications and Networking, Bari, Itália
13. Camarda P et al (2012) QoS provisioning in LTE-A networks with relay nodes. In: Proceedings of the IFIP Wireless Days Conference (WD'12). Dublin, Ireland
14. Capozzi F et al (2012) Downlink packet scheduling in lte cellular networks: key design issues and a survey. IEEE Communications Surveys and Tutorials, Bari, Itália
15. Grieco L et al (2012) A system-level simulation framework for LTE Femtocell. In: Proceedings of SIMUTools, international ICST conference on simulation tools and techniques, Desenzano, Itália
16. Piro G et al (2011a) Two-level downlink scheduling for real-time multimedia services in LTE networks, IEEE transactions on multimedia
17. ZDA Communications US LLC (2013) 450–470 MHz Yagi antennas. Columbia: ZDA Communications US LLC
18. 3rd Generation Partnership Project (3GPPa) (2013a) TR 37.840 V12.0.0: Study of radio frequency (RF) and electromagnetic compatibility (EMC) requirements for active antenna array system (AAS) base station. Valbonne
19. International Telecommunication Union—Radiocommunication Sector (ITU-R) (2009) Recommendation ITU-R P.1546-4, Oct. 2009. Method for point-to-area predictions for terrestrial services in the frequency range 30 MHz to 3000 MHz. Available at: https://www.itu.int/rec/T-REC-G.107-201112-I/en. Accessed on 17 September 2013
20. Brazil (2011) Casa civil. Decree 7,512, June 30, 2011 Available at: http://www.planalto.gov.br/ccivil_03/_Ato2011-2014/2011/Decreto/D7512.htm. Accessed on November 14 2013

Wavelet-Based Narrowband Interference Suppression in Long Term Evolution Physical Channels

João Paulo Miranda, Dick Carrillo, Fabiano Mathilde, Felipe A.P. de Figueiredo and Juliano João Bazzo

Abstract The interference caused by a narrowband system on another system that transmits wideband or spectrally spread signals is, in general, a known problem in wireless communications. However, analyses found in the literature often model the signal of interest as a generic transport channel whose subcarriers convey information of the same kind. This does not reflect the specific structure and application nature of signals conveyed through the different physical channels of the Long Term Evolution (LTE) standard. Having the candidacy of wavelets as adequate means to mitigate narrowband interference (NBI) in both the user and control planes of LTE previously confirmed in Miranda et al. (Narrowband Interference Suppression in Long Term Evolution Systems, pp. 707–711, 2014), in this chapter we extend our analysis to different wavelet types and operation conditions. Biorthogonal, Coiflets, Daubechies, and Haar wavelets are put to the test with respect to their ability to suppress NBI in the LTE downlink. Our simulations suggest that an optimized wavelet-based NBI suppression process calls for different wavelet types, the choice of which being dependent on the LTE physical

J.P. Miranda (✉) · D. Carrillo · F. Mathilde · F.A.P. de Figueiredo · J.J. Bazzo
CPqD Foundation, Campinas, SP, Brazil
e-mail: jmiranda@cpqd.com.br

D. Carrillo
e-mail: dickm@cpqd.com.br

F. Mathilde
e-mail: fabianom@cpqd.com.br

F.A.P. de Figueiredo
e-mail: felipep@cpqd.com.br

J.J. Bazzo
e-mail: jbazzo@cpqd.com.br

A. Paradisi et al. (eds.), *Long Term Evolution*, Telecommunications and Information Technology, DOI 10.1007/978-3-319-23823-4_5

channel considered. Daubechies are shown to be most convenient for synchronization channels, while Coiflets are found to be the best option when it comes to data shared channels.

1 Introduction

Narrowband interference (NBI) is the interference caused by a narrowband wireless communication system on another wireless communication system that uses wideband or spectrally spread signals. The effects of NBI manifest themselves as a wideband receiver within the coverage area of a narrowband transmitter does *not* pick up the noisy signals of interest (SOI), *but* a sum of SOI, narrowband signals and noise instead. Depending on the transmit power of the narrowband system, the undesired components present in the sum signal may introduce nonlinear distortions in the automatic gain control and analog-to-digital conversion blocks of the wideband receiver. This is a well-understood issue, and ways to tackle it are known for NBI of both non-intentional nature [1–6], and intentional nature, e.g., jamming in military communications [7, 8].

Narrowband systems may be found operating in frequencies designated for Long Term Evolution (LTE) systems, especially in bands where legacy (non-LTE) systems are in the process of being refarmed. Up until the point where spectrum refarming is complete, however, there is a need for LTE and narrowband systems to coexist. In order to characterize the NBI a LTE system may be subject to, we carried out in [9] field measurements in the 450–470 MHz range. The reason why we have chosen these frequencies is twofold. The first reason has its roots in the Brazilian National Broadband Plan (BNBP), which in May 2010 advanced the use of the 225–470 MHz range to accommodate new broadband services [10]. BNBP's goal is to increase the penetration rates of broadband services, especially in the countryside and remote areas where a significant number ($\approx$30 millions) of Brazilians live. Later in the same year, the Brazilian Regulatory Agency (ANATEL) allocated the 451–458 MHz and 461–468 MHz bands as uplink and downlink, respectively, for fixed and mobile radio services operating in frequency division duplex mode [11].

The second reason relates to the standardization of the 450 MHz band, designated as Band 31, by the Third Generation Partnership Project (3GPP) [12]. 3GPP's aim is to benefit from the superior propagation characteristics of lower frequencies in a new LTE profile for fourth generation systems operating in sparsely populated areas. On behalf of the Brazilian Ministry of Communications, CPqD supported 3GPP in the determination of appropriate channelization schemes, coexistence solutions, and transceiver radio parameters. These specifications will soon become available as part of LTE Release 12.

In what follows, we reproduce some findings of our measurement campaign reported in [9]. These will help motivating for the matter of NBI suppression in LTE networks, as well as for the work developed in the present chapter.

1.1 Characterization of NBI Sources and Signals

In Brazil, the Band 31 is predominantly assigned to voice services, whose channels are 12.5 kHz wide. The resolution of the spectrum analyzer was therefore set to 3 kHz, for 5 MHz (SOI) segments, and 0.3 kHz, for 12.5 kHz (NBI) segments. The antenna selected for the measurements was a custom-built J-pole antenna made of 15 mm copper tubes. A laptop running the software LabView allowed sample processing and storage to be carried out in an automated fashion. In the discussion that follows, we analyze the findings obtained using this setup in a measurement campaign carried out in Campinas, São Paulo. The exact measurement site coordinates and height above the terrain were 22º54′ S 47º02′ W and 667 m, respectively. A picture of our setup is shown in Fig. 1.

An analysis of the cumulative distribution function (CDF) of received power per segment revealed that, for most segments, the NBI power lies below the noise floor (due to the typically higher sensitivity of narrowband radios). However, high-power NBI −65 dBm and above) was found sitting at $f_1 = 463.5500$ MHz, $f_2 = 464.6000$ MHz, $f_3 = 457.5375$ MHz, and $f_4 = 469.1625$ MHz. According to [13], a search tool publicly made available by ANATEL, the first three frequencies

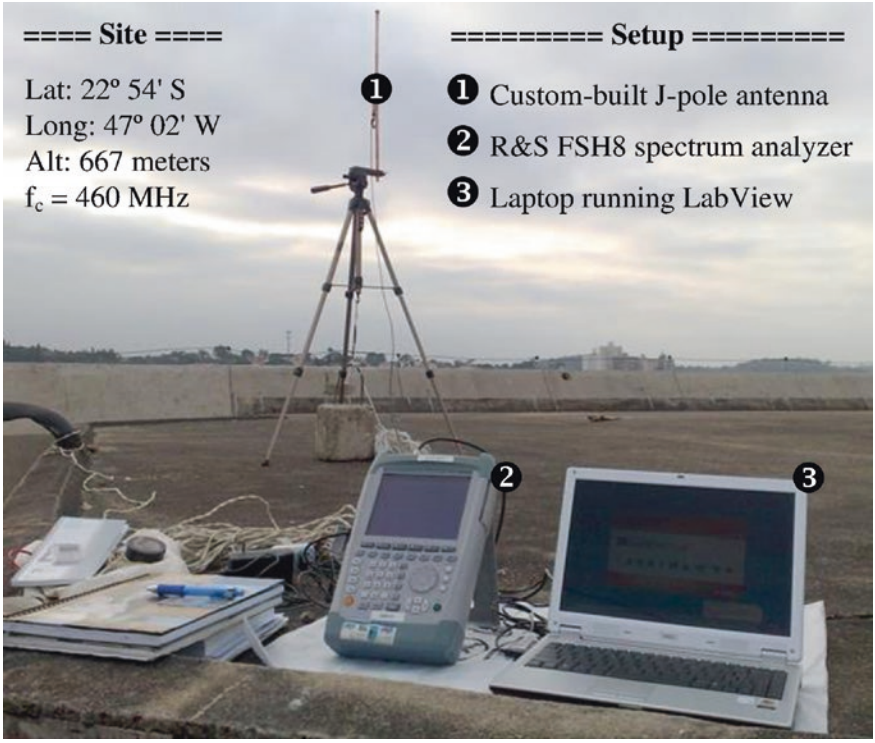

Fig. 1 Site information and setup used in the measurements

are granted to push-to-talk (PTT) systems used for highway control and oil and gas purposes. The fourth one is granted to the city town of Campinas for data transmissions. Another CDF analysis, now in terms of talk time, showed that PTT communications last up to 20 s for 90 % of the cases. The segment occupation was also found to lie around 30 % on average, for PTT signals, and 100 % of the time, for data signals.

Our measurements confirmed the presence of multiple narrowband systems in both uplink and downlink frequencies designated for the operation of LTE 450 MHz systems. Building on these findings, we can set requirements for NBI suppression so as to ascertain coexistence between LTE and narrowband systems.[1] Before we proceed, note that f_4 is about ten physical resource blocks (PRB) away from the LTE subcarrier conveyed by the highest frequency in the downlink. This is far enough for the corresponding data-based narrowband signals not to interfere with the LTE system. NBI suppression in the uplink is out of the scope of this chapter,[2] so the PTT-based narrowband signals sitting at f_3 will not be taken into consideration.

1.2 Motivation

Figure 2 depicts an exemplary shot of the signals received in the LTE downlink during our measurements. The narrowband signals x_1 ($@f_1 = 463.5500$ MHz) and x_2 ($@f_2 = 464.6000$ MHz) overlap different portions of the received LTE signal r. x_1 mainly affects data on the user plane, i.e., the physical downlink shared channels (PDSCH), whereas x_2 mainly affects control plane information. In particular, x_2 has potential to disrupt the Zadoff–Chu sequences conveying symbol timing and frequency offsets in the primary synchronization channels (PSCH). If so the LTE receiver fails to get time synchronized with the system, thus making it hard to extract frame timing and cell identity information transmitted in the secondary synchronization channels (SSCH). The lack of aforementioned information prevents the correct access on the part of the LTE receiver to basic operation parameters, e.g., channel bandwidth, cyclic prefix (CP) length, and antenna mode, transmitted in the physical broadcast channels (PBCH). As a consequence, the cell search procedure gets compromised and the receiver cannot register with the cell [14].

[1] Although such need for coexistence is clear in the context considered here, it may well be justified also in any other bands and/or locations where legacy (non-LTE) systems are in the process of being refarmed.

[2] Our field measurements suggest that the impact of NBI is more detrimental in the downlink because of its potential to cause the user terminal to lose connectivity with the base station, as explained later. An uplink analysis along the same lines used here should be straightforward to obtain.

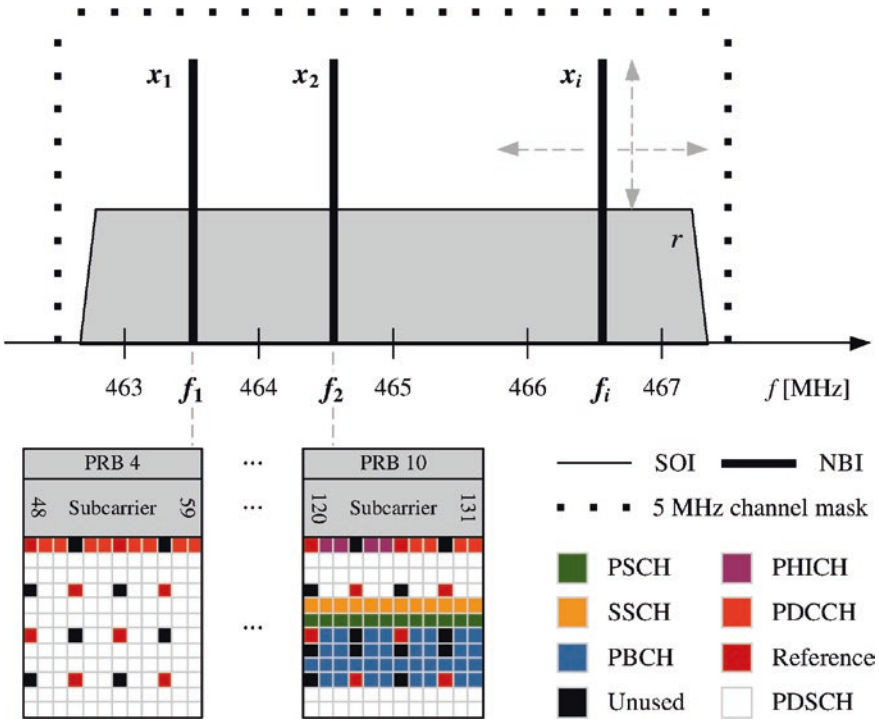

Fig. 2 Exemplary scenario of NBI in the LTE downlink. The signals x_1 and x_2 are real-world narrowband signals found in the Band 31. The signal x_i is an artificially created narrowband signal that introduces controlled NBI

It becomes evident from the above example that the analysis of NBI (and approaches to alleviate its deteriorating effects in the system performance) calls for modeling that takes *physical* channels into consideration. However, the literature on NBI has not managed so far to address this aspect, as most analyses typically rely on the assumption of a *generic* transport channel where all SOI subcarriers convey information of the same kind [1–8]. In answer to this need, we presented in [9] a standard-compliant assessment of the NBI suppression performance of some promising time–frequency distributions (TFDs). Among the TFDs evaluated therein, Daubechies wavelets were shown to offer the best compromise in terms of complexity and signal distortion regardless of the type of physical channel.

1.3 Contributions of This Chapter

Having confirmed the candidacy of wavelets as an adequate tool to mitigate NBI in LTE physical channels in our previous work, in this chapter we extend the analysis

to different wavelet types and operation conditions. Here, Biorthogonal, Coiflets, and Haar wavelets are evaluated in addition to Daubechies with respect to their ability to suppress NBI in the LTE downlink. It turns out from our simulation work that an optimized suppression process calls for different wavelet types, the choice of which being dependent on the physical channel considered. Daubechies are shown to be most convenient for synchronization channels (PSCH and SSCH), while Coiflets are found to be the best option when it comes to data shared channels (PDSCH).

The remainder of the chapter is organized as follows. Sect. 2 introduces the system model used throughout the chapter, overviews the fundamentals of any NBI suppression process, and reviews a number of different techniques that can be used to mitigate the problem we have at hand. For the sake of self-containment, Sect. 3 reproduces part of our previous work in [9]. This will prove to be of utmost importance as justification to our choice of further investigating wavelets, which in turn are explained in greater detail in Sect. 4. Simulation results are presented in this section, and the major contributions of the chapter are also discussed. Concluding remarks are offered in Sect. 5.

2 Fundamentals of NBI Suppression

This section is split into three parts that are as follows. First, we put in place a general system model that can be specialized so as to ease the identification and removal of NBI coefficients over different signal domains. In the second part, we provide a brief explanation of a few generic steps common to most NBI suppression techniques. A discussion about frequency-domain techniques, time-domain techniques, and techniques able to suppress NBI in both frequency and time domains, along with their strengths and weaknesses, is object of the third part.

2.1 General System Model

Let N_S denote the number of subcarriers, $C_f(e)$ the complex constellation transmitted by the eth subcarrier during the fth symbol, Δf the subcarrier spacing, T_{CP} the CP length, and T_{S} the sampling period. The LTE downlink Orthogonal Frequency-Division Multiplexing (OFDM) signal conveyed by the fth symbol is given by

$$s(t) = \sum_{e=-\lfloor N_s/2 \rfloor}^{\lceil N_s/2 \rceil} C_f(e) \exp\ (\mathrm{j}2\pi \Delta f e(t - T_{\mathrm{CP}} T_{\mathrm{S}})), \tag{1}$$

with a PRB formed by grouping F consecutive symbols into a block of E consecutive subcarriers, and $C_f(0) = 0$. Resource grid, physical signals and channels are then generated in detailed accordance to the standard [15]. In what follows, by abuse of notation, we shall refer to (1) as the SOI associated with a generic but standard-compliant LTE physical channel.

Suppose the SOI now becomes corrupted by $i = 0, 1, \ldots, I$ narrowband signals. The NBI sources statistically relevant in terms of transmit power and talk time were shown in [9] to be PTT radios in the case of the Band 31. The signals transmitted within such systems can be assumed, without loss of generality, based on frequency modulation (FM). Under this assumption, the FM signal transmitted by the ith NBI source can be written as

$$x_i(t) = A_i \cos\left[2\pi f_i t + 2\pi f_{\text{dev}} \int_0^t a_i(u)\mathrm{d}u + \theta_i\right], \tag{2}$$

where A_i, f_i, and f_{dev} are the magnitude, center frequency, and frequency deviation of the carrier used to modulate the audio signal a_i, and the random phase θ_i is uniformly distributed in the interval $(0, 2\pi)$.

After being passed through a multipath fading channel with impulse response h and L taps, the signal picked up by the LTE receiver (assumed not desensitized) corresponds to the SOI plus a sum of NBI contributions

$$z[n] = r[n] + \sum_{i=0}^{I} y_i[n] + w[n], \tag{3}$$

where $r[n]$ and $y_i[n]$ are filtered versions of (1) and (2), i.e.,

$$r[n] = \sum_{l=0}^{L-1} h[l]s[n - \sigma_l]$$

$$y_i[n] = \sum_{l=0}^{L-1} h'[l]x_i[n - \sigma_l],$$

σ_l is the channel delay spread associated with the lth channel tap, and w is additive white Gaussian noise (AWGN) statistically independent from tap to tap. Note that, in contrast to the static (and probably band specific) NBI scenario discussed earlier, the narrowband signals in (2) and (3) can be modified in terms of number, magnitude, and position. This allows the different LTE downlink physical channels to be fully exercised in the absence or presence of controlled NBI, e.g., as illustrated by the narrowband signal x_i in Fig. 2.

2.2 Step-by-Step of a Generic NBI Suppression Process

Most NBI suppression techniques have as their basis some sort of three-step process. The first step is the decomposition of the received signal z into some transform domain where the signal components corresponding to the NBI can be more easily identified. In case SOI and narrowband signals are distinguishable in the

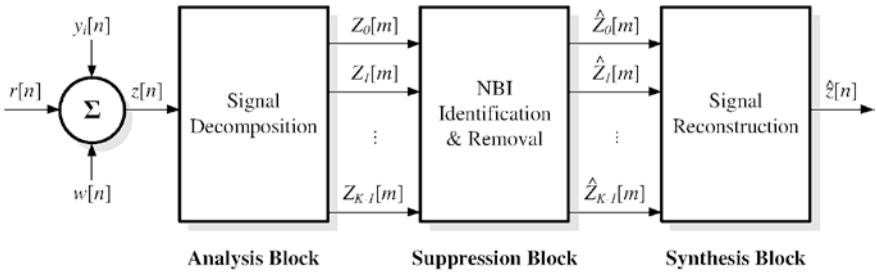

Fig. 3 Block diagram of a generic NBI suppression process

selected domain, the components due to the latter can be estimated via maximum likelihood (ML) [1], linear minimum mean square error (MMSE) [2], or a combination of compressive sensing and weighted least squares [3]. The second and third steps, respectively, involve the removal of such undesired components, and the reconstruction of an estimate of z, denoted as $\hat{z}$.

A generic representation of this process can be found in Fig. 3. The analysis block outputs the channel set Z_k, $k = 0, 1, \ldots, K-1$, which is fed into the suppression block. After the narrowband signals y_i have been estimated and cancelled out, $\hat{Z}_k$, $k = 0, 1, \ldots, K-1$, channels are made available for the synthesis block. This block reconstructs the noisy SOI, thus bringing the solution back to the original problem domain. To keep signal distortion low, the reconstructed signal $\hat{z}$ should provide a good approximation of (3) when $I = 0$, i.e., as in the no NBI case.

2.3 Review of NBI Suppression Techniques

In what follows, we review some techniques regarded as promising in the NBI suppression literature. Any of them can theoretically be employed to specialize system model and process described earlier in this section. To support selection of a given technique among those reviewed, the pros and cons associated with each technique and signal domain where it works are also discussed.

2.3.1 Frequency-Domain Techniques

Frequency-domain techniques, also known as excision approaches, exploit the fact that NBI often comes into play in the form of high-power signals that can be distinguished from lower-power SOI in the frequency domain. Robustness against narrowband signals with center frequencies that change over time, and frequency-selective fading are among their advantages. However, when the NBI spectra do not sit at frequencies coinciding with the bins of the discrete-time Fourier

transform (DFT), carried out at the demodulator, spectral leakage occurs. The higher the NBI power, the larger the number of corrupted subcarriers in $\hat{z}$. This issue can be circumvented by mapping the data only to those subcarriers whose powers exceed a given signal-to-interference ratio [4], but the resulting system may fail to comply with currently DFT-based wireless standards.

2.3.2 Time-Domain Techniques

Techniques that operate in the time domain avoid spectral leakage by applying cancellation filters before the DFT block. Time-domain cancellers require less prior knowledge to work than their frequency-domain counterparts, e.g., only estimates of the frequencies where the NBI spectrum sits at and/or its power per subcarrier. As for the limitations, performance may deteriorate in the presence of frequency offsets. This is exactly the case with phase-locked loops [5], which may undergo a further drop in performance if quadrature phase shift keying (QPSK) is in use. Care must also be taken when it comes to filter design, as impulse responses longer than the CP length introduce intersymbol interference (ISI).

2.3.3 Bidimensional Techniques

In general, NBI suppression in frequency *and* time domains offer flexibility and resolution superior to those obtained in a single domain. Wavelet transforms [6], multirate digital filter banks (MDFBs) [7], and bilinear signal distributions [8] are TFDs that offer relatively lower complexity and near-perfect signal reconstruction at the expense of none or very few prior knowledge of the systems and signals causing NBI. Another advantage is that, by directly representing the frequency content of the signal while keeping the time description parameter, the linear progression of the frequency with time can be observed [16]. However, despite its potential for robustness against NBI, the application of TFDs has been limited to spectrally spread systems [6–8] and a better understanding is needed in the context of multicarrier wideband systems.

2.3.4 Discussion

In light of the literature review above, we can conclude that candidate solutions for NBI suppression in the LTE systems operating in the Band 31 (or in any other spectra where the conditions for coexistence with narrowband systems are similar to those determined here) should be designed bearing the following requirements in mind:

- Low signal distortion: LTE operation occurs most of the time (up to 70 %) in the absence of high-power NBI. Near-perfect signal reconstruction is crucial to maintain the bit error rate (BER) of the system.

- Prior knowledge: For the sake of flexibility and practical feasibility, the amount of information known a priori about narrowband signals should be kept as low as it can possibly be, i.e., blind techniques are preferred.
- Low computational complexity: Narrowband systems currently found in LTE operation bands may not be refarmed nor undergo modifications of any kind soon. NBI originated from these systems can be suppressed at the receive side, where low-complex approaches are preferred.

3 Previous Work

In answer to the aforementioned needs, we assessed the NBI suppression performance of Daubechies wavelets, a polyphase implementation of MDFBs, and a custom Wigner–Ville distribution (WVD) aided time-domain canceller [9]. For the sake of self-containment, we reproduce in the sequel a smaller set of results illustrating the performance of such techniques. The underlying theory behind each of these techniques is briefly discussed here too, except for wavelets to which we dedicate the entire Sect. 4.

3.1 Multirate Digital Filter Banks

Provided that the Z_k channels in Fig. 3 are uniformly and contiguously spaced, and critically sampled, an efficient option is to decompose z using [7]

$$Z_k[m] = \sum_{\rho=0}^{M-1} \sum_{r=-\infty}^{\infty} \bar{p}_\rho[r] z_\rho[m-r] W_M^{-k\rho}, \tag{4}$$

where the sample index m may differ from n, the decimation and interpolation ratio M is equal to K, $\bar{p}_\rho[m] = h_\mathrm{A}[mM - \rho]$ is the ρth polyphase branch of a lowpass analysis filter h_A, $r = [n + \rho]/M$, and $W_M = \exp(\mathrm{j}2\pi)/M$.

NBI suppression is carried out along the same lines described later for wavelets, i.e., by exploiting the prior knowledge of the center frequencies where narrowband signals sit at. Signal reconstruction can be efficiently implemented using

$$\hat{z}_\rho[r] = \frac{1}{M} \sum_{k=0}^{M-1} \sum_{m=-\infty}^{\infty} q_\rho[r-m] \hat{Z}_k[m] W_M^{k\rho}, \tag{5}$$

where $q_\rho[m] = h_\mathrm{S}[mM + \rho]$ denotes the ρth polyphase branch of a lowpass synthesis filter h_S.

A parallel implementation of sets of filters $\bar{p}_\rho$ and q_ρ is a *polyphase network*, and the polyphase structures in (4) and (5) are known to be mathematically equivalent to the banks of lowpass filters and decimators/interpolators that would result from the direct mechanization of analysis and synthesis blocks based on MDFBs.

3.2 Bilinear Signal Distributions

A filter bank is also a special quadratic TFD that represents the signal in a joint time-frequency domain. Among bilinear TFDs, the representation regarded as the most powerful and fundamental is the WVD due to the superior covariance properties it possesses.

The discrete-time WVD (DWVD) can be written as [17]

$$Z_k[n] = \sum_{r=-N}^{N} z[n+m]z^*[n-m]w[m]w^*[-m]W_4^{km}, \tag{6}$$

where the window $w = 0$ for $|m| > N$, N an integer, and $W_4 = \exp(-\mathrm{j}4\pi/K)$. The additional power of 2 in W_4 is a scaling in frequency that is negligible, so in practice it can be replaced by the standard twiddle factor $W_2 = \exp(-\mathrm{j}2\pi/K)$ used in the DFT.

Different synthesis procedures can be employed to obtain the reconstructed signal $\hat{z}$ [18], but they are somewhat cumbersome to implement in practice. We therefore decided to exploit the superior visualization of DWVD-based analysis in a simple time-domain NBI canceller. Since SOI subcarriers are all transmitted at the same power level for a given modulation scheme and data traffic, the indices of subcarriers corrupted by NBI can be *blindly* identified using the DWVD over the entire received signal bandwidth. Having confirmed the presence of in-band narrowband signals (which are clearly distinguishable from the SOI in the DWVD domain), we "blank" corrupted subcarriers in the time domain, bringing their gains back to the expected value. The blanking threshold used to this end is computed on the basis of the average standard deviation of the power received over all subcarriers.

3.3 Simulation Settings and Preliminary Results

In this section, we discuss some preliminary results obtained using a custom-built Matlab simulator that implements the LTE PHY in detailed accordance to the standard [14, 15]. The simulation settings common to all techniques and those that are technique-specific are both summarized in Table 1. We conducted simulations for the cases 'NBI Off' ($I = 0$), 'NBI On' ($I = 1$ without suppression), and 'Technique', which means that NBI is suppressed using the corresponding technique. The latter two cases introduce NBI at $f_1 = 463.5500$ MHz and $f_2 = 464.6000$ MHz, one frequency at a time, so we can evaluate the impact on the performance of PDSCH and PSCH/SSCH. The NBI/SOI power ratio is set to 15 dB, which corresponds to the worst-case condition observed in our measurements.

3GPP has been developing channel models for LTE. However, to the best of our knowledge, no standardized (nor widely accepted) model reflecting LTE

Table 1 General and specific settings (1st round of simulations)

SOI parameters					
N_s	Δf	T_{CP}	$1/T_S$	f_c	BW
512	15 kHz	4.69/16.67 μs	30.72 MS/s	465 MHz	5 MHz
NBI parameters					
A_i	f_i	f_{dev}	I	BW	
NBI/SOI = 15 dB	f_1, f_2	5 kHz	{0, 1}	12.5 kHz	
Parameters/technique		MDFBs	Wavelets	Bilinear	
Type of implementation		Polyphase	Daubechies	DWVD	
Number of parallel channels, K		16	2 per level	512	
Decimation/interpolation ratio, M		16	2	–	
Number of resolution levels, J		1	8	1	
Filter/window length		256 taps	16 taps	512 bins	

operation in the Band 31 was available at the time of writing. A suitable alternative is the 6-tap channel model established within the IEEE 802.22 standard [19], which meets most requirements mandated by [11] (see Table 2). In the sequel, we present a smaller set of results obtained using the 'Profile A' of the 802.22 channel model. Upon passing through this channel, PTT and LTE signals will undergo flat and frequency-selective fading, respectively, but both signals will be subject to less destructive slow fading characteristics. One issue brought about by the choice of this channel, however, is that the maximum delay spread of 21 μs (see Table 3) cannot be absorbed by the standard CP lengths, $T_{CP} = N_S/T_S \approx 4.69$ μs for normal CP, and $T_{CP} = 16.67$ μs for extended CP, used in LTE. In this setting, ISI is the dominating effect and less will likely be seen in terms of NBI suppression regardless of the CP length used. Nevertheless, and since the simulation is under multipath fading, the CP is set to extended and the modulation to QPSK with code rate 1/3. Antenna mode is SISO, channel estimation is assumed ideal, and equalization relies on MMSE. 5×10^7 Monte Carlo trials are carried out for each signal-to-noise (SNR) point.

Table 2 LTE channel model configuration parameters

Parameters	Band 31 [11]	IEEE 802.22 [19]
Transmitter–receiver separation	≈30 km	10–100 km
Radio frequency	450–470 MHz	30–3000 MHz
Channel bandwidth	5 MHz	5, 6, or 7 MHz
Propagation conditions	LOS, NLOS	LOS, NLOS
Environment type	Rural	Rural, suburban, or urban
Transmit antenna height	40 m	30–1000 m
Receive antenna height	5–10 m	10 m
Multipath profiles	Not available	See Table 3
Seasons of operation	All	All

Table 3 Profile used in the simulations of multipath fading

Profile "A"	Path 1	Path 2	Path 3	Path 4	Path 5	Path 6
α_l (dB)	0	−7	−15	−22	−24	−19
σ_l (μs)	0	3	8	11	13	21
f_l (Hz)	0	0.10	2.50	0.13	0.17	0.37

As seen in Fig. 4, the best suppression results are obtained using wavelets regardless of the physical channel type. This is in good agreement with our expectations because the resolution achieved by the 8-level DWT used is about 20 times finer than that of the 256-tap polyphase implementation, here referred to simply as 'PolyNets'. While the multilevel DWT is capable of cancelling out NBI in a highly localized fashion, PolyNets and our DWVD-based approach act on the entire SOI bandwidth. In fact, it turns out that the use of MDFBs for NBI suppression in systems with non-overlapping designs is not advisable, as the attenuation outside the filters' stopband regions can never be infinite in practice. This harms the subcarrier orthogonality of OFDM (introducing signal distortions), thus explaining the poor performance of PolyNets observed here. Despite being the best performer, the DWT needs to know the center frequencies where NBI sits at in order to suppress it. The simple DWVD-based approach proposed has also shown value in some cases, and its application can be considered as a blind alternative to wavelets when no such prior knowledge is available.

Among the TFDs considered, Daubechies are shown the best compromise in terms of complexity and signal distortion regardless of the physical channel type. A question that remains open so far is whether wavelet types other than Daubechies can improve performance further, and, if so, what type best suits each physical channel. This may well be the case since the wavelet choice is dictated by the signal characteristics (recall the distinct structure of signals conveyed through different LTE physical channels) and application nature. But before we carry on with the selection of candidate wavelets, let us briefly review their theory and look into efficient ways to implement a practical wavelet-based NBI suppressor.

4 Wavelet-Based NBI Suppression

4.1 The Discrete Wavelet Transform

The idea of the wavelet transform is to project a signal on a family of zero-mean functions $\Psi_{u,v}(t)$, u, v integers, deduced from an elementary function $\Psi(t)$ by translations and dilations, i.e., $\Psi_{u,v}(t) = \Psi(a_0^v t - ut_0)$. The full representation of z using coefficients of the form [16]

$$WT_z(u, v; \Psi) = a_0^{v/2} \int_{-\infty}^{+\infty} z(t)\Psi_{u,v}^* \mathrm{d}t \tag{7}$$

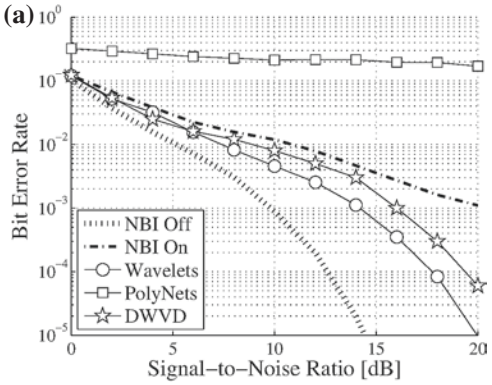

PDSCH@f_1 = 463.5500MHz

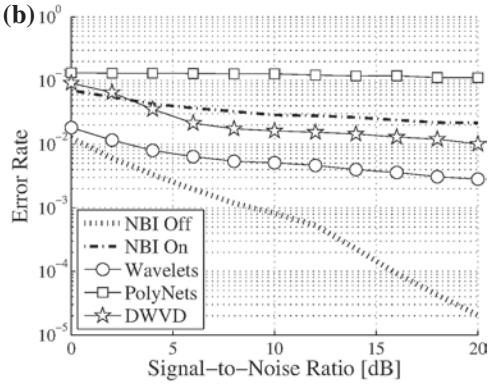

PSCH@f_2 = 464.6000MHz

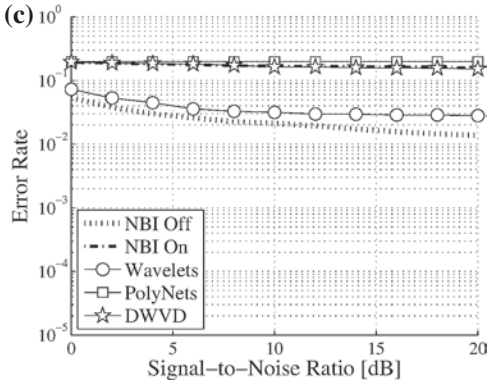

SSCH@f_2 = 464.6000MHz

Fig. 4 Performance obtained over LTE physical channels using different NBI suppression techniques. User plane performance evaluated in **a** is characterized in terms of bit error rate, while control plane performance evaluated in **b** and **c** is characterized as a simple error rate

requires the number of scaling steps, a_0, and time dilations, t_0, to be infinite. Fortunately, this limitation can be overcome by exploiting the close relationship of MDFBs with the discrete wavelet transform (DWT). Using the DWT, the implementation of the analysis (synthesis) block in Fig. 3 requires only a pair of lowpass and highpass filters, whose outputs are both downsampled (upsampled) by 2. In each scale obtained at the output of the bank of filters, NBI is suppressed by cancelling out the coefficients associated with narrowband components. The threshold applied to this end can be set using [6]

$$\gamma = \sigma_s^2 \sqrt{2} \mathrm{erf}^{-1}(P_{\mathrm{fa}}), \tag{8}$$

where σ_s^2 is the variance of the SOI and P_{fa} is the probability of a sample crossing the threshold γ in the absence of interference. The multilevel DWT involves the repetitive application of uniform filter banks on the low-frequency channel, meaning that redundancy is introduced more in that channel as compared to the high-frequency channel. In such multilevel settings, finer resolution is achieved but the recursive coefficient computation raises the need to store intermediate coefficients. This burden can be avoided by replacing the cascaded lowpass filters and subsampling by 2 at each resolution level of the analysis block by an equivalent analysis filter, defined in the z-domain as [20]:

$$H_{\mathrm{A}}^{J}(z) = \prod_{j=0}^{J-1} H_{\mathrm{A}}(z^{2^j}) \tag{9}$$

An equivalent synthesis filter $H_S^J(z)$ can be generated accordingly to replace the cascaded highpass filters and upsampling by 2 used in the synthesis block. In either case, the coefficients of the jth level can now be computed without prior knowledge of the coefficients of the $(j-1)$th level. Such an equivalent filter implementation of the multilevel DWT is exemplified in Fig. 5 for the case of a three-level MDFB ($J = 3$).

In such an implementation, the wavelet type used at each level needs to be compactly supported, i.e., so as to allow discrete-time analysis based on the DWT. Another requirement, determined by the application nature, is that the wavelet

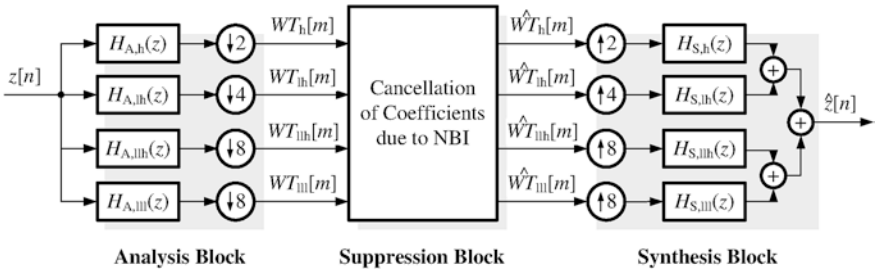

Fig. 5 Exemplary multilevel wavelet-based NBI suppression process ($J = 3$)

Table 4 Selected candidate wavelets and their characteristics

Wavelet type	Short name	L_{sup}	W
Biorthogonal	BiorN_d • N_r	$2N + 1$	Max($2N_d$, $2N_r$) + 2
Coiflets	Coif-N	$6N - 1$	$6N$
Daubechies	Daub-N	$2N - 1$	$2N$
Haar	Haar	1	2

considered should possess the perfect reconstruction property. This led us to the candidates listed in Table 4, alongside some distinguishing characteristics [21]. Coiflets, Daubechies, and Haar are orthogonal wavelets, for which support length (L_{sup}) and filter length (W) are determined by the number of vanishing moments (N). Biorthogonal wavelets differ from others in the table in that a different N can be used for decomposition (N_d) and reconstruction (N_r). All types considered are symmetric, except for Coiflets and Daubechies which are only approximately symmetric and asymmetric, respectively.

4.2 Simulation Work

The simulator and simulation settings used in this second round of simulations are basically the same as described in Sect. 3. The settings common to all simulation campaigns (unless mentioned otherwise) and those that are wavelet-specific are summarized in Table 5. As before, we consider the cases 'NBI Off' ($I = 0$), 'NBI On' ($I = 1$ without suppression), and 'WaveletType', which means that NBI is suppressed using the corresponding type of wavelet). The NBI/SOI power ratio

Table 5 General and specific settings (2nd round of simulations)

SOI parameters					
N_s	Δf	T_{CP}	$1/T_S$	f_c	BW
512	15 kHz	4.69 μs	30.72 MS/s	465 MHz	5 MHz
NBI parameters					
A_i	f_i	f_{dev}	I	BW	
NBI/SOI = 15 dB	f_1, f_2	5 kHz	{0, 1}	12.5 kHz	
Wavelet-specific parameters					
Wavelet type	Short name	N	L_{sup}	W	
Biorthogonal	BiorN_d • N_r	9.3	19.7	20 taps	
Coiflets	Coif-N	5	29	30 taps	
Daubechies	Daub-N	8	15	16 taps	
Haar	Haar	1	1	2 taps	
Filter/window length		256 taps	16 taps	512 bins	

is 15 dB, the narrowband signals are FM modulated, the SOI is QPSK modulated with code rate 1/3, single-antenna mode, and MMSE equalization. The number of vanishing moments used within each wavelet type is carefully chosen by means of small-scale simulations so as to produce the best results for fixed resolution ($J = 8$) and probability of false alarm ($P_{\text{fa}} = 0.01$). As many as 5×10^7 Monte Carlo trials are carried out for each SNR point.

4.2.1 AWGN Channel

In this simulation campaign, we assess the performance of wavelet-based NBI suppression in the presence of AWGN. Such an evaluation scenario, where additive noise and NBI are the sole mechanisms at work, will be used as benchmark later on to help us determine the impact of fading in the NBI suppression process. Results are given in Fig. 6, where the use of different wavelet types across different LTE physical channels yields to improved suppression results. Haar wavelets are not recommended for PDSCH because, as shown in Fig. 6a, they introduce performance losses with respect to the 'NBI On' case. Coiflets, in contrast, are clearly the best option, with performance matching that of the 'NBI Off' case. Thanks to the robustness of the Zadoff–Chu sequences conveyed in the PSCH, both Daubechies and Biorthogonal wavelets match the 'NBI Off' case performance in Fig. 6b also with no single error measured. While this is not the case in Fig. 6c, due to the weaker pseudo-random sequences conveyed in SSCH, Coiflets again outperform all other wavelet types considered.

4.2.2 Flat Fading Channel

A second simulation campaign was carried out to determine the performance derived when the received signal is subjected to flat fading, i.e., all of its frequencies are equally affected by the channel. The corresponding results are shown in Fig. 7, where we again see that different performances can be derived by employing different wavelets. In Fig. 7a, Daubechies and Coiflets give similar results for PDSCH until SNR of about 10 dB, with the latter becoming better than the former from that point on. Figure 7b shows that all the types of wavelets but Daubechies perform approximately same. Daubechies offer gains of up to 20 dB over the 'NBI On' case, thus having their selection justified for PSCH. A similar behavior is observed in Fig. 7c, where Coiflets also prove to be an interesting option for SSCH provided that the SNR is high enough.

4.2.3 Frequency-Selective Channel

In this simulation campaign, we again consider the 'Profile A' of the 802.22 channel model with profile given in Table 3. However, in order to circumvent the limitation experienced in our first simulation round, thus allowing the LTE system to

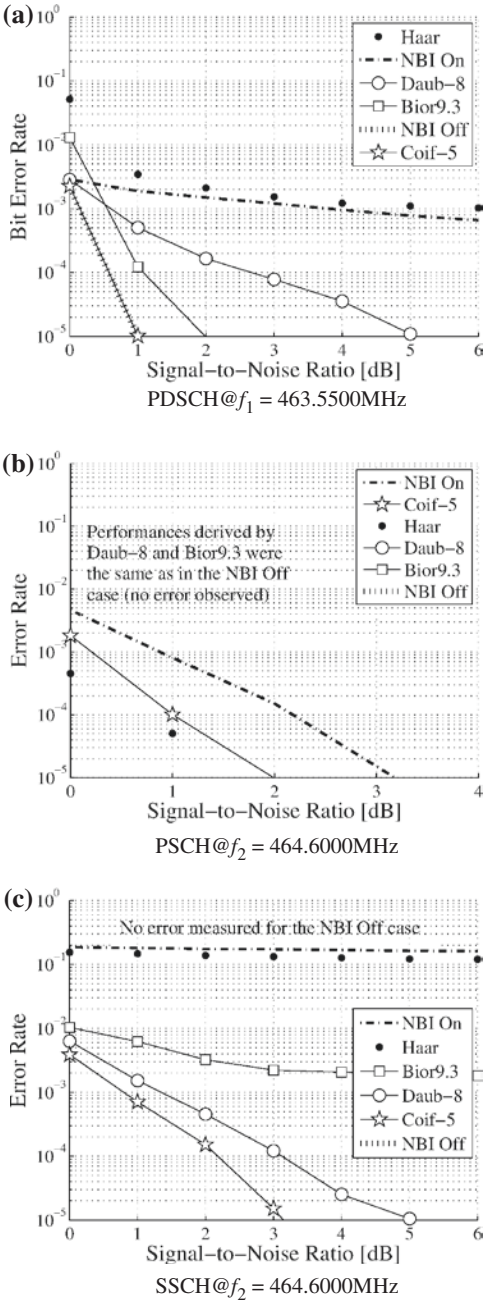

Fig. 6 NBI suppression performance obtained over LTE physical channels using different wavelet types in the presence of AWGN only

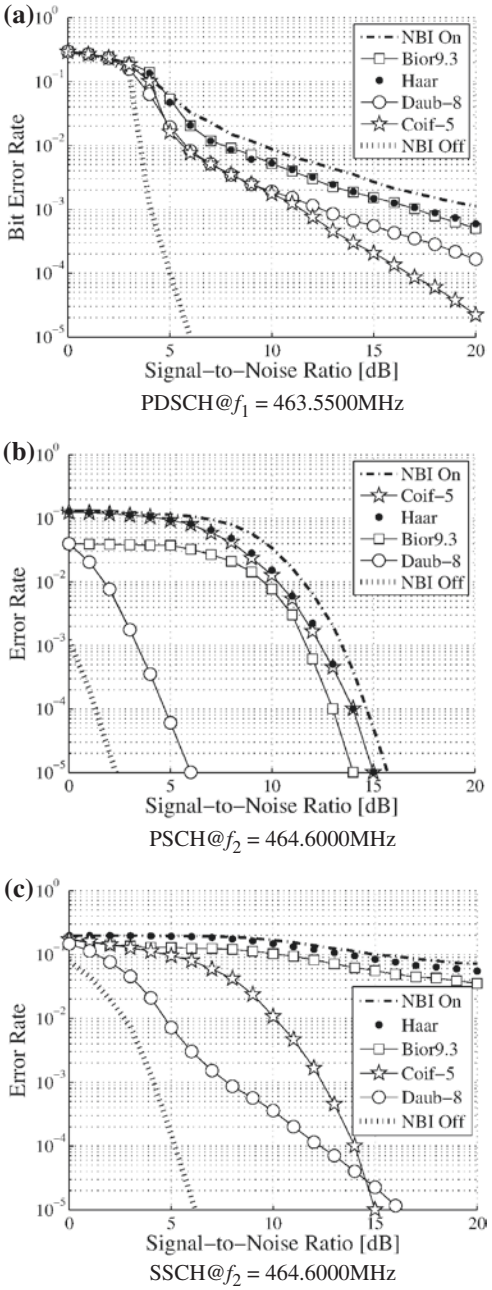

Fig. 7 NBI suppression performance obtained over LTE physical channels using different wavelet types in the presence of flat fading

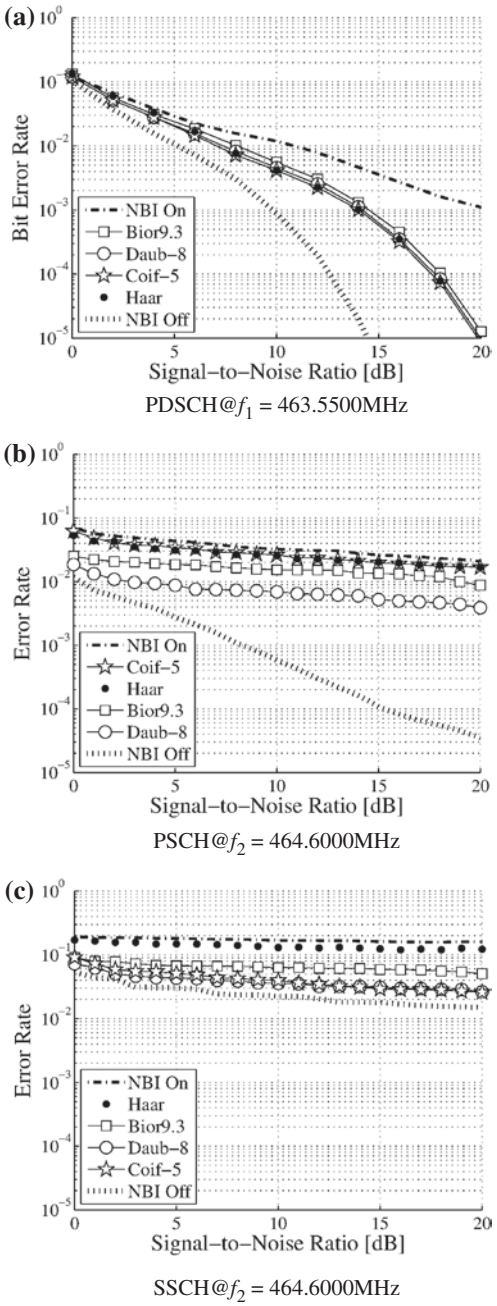

Fig. 8 NBI suppression performance obtained over LTE physical channels using different wavelet types in the presence of frequency-selective fading

work in the ISI-free region, we arbitrarily set the maximum delay spread of the channel to 15 μs, and select the extended CP. Nevertheless, the benefit of NBI suppression can only be better visualized when ideal channel estimation is used. Under this assumption, Fig. 8a suggests that any type of wavelet chosen among

the candidates considered outperforms the 'NBI On' case in excess of 5 dB. Apparently, and unlike the results just discussed for PDSCH, the assumption of ideal channel estimation seems to play a less critical role for synchronization channels. This is seen for PSCH and SSCH in Fig. 8b, c, respectively, whose curves are roughly same as those obtained using MMSE channel estimation (not shown in the figures).

4.3 Discussion

Table 6 summarizes the results of all simulation campaigns carried out in this chapter. One conclusion drawn from this table is that the optimization of the NBI suppression process across the LTE physical channels calls for different types of wavelets. The use of Coiflets has proven most suitable for cancelling out narrowband signals in the user plan, characterized in terms of PDSCH here. Daubechies have been shown as the best option when it comes to NBI in the control plane, especially in PSCH. As for SSCH, either Coiflets or Daubechies can be applied thanks to their similar suppression performances.

Besides having determined the matches among physical channels and wavelet types that offer the best NBI suppression results for LTE systems, this chapter has illustrated the extent to which the wavelet-based approach depends on the wireless channel considered. In fact, our simulation work suggests that choosing the "right match" yields to ideal performance under AWGN for most physical channels. However, the performance losses (with respect to the ideal 'NBI Off' case) progressively increase as more realistic operation conditions such as shadowing and multipath fading are taken into consideration. This is in good agreement with our expectations, as multiplicative mechanisms create oscillations in the received power level whose contributions have potential to dominate the contribution due to NBI. In this case, the performances observed for scenarios 'NBI Off' and 'NBI On' become so close to each other that the gains derived by using wavelets dramatically decrease.

We believe that these results are, in part, due to the ability to reject frequencies out of the band of interest, and complementarity of the quadrature mirror filters (QMF) pair used in the analysis and synthesis blocks. As shown in Fig. 9, Bior9.3 and Haar QMF pairs are, respectively, the least complementary and weakest in terms of out-of-band attenuation. In contrast, Coif-5 and Daub-8 are the

Table 6 Summary of simulation results

Channel type	PDSCH	PSCH	SSCH
AWGN	Coif-5	Bior9.3, Daub-8	Coif-5
Flat fading	Coif-5	Daub-8	Coif-5, Daub-8
Frequency-selective fading	Coif-5	Daub-8	Coif-5, Daub-8

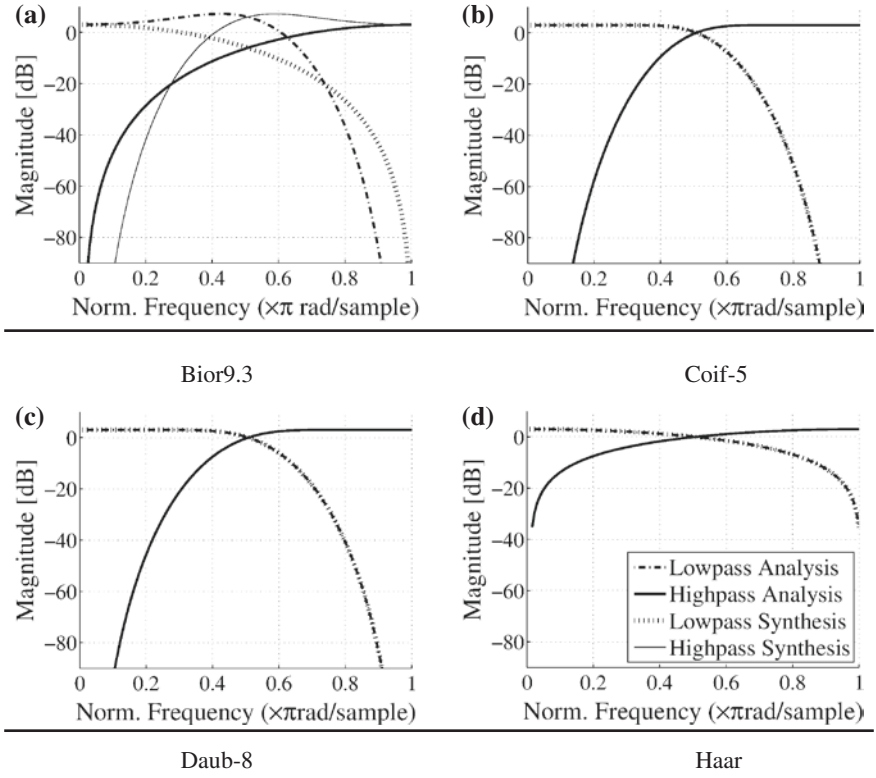

Fig. 9 Magnitude responses of the corresponding wavelet filters for a given resolution level. The legend of subplot **d** holds also for subplots **a**–**c**

most complementary and effective QMF pairs. However, recalling that the wavelet choice tightly relates to the SOI, and symmetry (or asymmetry, as in Coiflets and Daubechies) may also play a role in the NBI suppression process, in our future work we will deepen the study by looking into the structures of QPSK signals, Zadoff–Chu sequences and pseudo-random sequences, respectively, conveyed through PDSCH, PSCH, and SSCH.

5 Concluding Remarks

This chapter has described a wavelet-based approach aimed at mitigating NBI in LTE physical channels. Our simulations suggest that an optimized NBI suppression process calls for different wavelet types, the choice of which being dependent on the physical channel considered. Daubechies are shown to be most convenient for synchronization channels (PSCH and SSCH), while Coiflets are found to be the best option when it comes to data shared channels (PDSCH).

Acknowledgments This chapter is based upon work supported by FUNTTEL/FINEP under Grants 01.12.0481.00 and 01.09.0631.00. The authors are also grateful to Dr. L.C. Pereira for fruitful discussions on the suitability of the 802.22 channel model for simulations in the 3GPP Band 31.

References

1. Sahin ME, Guvenc I, Arslan H (2011) An iterative interference cancellation method for co-channel multicarrier and narrowband systems. Phys Commun 4(1):13–25
2. Nilsson R, Sjoberg F, LeBlanc JP (2003) A rank-reduced LMMSE canceller for narrowband interference suppression in OFDM-based systems. IEEE Trans Commun 51(12):2126–2140
3. Gomaa A, Al-Dhahir N (2010) A compressive sensing approach to NBI cancellation in mobile OFDM systems. In: Proceedings of the IEEE Globecom, Dec 2010, pp 1–5
4. Mei L, Zhang Q, Sha X, Zhang N (2013) WFRFT precoding for narrowband interference suppression in DFT-based block transmission systems. IEEE Commun Lett 17(10):1916–1919
5. Coulson AJ (2006) Bit error rate performance of OFDM in narrowband interference with excision filtering. IEEE Trans Wireless Commun 5(9):2484–2492
6. Dovis F, Musumeci L (2011) Use of wavelet transforms for interference mitigation. In: Proceedings of the ICL-GNSS, June 2011, pp 116–121
7. Jones WW, Jones KR (1992) Narrowband interference suppression using filter-bank analysis/synthesis techniques. In: Proceedings of the IEEE Milcom, Oct 1992, vol. 3, pp 898–902
8. Zhang Y, Amin MG, Lindsey AR (2001) Anti-jamming GPS receivers based on bilinear signal distributions. In: Proceedings of the IEEE Milcom, Oct 2001, pp 1070–1074
9. Miranda JP et al (2014) Narrowband interference suppression in long term evolution systems. In: Proceedings of the IEEE PIMRC, Sept 2014, pp 707–711
10. Brazilian Ministry of Communications (2009) A national plan for broadband: Brazil in high speed (in Portuguese)
11. Brazilian National Agency of Communications (ANATEL) (2010) Resolution no. 558, regulations on channelization and use conditions of radiofrequencies in the 450–470 MHz band, Dec 2010 (in Portuguese)
12. 3GPP TR 36.840, LTE 450 MHz in Brazil work item technical report, Sept 2013
13. Brazilian National Agency of Communications (ANATEL). The STEL system (Online). Available http://sistemas.anatel.gov.br/stel/
14. 3GPP TS 36.213 (2012) Physical layer procedures, Sept 2012
15. 3GPP TS 36.211 (2012) Physical channels and modulation, Sept 2012
16. Auger F, Flandrin P, Goncalves P, Lemoine O (2005) Time frequency toolbox for use with matlab, CNRS and Rice University, Oct 2005
17. Boashash B, Black PJ (1987) An efficient real-time implementation of the Wigner-Ville distribution. IEEE Trans Acoust Speech Signal Process 35(11):1611–1618
18. Kootsookos PJ, Boashash B (1987) Signal synthesis in a time-frequency domain using the Wigner-Ville Distribution. In: Proceedings of the IREE conference, pp 845–848
19. Sofer E,Chouinard G (2005) WRAN channel modeling, IEEE 802.22-05/0055r7, Sept 2005
20. Shukla KK, Tiwari AK (2013) Efficient algorithms for discrete wavelet transform with applications to denoising and fuzzy inference systems. Springer, Berlin
21. Misiti M, Misiti Y, Oppenheim G, Poggi J-M (2014) Wavelet toolbox—matlab user's guide

Link Adaptation in LTE Systems

Ricardo Toguchi Caldeira and Gilberto Gambugge Neto

Abstract This chapter explains the link adaptation mechanism used in a Long Term Evolution (LTE) system. For downlink data transmission in LTE systems, the Base Station usually selects modulation scheme and code rate depending on the prediction of the downlink channel conditions. A piece of information crucial to this selection process is the feedback from the Channel Quality Indicator (CQI) transmitted by the User Equipment (UE) in the uplink channel. For uplink transmissions in LTE systems, the link adaptation process is similar to the downlink process, with the Base Station handling the selection of the modulation and coding scheme (MCS).

1 Introduction

The principle of link adaptation is essential for the development of a radio interface project for efficient packet switching data traffic [1, 2]. Link adaptation in Long Term Evolution (LTE) systems dynamically adjusts the data rate of transmitted information (modulation scheme and channel code rate) to equalize the existing radio channel capacity assigned for each user. Link adaptation is therefore closely related to the channel code scheme project used for forward error correction (FEC).

R.T. Caldeira (✉) · G.G. Neto
CPqD Foundation, Campinas, SP, Brazil
e-mail: rtoguchi@cpqd.com.br

G.G. Neto
e-mail: gneto@cpqd.com.br

A. Paradisi et al. (eds.), *Long Term Evolution*, Telecommunications and Information Technology, DOI 10.1007/978-3-319-23823-4_6

For downlink data transmission in LTE systems, the Base Station or Evolved Node B (eNodeB) usually selects the modulation scheme and the code rate depending on the prediction of the downlink channel conditions [3]. An important piece of information for this selection process is the Channel Quality Indicator (CQI) feedback transmitted by the User Equipment (UE) in the uplink channel. CQI feedback is an indicator of the data rate that the channel can support, taking into consideration the Signal to Interference plus Noise Ratio (SINR) and the receiving characteristics of the UE [4, 5, 6]. This chapter explains the link adaptation principles applied to the LTE system. It will also show how the eNodeB can select one of the two different CQI feedback schemes, namely periodic mode or aperiodic mode.

The eNodeB will create a trade-off between the best downlink adaptation, based on the CQI (considering the informed channel quality), and the overload on the uplink channel caused by the CQI itself, i.e., channel quality control traffic. There exists therefore a trade-off between downlink adaptation and uplink overload.

LTE specifications are designed to provide the needed indicators for interoperability between eNodeB and UE, enabling the eNodeB to optimize link adaptation. The method that the eNodeB will use to explore available information is not standardized and as such left up to the manufacturer.

In general, in response to CQI feedback, the eNodeB can choose between different modulation schemes (QPSK, 16-QAM and 64-QAM) and a wide range of code rates. As it will be discussed later on in this chapter, the ideal switching point between the different modulation combinations and the code rate depends on a series of factors that include the required Quality of Service (QoS) and the cell throughput.

The channel code scheme for FEC, which is the basis for the code rate adaptation mechanism, was the object of an in-depth study during the LTE standardization process. The channel coding theory has been intensely researched over the last decades, especially with the discovery of turbo codes, offering performance close to the Shannon limit and the development of general iterative processing techniques. More advanced channel coding resources were added, with the introduction of link adaptation, including Hybrid Automatic Repeat reQuest (HARQ), a combination of ARQ and channel coding, improving robustness against channel fading. These schemes include incremental redundancy, by means of which the code rate is progressively reduced, transmitting additional parity information at each retransmission.

For LTE uplink transmission, the link adaptation process is similar to the downlink adaptation process, again with the eNodeB handling the selection of modulation and coding schemes (MCS). An identical channel coding structure is used for the uplink, while the modulation scheme can be either QPSK or 16-QAM, and for the maximum UE category, 64-QAM modulation is also available. The main difference between the uplink and downlink is that, instead of basing link adaptation on CQI feedback, the eNodeB can make its own estimate of the uplink data rate that the sounding channel can handle, e.g, by using Sounding Reference Signals (SRS).

An important final aspect regarding link adaptation is its use for time and frequency scheduling of multiple users, which allows radio transmission resources to be efficiently shared among the users (since the channel capacity for individual users varies). CQI can therefore be used not only to adapt code rate and modulation in response to actual channel conditions, but for optimal time-frequency selective scheduling and for managing interference among the cells.

The remainder of the chapter is organized as follows: in Sect. 2 the principles of link adaptation are described; in Sect. 3,the mechanism of CQI feedback in LTE is described; in Sects. 4 and 5, the two types of CQI reporting are described: aperiodic and periodic; and in Sect. 6 experimental laboratory experiments and their corresponding results are described.

2 Link Adaptation and Feedback Computation

In cellular communication systems, the quality of the signal received by a UE depends on a number of aspects, including channel quality level of interference from other cells, and noise level. In order to optimize system capacity and coverage for a specific transmission power, the transmitter (eNodeB, in LTE systems) must try to combine the data rate of each user based on the variations in quality of the received signal [1, 2]. This method is commonly called link adaptation and is usually based on Adaptive Modulation and Coding (AMC).

The degrees of freedom for AMC consist in the following (existing) MCS:

- Modulation scheme: Low-order modulation (few data bits per modulated symbol, e.g, 2 bits per symbol in QPSK) is the most robust scheme and can tolerate high levels of interference at the cost of lower transmission bit rates. In contrast, high-order modulation (more bits per modulated symbol, e.g, 6 bits per symbol in 64-QAM) offers higher bit rate but it is more prone to errors due to its greater sensibility to interference, noise, and channel estimate errors. The latter scheme is therefore useful only when the SINR is sufficiently high;
- Code rate: For a given modulation scheme, the code rate can be chosen based on the radio link conditions. Lower code rates can be used in the presence of poor channel conditions, whereas higher code rates can be used when the SINR is high enough. The adaptation of the code rate is achieved by applying puncturing or code repetition to reduce the code rate to the output of a code matrix.

A key issue in AMC design for LTE systems was whether all Resource Blocks (RBs) allocated to a user in a subframe should use the same MCS [3–6] or if the MCS should be frequency dependent within each subframe. It was shown that, in general, only a slight throughput improvement arises from a frequency-dependent MCS, compared with a RB-common MCS, in the absence of transmission power control. However, the additional overload control signaling overhead associated with frequency-dependent MCS is hard to justify. Therefore, in LTE systems, the modulation and channel coding rates are constant over the allocated frequency

resources for a given user, and time-domain channel-dependent scheduling and AMC are supported instead. In addition, when multiple transport blocks are transmitted to one user in a given subframe using multistream Multiple-Input Multiple-Output (MIMO), each transport block can use an independent MCS.

In LTE systems, the UE can be set up to report CQIs to assist the eNodeB in selecting an appropriate MCS to use for downlink transmissions. The CQI reports are derived from the received downlink signal quality, typically based on the respective measurements of the downlink reference signals. It is important to note that in LTE, the reported CQI is not a direct indication of SINR. Instead, the UE reports the highest MCS that it can decode with a transport block error rate (BLER) probability not exceeding 10 %. Thus, the information received by the eNodeB takes into account the characteristics of the UE receiver, and not just the prevailing radio channel quality. Hence, a UE designed with advanced signal processing algorithms (for example, using interference cancellation techniques) can report a higher channel quality, and depending on the characteristics of the eNodeB's scheduler, receive a higher data rate.

A simple method for the UE to choose an appropriate CQI value could be based on a set of BLER thresholds. Thereby, the UE would report the CQI value corresponding to the MCS that ensures a given BLER, based on the measured received signal quality. The list of modulation schemes and code rates, which can be signaled by means of a CQI value, is shown in Table 1 [7].

AMC can exploit the UE feedback by assuming that channel fading was sufficiently slow. This requires the channel coherence time to be at least as long as the time between the UE's measurement of the downlink reference signals and the

Table 1 CQI index for each modulation scheme and code rate

CQI index	Modulation	Approximate code rate	Efficiency (information bits per symbol)
0	No transmission	–	–
1	QPSK	0.076	0.1523
2	QPSK	0.12	0.2344
3	QPSK	0.19	0.3770
4	QPSK	0.3	0.6016
5	QPSK	0.44	0.8770
6	QPSK	0.59	1.1758
7	16QAM	0.37	1.4766
8	16QAM	0.48	1.9141
9	16QAM	0.6	2.4063
10	64QAM	0.45	2.7305
11	64QAM	0.55	3.3223
12	64QAM	0.65	3.9023
13	64QAM	0.75	4.5234
14	64QAM	0.85	5.1152
15	64QAM	0.93	5.5547

subframe containing the correspondingly adapted downlink transmission on the Physical Downlink Shared CHannel (PDSCH).

However, a trade-off exists between the amount of CQI information reported by the UE and the accuracy with which the AMC can match prevailing conditions. Frequent reports of the CQI in the time domain allow better matching to the channel and interference variations, while fine resolution in the frequency domain allows better exploitation of frequency-domain scheduling. However, both lead to increased feedback overhead in the uplink. Therefore, the eNodeB can configure both the time-domain update rate and the frequency-domain resolution of the CQI, as discussed in the following section.

3 CQI Feedback in LTE

Both periodicity and frequency resolution to be used by a UE to report CQI are controlled by the eNodeB. In the time domain, periodic and aperiodic CQI reporting are supported. The Physical Uplink Control CHannel (PUCCH) is used only for periodic CQI reporting; while the Physical Uplink Shared CHannel (PUSCH) is mainly used for aperiodic reporting of the CQI. This is how the eNodeB specifically instructs the UE to send an individual CQI report embedded into a resource that is scheduled for uplink data transmission.

The frequency granularity of the CQI reporting is determined by defining a number of sub-bands (N), each comprised of k contiguous Physical Resource Blocks (PRBs). The value of k depends on the type of CQI report considered. In each case the number of sub-bands spans the whole system bandwidth and is given by

$$N = \left[N_{\mathrm{RB}}^{\mathrm{DL}} / k \right] \tag{1}$$

where $N_{\mathrm{RB}}^{\mathrm{DL}}$ is the number of RBs which comprise the system bandwidth. The CQI reporting modes can be wideband CQI, eNodeB-configured sub-band feedback, or UE-selected sub-band feedback. These modes are explained in detail in the following section. In addition, in the case of multiple transmit antennas at the eNodeB, CQI value(s) may be reported for a second codeword.

For some downlink transmission modes, additional feedback signaling is transmitted by the UE, consisting of Precoding Matrix Indicators (PMI) and Rank Indicators (RI).

4 Aperiodic CQI Reporting

Aperiodic CQI reporting transmitted on the PUSCH is scheduled by the eNodeB by setting a CQI request bit in an uplink resource grant sent on the Physical Downlink Control CHannel (PDCCH). The type of CQI report is configured by

the eNodeB via RRC signaling. Table 2 summarizes the relationship between the configured downlink transmission mode and the Aperiodic CQI reporting mode, which can be:

(a) **Wideband feedback**: The UE reports one wideband CQI value for the whole system bandwidth.
(b) **eNodeB-configured sub-band feedback**: The UE reports a wideband CQI value for the whole system bandwidth. In addition, the UE reports a CQI value for each sub- band, calculated assuming transmission only in the relevant sub-band. The size of sub-band k is a function of the system bandwidth, as resumed in Table 3.
(c) ***UE-selected sub-band feedback***: The UE selects M preferred sub-bands of size k in the whole system bandwidth (where *k* and *M* are presented in Table 4 for each bandwidth). The UE reports one wideband CQI value and one CQI value presenting the average quality of the M-selected sub-bands.

Table 2 Aperiodic CQI feedback types on PUSCH for each PDSCH transmission mode

PDSCH transmission mode	Wideband only	UE-selected sub-bands	eNodeB-configured sub-bands
Mode 1: single antenna port		X	X
Mode 2: transmission diversity		X	X
Mode 3: open-loop spatial multiplexing		X	X
Mode 4: closed-loop spatial multiplexing	X	X	X
Mode 5: multi-user MIMO			X
Mode 6: closed-loop rank-1 precoding	X	X	X
Mode 7: UE-selected reference signals		X	X

Table 3 Sub-band size *k* versus system bandwidth for eNodeB-configured aperiodic CQI reports

System bandwidth (RBs)	Sub-band size (*k* RBs)
6–7	Wideband CQI only
8–10	4
11–26	4
27–63	6
64–110	8

Table 4 Sub-band size k and number of preferred sub-bands (M) versus downlink system bandwidth for aperiodic CQI reports for UE-selected sub-bands feedback

System bandwidth (RBs)	Sub-band size (k RBs)	Number of preferred sub-bands (M)
6–7	Wideband CQI only	Wideband CQI only
8–10	2	1
11–26	2	3
27–63	3	5
64–110	4	6

Table 5 Periodic UE-selected sub-band CQI reporting sub-band size (k) and bandwidth parts (J) versus downlink system bandwidth

System bandwidth (RBs)	Sub-band size (k RBs)	Number of bandwidth parts (J)
6–7	Wideband CQI only	1
8–10	4	1
11–26	4	2
27–63	6	3
64–110	8	4

5 Periodic CQI Reporting

If the eNodeB wants to receive periodic CQI reports from the UE, the UE will transmit the reports over PUCCH. If the PUSCH transmission resources are allocated to the UE in one of the periodic subframes, the periodic CQI report is sent over PUSCH. Only wideband and UE-selected sub-band feedback are available for periodic CQI reporting for all downlink transmission modes. As in the case of aperiodic CQI reports, the type of periodic report is decided by eNodeB via RRC signaling.

While wideband feedback mode is similar to reports sent over PUSCH, the CQI from UE-selected sub-band is different. In this case, the total number of sub-bands N is divided into J fractions called bandwidth parts. The value of J depends on system bandwidth, as summarized in Table 5. In the case of periodic UE-selected sub-band CQI reporting, one CQI value is computed and reported for a single selected sub-band from each bandwidth part, along with the corresponding sub-band index.

6 Experimental Results

In order to illustrate the LTE link adaptation performance, an experimental setup, which was composed of real eNodeBs and UEs with variable attenuators to simulate the link path loss, was built. By varying link attenuation under controlled

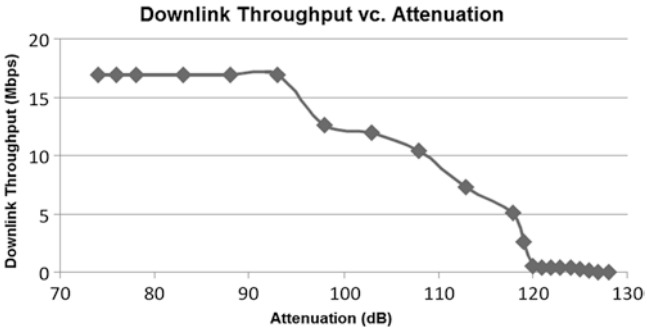

Fig. 1 Downlink throughput (Mbps) versus attenuation (dB)

conditions and environment, corresponding variations of MCS, SNR, and RSSI_RS were evaluated.

The following configuration was used in the reference setup of the LTE system:

- 5 MHz bandwidth (25 RBs)
- Attenuation variation: from 74 to 128 dB
- CQI reporting mode 1-0 (periodic wideband CQI reporting)
- Transmission mode: TM2
- UDP and TCP traffic generated with iperf tool [8]

Figure 1 shows the downlink throughput and Fig. 2 shows the modulation and code model based on attenuation variation. The terminal can connect to a network with a link attenuation of up to 118 dB, and once connected, downlink channel can operate with attenuation level up to 128 dB.

A downlink MCS varying from 0 to 9 corresponds to QPSK modulation (2 bits per symbol); a downlink MCS varying from 10 to 16 corresponds to 16-QAM modulation (4 bits per symbol); and a downlink MCS varying from 17 to 28 corresponds to 64-QAM modulation (6 bits per symbol). Only downlink traffic was used to calculate UE sensitivity.

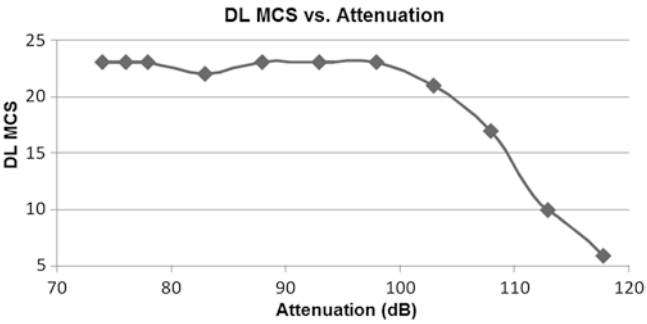

Fig. 2 Downlink MCS versus attenuation (dB)

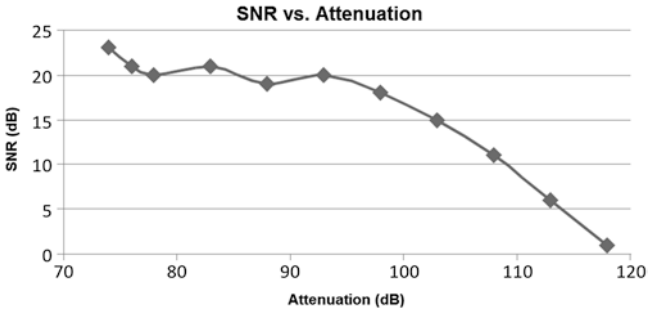

Fig. 3 SNR versus attenuation (dB)

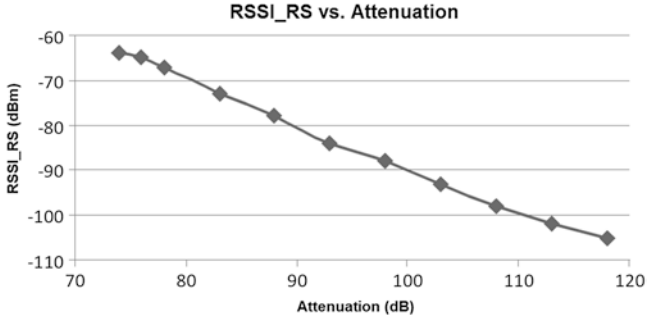

Fig. 4 RSSI_RS versus attenuation (dB)

Figure 3 presents the SNR based on attenuation. And Fig. 4 shows the RSSI_RS based on attenuation. RSSI_RS is defined as the total wideband power received by the UE of all reference signal (RS) subcarriers.

7 Conclusion

This chapter has explained the link adaptation mechanism used in LTE systems. For downlink data transmission in LTE systems, the eNodeB usually selects modulation scheme and code rate depending on the prediction of the downlink channel conditions. An important piece of information for this selection process is feedback from the CQI transmitted by the UE in the uplink channel. For uplink transmissions in LTE systems, the link adaptation process is similar to the downlink process, with the eNodeB handling the selection of the MCS.

As described, the degrees of freedom for the link adaptation mechanism AMC consist in the existing MCS. Furthermore, CQI feedback mechanisms in LTE comprise aperiodic CQI reports (wideband feedback, eNodeB-configured sub-band feedback, and UE-selected sub-band feedback) and periodic CQI reports.

Acknowledgments The authors would like to thank the support received for this project, developed within the scope of the RASFA Project – Advanced Wireless Access Network, sponsored by FUNTTEL, under Agreement No. 01.09.0631.00.

References

1. Goldsmith AJ, Chua SG (1998) Adaptive coded modulation for fading channels. IEEE Trans Commun 46(5):595–602
2. HAYES J (1968) Adaptive feedback communications. IEEE Trans Commun Technol 16:15–22
3. LG Electronics (2013) **R1-060051**: link adaptation in E-UTRA Downlink., 3GPP TSG RAN WG1 LTE ad Hoc, Helsinki, Finland, January 2006c. Available at: http://www.3gpp.org/ftp/tsg_ran/wg1_rl1/TSGR1_AH/LTE_AH_January-06/Docs/. Accessed on: 01 ago. 2013
4. 3rd GENERATION PARTNERSHIP PROJECT (3GPP) NTT DoCoMo, Fujitsu (2006a) Mitsubishi Electric Corporation, NEC, QUALCOMM Europe, Sharp, and Toshiba Corporation, **R1-060039**: Adaptive Modulation and Channel Coding Rate Control for Single-antenna Transmission in Frequency Domain Scheduling in E-UTRA Downlink. 3GPP TSG RAN WG1 LTE Ad Hoc, Helsinki, Finland. Available at: http://www.3gpp.org/ftp/tsg_ran/wg1_rl1/TSGR1_AH/LTE_AH_January-06/Docs/. Accessed on: 01 ago. 2013
5. NTT DoCoMo, Fujitsu, Mitsubishi Electric Corporation (2006b) NEC, Sharp, and Toshiba Corporation. **R1-060040**: adaptive modulation and channel coding rate control for MIMO transmission with frequency domain scheduling in E-UTRA Downlink. 3GPP TSG RAN WG1 LTE ad Hoc, Helsinki, Finland. Available at: http://www.3gpp.org/ftp/tsg_ran/wg1_rl1/TSGR1_AH/LTE_AH_January-06/Docs/. Accessed on: 01 ago. 2013
6. Samsung (2013) **R1-060076**: Adaptive Modulation and Channel Coding Rate. 3GPP TSG RAN WG1 LTE ad Hoc, Helsinki, Finland, January 2006d. Available at: http://www.3gpp.org/ftp/tsg_ran/wg1_rl1/TSGR1_AH/LTE_AH_January-06/Docs/. Accessed on: 01 ago. 2013
7. Technical Specification **36.213** (2013) Evolved Universal Terrestrial Radio Access (E-UTRA); Physical Layer Procedures (Release 8). 2008. Available at: http://www.3gpp.org/DynaReport/36213.htm. Accessed on: 01 ago. 2013
8. Iperf (2015) Available at: https://iperf.fr/. Acessed on: 09 June 2015

Method and Test Environment for the Validation of Random Access Channel for Long Term Evolution Systems in 450 MHz

Ricardo Toguchi Caldeira, Juliano João Bazzo, Elisabete Banza de Arruda Faber and João Paulo Miranda

Abstract Field tests usually demand resources such as human, equipment, and materials. Moreover, other factors that cannot be controlled, such as weather conditions and the presence of interfering signals, result in the unpredictability and increase of test execution time when compared with laboratory tests. This chapter presents a validation method for the Physical Random Access Channel (PRACH) from the 450 MHz Long Term Evolution (LTE) system. The proposed method results in significant reduction of the execution time and costs involved in the experiments when compared with experiments executed in the field. The method does not fully replace the field tests, however it has the advantage of allowing greater flexibility in terms of test scenarios, thus having a positive effect, mainly during the product development phases. Laboratory test setup using the proposed method and experimental results are also presented.

R.T. Caldeira (✉) · J.J. Bazzo · E.B. de Arruda Faber · J.P. Miranda
CPqD Foundation, Campinas/SP, Brazil
e-mail: rtoguchi@cpqd.com.br

J.J. Bazzo
e-mail: jbazzo@cpqd.com.br

E.B. de Arruda Faber
e-mail: efaber@cpqd.com.br

J.P. Miranda
e-mail: jmiranda@cpqd.com.br

A. Paradisi et al. (eds.), *Long Term Evolution*, Telecommunications and Information Technology, DOI 10.1007/978-3-319-23823-4_7

1 Introduction

Mobile communication technology systems have been improving constantly to meet the increasing demand of traffic generated by video and Web access applications. The Long Term Evolution (LTE), which began to gain more attention from 2008 with the consolidation of its Release 8, has undergone constant evolution, achieved mainly in anticipation of completion of the Release 12 by the 3rd Generation Partnership Project [1].

This new standardization effort has acted in several areas, such as the interference cancellation, cooperation between cells, carrier aggregation, multiple antennas, among others, making the system more and more complex. LTE, operating in the band of 450 MHz, mainly emerged as a proposal within the scope of Release 12, to bring broadband and communication services to areas served precariously or even devoid of any telecommunications service, such as the rural and remote locations. This is a new profile of LTE technology with the operation in the 450–470 MHz band, which can provide more favorable propagation conditions than those obtained in higher frequency bands, resulting in higher than the radii of coverage of the current profiles standardized in 3GPP.

The effort for the specification and the development of LTE 450 MHz has started focusing on the Brazilian scenario, where the deployment of this technology should contribute to the government's goal of providing universal access to broadband services throughout the country, trying to reach all Brazilian citizens [2]. This means providing these services also to rural areas, covering a vast territory of Brazil, with a population of about 30 million people. To this end, the Brazilian government recently established policies to enable the use of this spectrum in 450 MHz for rural areas, which culminated in 2012 with the auction of operating licenses, based on Resolution 558 of Anatel [3]. Other more recent initiatives of the government include the National Broadband Plan (PNBL), also driven by the availability of LTE 450 MHz as a viable alternative to meet the objectives of this program in rural areas. These actions are complementary and create investment leverage conditions for the telecommunications industry, contributing to the development of an even more promising and dynamic scenario.

The application of LTE 450 MHz is not restricted to the Brazilian scenario. The 3GPP considers this profile as a global application and as an appropriate option for deployment of Fourth Generation (4G) cellular networks in regions with low population density. The completion of this expansion is challenging, depending on the definition of economically sustainable models, particularly when we consider the deployment, operation, and maintenance of networks.

The standardization process of the 450 MHz band for LTE was launched in September 2012 for a Brazilian company in the 3GPP for the first time. Several challenges were faced and overcome, related to spectrum plumbing, coexistence with adjacent services, and definition and adjustment of transmission/reception performance parameters [4]. The goal was to create conditions which will allow the cell coverage of the order of tens of kilometers, more adequate to scenarios

lacking appropriate infrastructure, including items such as backhaul and electrical installation.

Finally, in June 2013, the 450 MHz band became part of the LTE standard, called band 31 [5], representing an important milestone for operators and industries to intensify its investment in LTE technology for this band.

For the industry, this means developing products able to meet the specific operating conditions of the mentioned priority application scenarios, with the attendance of cells covering extensive areas as one of the most important scenarios. This directly impacts the random access procedure of PRACH, which must be adequate and properly assessed.

Therefore, this chapter aims to present an efficient method which enables the evaluation, adaptation, and validation of the random access procedure of the Physical Random Access Channel (PRACH) in the laboratory, resulting in a positive impact on the development of the algorithms used in this procedure. The presentation of this work includes a description of the implementation of the testing scenario in laboratory, the analysis of the results obtained in the laboratory by such implementation, and a comparison with the results obtained in field tests to validate the results obtained in the laboratory.

The remainder of the chapter is organized as follows. Sect. 2 describes the random access procedure in the LTE system. Sect. 3 presents relevant aspects of the Radio over Fiber (RoF) technology used as basis for the development of the laboratory setup. Sect. 4 details the implementation of the experimental evaluation scenario and provides an analysis of the results. Finally, conclusions are offered in Sect. 5.

2 Random Access Procedure in LTE

A fundamental requirement for any mobile system is the possibility of the terminal request for a connection configuration on the reverse link (or uplink), commonly referred to as random access. This connection configuration is performed in the LTE system through a specific channel called PRACH. This channel allows initial network access and synchronization, on the uplink direction, of the User Equipment (UE) transmissions with the temporal frame structure determined by the Base Station or Evolved Node B (eNodeB). Thus, once the connection is established in the uplink, the UE may receive sufficient bandwidth allocation for data transmissions on the Physical Uplink Shared CHannel (PUSCH) and control on the Physical Uplink Control CHannel (PUCCH).

Therefore, the LTE PRACH is a physical channel designed for transmission by the UE characterized as a signal preamble, which enables the eNodeB to calculate the frame synchronization parameter known as Timing Advance (TA). This parameter is then informed by the eNodeB to the UE by the forward link (descent or downlink), enabling the UE to do the temporal setting of transmissions, as the uplink frame structure [6].

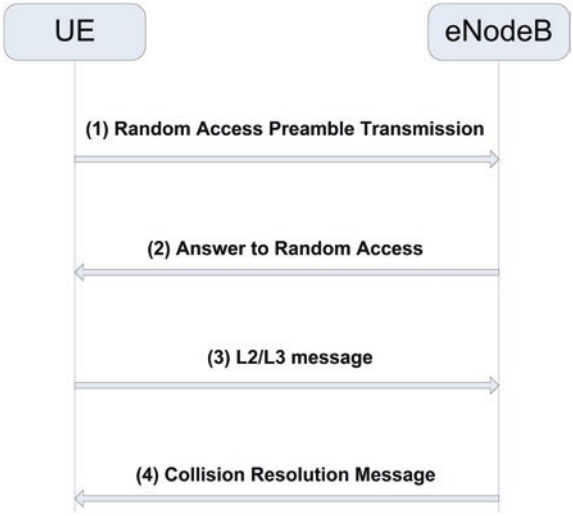

Fig. 1 Random access procedure based on dispute

In LTE, a fixed number of up to 64 preambles (or signatures) are available in each cell [7] and the operation of the two kinds of PRACH procedures, based on the occurrence or the absence of possibility of collision, depends on the partition of these signatures between these two types of procedures.

For the PRACH procedure with possibility of collision occurrence (also known as Contention Based, it will be described in this chapter in more detail because it is the procedure adopted during the first attempt by the UE connection), four steps are identified [6, 8]. These steps are illustrated in Fig. 1 and detailed below.

2.1 Step 1: Transmission of Random Access Preamble

It has 1 byte information, indicating the L2/L3 (Layer 2 and Layer 3) message length which will be transmitted in Step 3. The primary purpose of transmission of the preamble is the eNodeB to indicate the presence of a random access attempt and allow eNodeB to estimate the delay associated with the distance from the terminal. The estimated delay is used in Step 2 to adjust the timing of transmission in the uplink frame.

2.2 Step 2: Answer to Random Access

Used to adjust the time of transmission of the terminal, it is estimated based on estimated delay in Step 1. The Random Access Response (RAR) is sent by the eNodeB in the Physical Downlink Shared Channel (PDSCH) and addressed with

an identification (ID), called Random Access Radio Network Temporary Identifier (RA-RNTI), identifying the time–frequency slot in which the preamble has been detected. The RAR carries:

(a) The identity of the detected preamble, i.e., the signature to be used by the UE;
(b) TA instruction, which aims to synchronize the subsequent uplink UE transmissions with the eNodeB;
(c) A permit or initial grant of uplink resources (scheduling grant) for L2/L3 message transmission in Step 3;
(d) The assignment of a Temporary Cell/Cell-Radio Network Temporary Identifier (TC-RNTI or C-RNTI) used to enable communication between the terminal and the core network.

2.3 Step 3: L2/L3 Message

L2/L3 Message and terminal ID. This message is the first uplink transmission allocated in the PUSCH and makes use of Hybrid Automatic Repeat reQuest (HARQ). It includes the Temporary C-RNTI allocated to the RAR in accordance with Step 2 or C-RNTI if the UE has already entered the RRC_CONNECTED state, or the 48-bit unique identification of the UE, if it is the first UE access to the service provider's network.

In case a preamble collision occurred in Step 1, the colliding UEs receive the same Temporary C-RNTI via RAR, resulting in the superposition of uplink time–frequency resources when the UEs transmit their L2/L3 messages. The following downlink message (in Step 4) allows a quick resolution of this conflict.

2.4 Step 4: Collision Resolution Message

The last step consists in transmitting a conflict resolution message from the Radio Access Network (RAN), on the DL-SCH addressed to the terminal. This step also enables the resolution of any conflict arising from attempts by several terminals to access the system using the same resource available for random access.

It is important to highlight that the random access procedure in LTE does not employ any mechanism for carrier sense. Thus, to detect whether there is transmission in the PRACH in order to minimize the possibility of collision becomes meaningless, since even when the PRACH is already occupied by another UE, it still can be transmitted through this channel since the preamble sequences used by different UEs are orthogonal. In fact, it is considered that there is a collision only when more than one UE transmits with the same sequence selected among the 64 possible preambles and occupies a single time–frequency resource. To avoid collisions, the cells can be configured in the access network using statistics previously

obtained in access occurrences. However, in this configuration, there is a trade-off between the cell data flow and the magnitude of the resources available to the PRACH. For a cell where there are a large number of hits, it is necessary to set up more opportunities or resources (subframes) for the PRACH in the same frame. However, allocating more resources for the PRACH implies decreasing resources for data transmission in the PUSCH, causing a reduction in the total throughput of the cell.

The PRACH procedure without considering the possibility of collision (also known as contention free) is only used in handover scenarios or when data is received in the downlink with the UE in RRC_CONNECTED state. In this procedure, the eNodeB reserves a set of preambles and in the occurrence of an applicable scenario, the eNodeB allocates one of these preambles. As this procedure is completely controlled by the eNodeB, there are no bumps and the UE is informed exactly when and which preamble sequence it should transmit.

3 Radio Over Fiber

RoF systems have a diversity of applications based on the possibility of distribution of Radio Remote Units (RRU) comprising the antenna and the transmission and reception chains consisting of radio frequency devices.

The applications of these systems benefit from the low transmission losses and distortion of signals carried over optical fiber, increasing flexibility and the range of applications.

Examples of this flexibility that can be cited are the distribution, extent, and cell formatting in mobile system [9], the centralization of the installation of the baseband units of base stations in a sheltered and air conditioned environment, and the implementing transmission diversity schemes using multiple remote units and antennas (Multiple-Input Multiple-Output—MIMO) [10].

In some of these applications, when the objective is to provide wireless infrastructure in urban areas with high density, installation within commercial buildings and airport terminals, or in industrial environments characterized by high level of electromagnetic interference and therefore subject to special requirements of service availability, radio-over-fiber solution has additional advantages. These advantages come from the ease of installation, operation and maintenance, as well as the support for product-specific requirements, which result in significant cost savings.

In short, the fiber-radio system is fundamentally an analog transmission system because it distributes the “waveform” directly on the frequency of the radio bearer, a central unit to the Remote Access Unit (RAU), or remote units for systems using MIMO or multisector base stations. In the case of LTE signal, comprising a set of subcarriers dynamically allocated, and high-level modulation, the radio-over-fiber system becomes quite interesting because it shows the possibility of signal transmission over long distances, without loss of capacity. These characteristics have been proven, for example, for standard Worldwide Interoperability

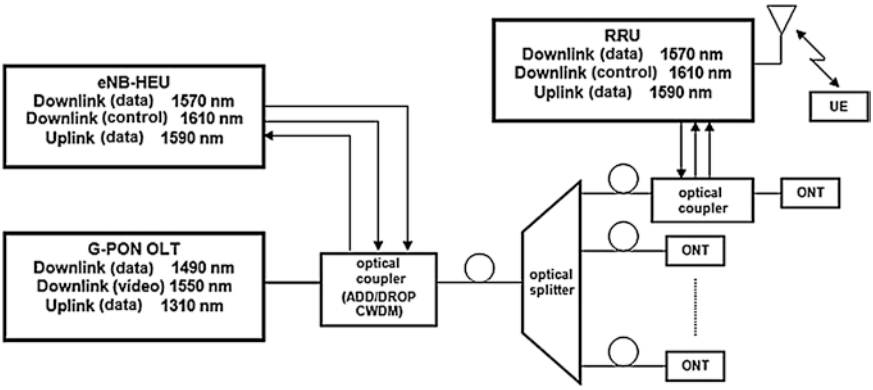

Fig. 2 Integration of the LTE system using RoF over a G-PON infrastructure

for Microwave Access (WiMAX) signals, which also uses Orthogonal Frequency-Division Multiplexing (OFDM) technology and high-level modulations [11].

Essential components of typical RoF solutions are electro-optical converter and optical coupler. The first is an active device that converts an electrical RF signal, modulated and with analog information in its input to an optical signal at its output, which carries these analog information. To compose the optical link two conversion devices are needed: the transmitter and the receiver. The coupler allows the insertion of optical signal into the fiber, enabling the sharing with other systems, for example, Gigabit Passive Optical Network (G-PON) point-multipoint or other patterns, making it a more economically attractive solution, especially in cases where there are large distances between RAUs and the baseband of a wireless broadband system.

Figure 2 illustrates the possibility of integrating an LTE broadband transmission system operating in Frequency Division Duplexing (FDD) mode with a G-PON network. In the figure the connections between the RAU and the unit containing the baseband, Head End Unit (HEU), using the RoF transmission inserted in the G-PON's optical fiber infrastructure network, are illustrated schematically.

The infrastructure connects the Optical Line Terminal (OLT) to the Optical Network Terminal (ONT). In such integration, performed in the laboratory at CPqD, but using the standard WiMAX 802.16e operating in Time Division Duplexing (TDD) mode, the viability was checked via direct transmission signals (downlink) on 64-QAM modulation, over 20 km of fiber.

Figure 3 is a picture of the laboratory setup used. With this setup it was found that the losses of efficiency of the system depend on the configuration of the optical network, mainly on the type of splitter used in the distribution.

Figure 4 lists the relative transmission efficiency at its maximum rate (64-QAM modulation) on the downlink as a function of the maximum attenuation (dynamic range) and distance of optical link (4.14–20 km).

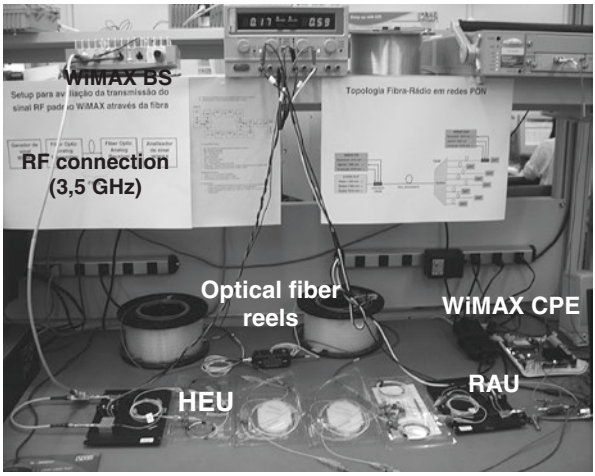

Fig. 3 RoF evaluation setup in laboratory

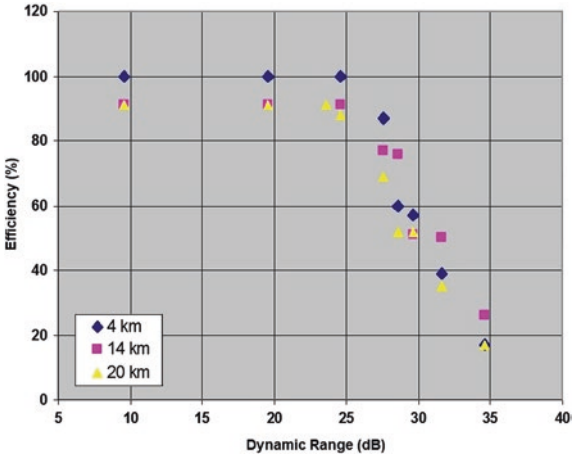

Fig. 4 RoF's transmittion efficiency

4 Test Execution and Results

4.1 Test Environment

The method proposed in this chapter consists in the usage of the test environment shown in Fig. 5, which implements the test scenario to evaluate the PRACH in the laboratory.

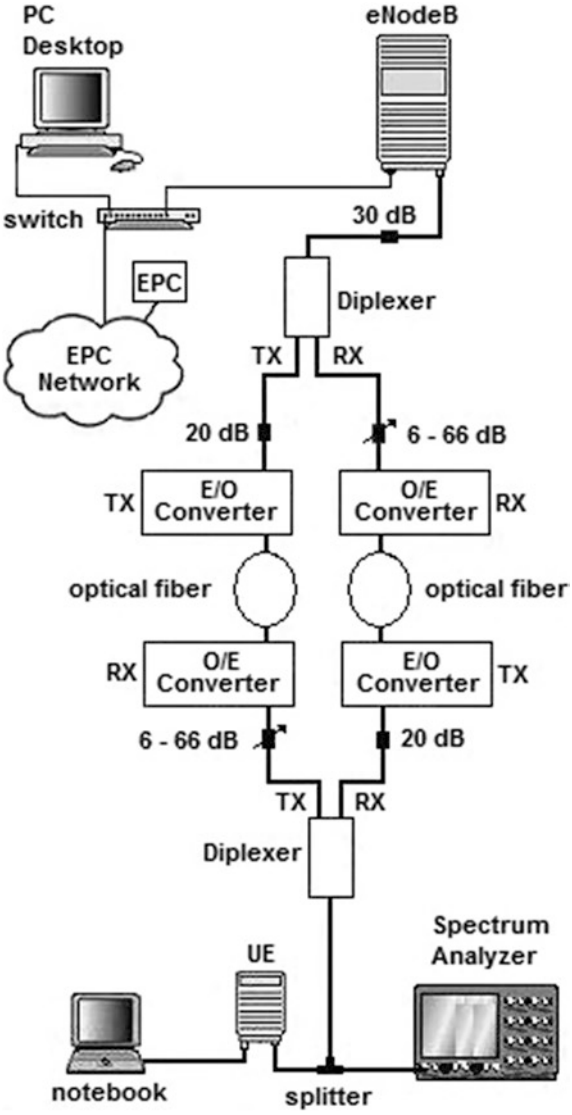

Fig. 5 Test environment in laboratory

The following elements are used to implement the test environment:

(a) eNodeB LTE;
(b) UE LTE;
(c) *Diplexers*: used to separate or unite the transmission (Tx) and receive (Rx) channels, spaced in frequency (FDD), used in the RF link established between the eNodeB and the UE;

(d) Electro-optical converters: used in signal conversion, from RF to optical (before passing the optical fibers) and from optical signal to RF (after passing through the optical fiber). Includes optical couplers that can perform the insertion of the optical signal into the fiber;
(e) Fiber optic reels: used to simulate long distance links. With the use of very compact spools with fiber lengths of the order of tens of km, the emulation of large distance links in the lab's confined environment, becomes possible;
(f) Attenuators (fixed and variable): fixed 20 dB attenuators connected to the input of the electro-optical converters (transmitting) to assure the linearity of the optical signal injected into or extracted from the fiber and thus maintaining the best operating point at the optical link. The variable attenuators connected to the outputs of the optical-to-RF converters have the function of simulating the path loss at the link by the introduction of a compatible attenuation with distance from the link to be tested. Values used were close to those observed in field tests, allowing to take into account other factors apart from path loss. For instance, the loss due to the partial line of sight obstructions.

The main purpose of this test is to check the operation of PRACH channel algorithms, as well as the validation of the settings that allow the UE attach procedure at maximum specified distance.

In other words, the goal is to validate the maximum cell radius set in the eNodeB in a controlled laboratory setting. This approach significantly facilitates the subsequent execution of field tests.

To calculate the length of the air link simulated by the optical link, we use a factor of 1.5, i.e., every 1 km of optical fiber link corresponds to 1.5 km of air link. This correspondence is determined by the refractive index of the optical fiber (approximately 1.5 compared to air), which directly affects the speed of light in the fiber, that is, 50 % lower than the speed over the air [12].

In the eNodeB configuration files, the following standard parameters for the PRACH configuration are changed to enable the maximum distance to be considered between the UE and the eNodeB:

- *rootSequenceIndex*: corresponding to the index of the Zadoff–Chu sequence, identified by the parameter RACH_ROOT_SEQUENCE, used in determining the 64 possible PRACH sequences of the random access preamble provided in the cell;
- *zeroCorrelationZoneConfig*: used in the calculation of the preamble sequence;
- *highSpeedFlag*: this flag, when active, indicates that the UE's scenario usage involves moving at high speed, resulting in higher frequency shifts as a result of the Doppler effect;
- *prach_ConfigIndex*: used in the definition of the frame resource allocation for PRACH;
- *prach_FreqOffset*: defines the first physical resource block to be allocated in an access attempt through PRACH procedure.

4.2 Validation Method

The validation of the implementation of the PRACH procedure in the laboratory consists of the following steps presented in the execution sequence below:

(1) eNodeB configuration, according to the cell size and the preamble format;
(2) Setting the variable attenuation on the output of the O/E converter in order to simulate the estimated path loss for the distance to be tested;
(3) Calculating the lengths of optical fiber spools used in the test, corresponding to the distance to be validated;
(4) After the eNodeB activation, verify that the UE makes the Public Land Mobile Network (PLMN) search procedure (i.e., detects and processes the signal transmitted by the eNodeB). Subsequently, measure the parameters related to the signal levels received by the UE Received Signal Received Power (RSRP) or Received Signal Strength Indicator (RSSI) and signal-to-noise ratio (SNR);
(5) Verification of the implementation of the UE attach procedure (connect and register the user). This is the most important step, as it is the procedure that occurs to validate the PRACH algorithm;
(6) Performance evaluation of the link, including throughput testing and data file transfer.

Note that the setup shown in Fig. 5 was set to equipment supporting operation in transmission with Single-Input Single-Output (SISO) mode at eNodeB and UE, simplifying the test scenario. However, this characteristic does not invalidate the above-described procedure or the proposed method, since the PRACH procedure is not dependent on the transmission mode.

4.3 Experimental Results

The test scenario described in the previous section, used during the development of software responsible for implementing the PRACH procedure, is illustrated in Fig. 6.

Several versions of the software were generated and tested, and some of the results from tests performed in the laboratory were compared with those obtained in field tests. The similarity of the results proves the effectiveness of the method.

To obtain the results presented in this chapter, a software version developed to support the preamble format 0 was used and the following set of parameters for the PRACH was used:

(a) $rootSequenceIndex = 328$
(b) $zeroCorrelationZoneConfig = 14$
(c) $highSpeedFlag = 0$
(d) $prach\_ConfigIndex = 0$
(e) $prach\_FreqOffset = 10$

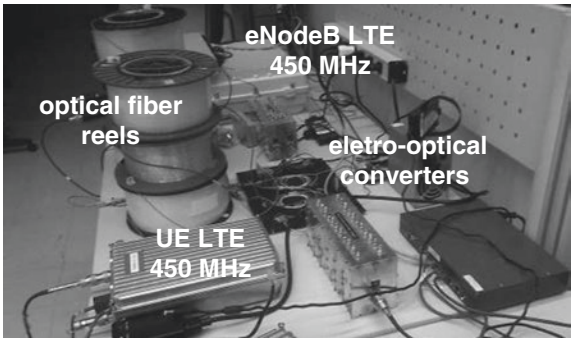

Fig. 6 Laboratory test *setup* of LTE 450 MHz system using optical fibers

Table 1 Length of optical fiber reels used in the laboratory tests

Length of the optical link (km)	Equivalent distance in the link over the air (km)
10	15.0
20	30.0
24	36.0
27	40.5
30	45.0

Table 2 Values of attenuation used to simulate path loss in laboratory tests

Distance simulated (km)	Additional attenuation (dB)	Total path loss (dB)
15.0	30	80
30.0	45	95
36.0	50	100
40.5	55	105
45.0	58	108

This setting is compatible with a theoretical coverage radius cell to 38.84 km [8].

For the test in the laboratory, measurements were made for the lengths of optical fiber reels described in Table 1.

In order to simulate the path loss corresponding to the distances of the links simulated in the optical fiber environment, an additional attenuation was inserted with the variable attenuator, as shown in Table 2.

Table 3 shows the results obtained under these conditions and according to the procedure described in Sect. 4.

It is noteworthy that, in the laboratory, even the much larger distances to those specified for a successful connection of the UE, it is possible to perform part of the procedure, proven by detecting and processing, in the UE, the signal transmitted by the eNodeB. In other words, failure of UE attach procedure is not necessarily the result of a low signal level received by the UE, but by the impossibility of a

Table 3 Laboratory test results, UE distance (km)

	PLMN search	RSSI (dBm)	SNR (dB)	UE attach
15.0	OK	−64	27	OK
30.0	OK	−84	22	OK
36.0	OK	−88	20	OK
40.5	OK	−91	17	NOK
45.0	OK	−94	12	NOK

Table 4 Field test results, near Campinas (SP)

UE distance (km)	PLMN search	RSSI (dBm)	SNR (dB)	UE attach
13	OK	−71	20	OK
16	OK	−80	20	OK
27	OK	−91	10	OK
30	OK	−90	14	OK
36	OK	−74	22	OK

Table 5 Field test results, near Brasília (DF)

UE distance (km)	PLMN search	RSSI (dBm)	SNR (dB)	UE attach
37	OK	−78	21	OK
38	OK	−84	17	NOK
40	OK	−92	12	NOK
52	NOK	–	–	–

frame synchronization establishment, an essential step for the correct operation of the processes in charge of the layers 2 and 3 of LTE.

After system validation in laboratory, field tests were conducted in various scenarios for UE locations in points with the following distances from eNodeB: 13, 16, 27, 30, 36, 37, 38, 40, and 52 km.

For the distances presented in Tables 4 and 5, the results obtained in the field tests are presented, considering the same parameters as used in the laboratory tests (with results presented in Table 3).

Regrettably, it was not possible to perform field tests for the same distances simulated in laboratory tests, because for the field tests we chose the most favorable points for the measurements.

It is important to note that for tests carried out at distances up to 30 km an omnidirectional antenna was used, with a gain of 5 dBi, installed on the roof of the car used in the tests, while for the tests at distances exceeding 30 km, a Yagi antenna (directional) with a gain of 13 dBi was used. The difference in performance is visible in Table 4, because the test 36 km showed better values of RSSI and SNR, when compared with the values obtained in the test 30 km.

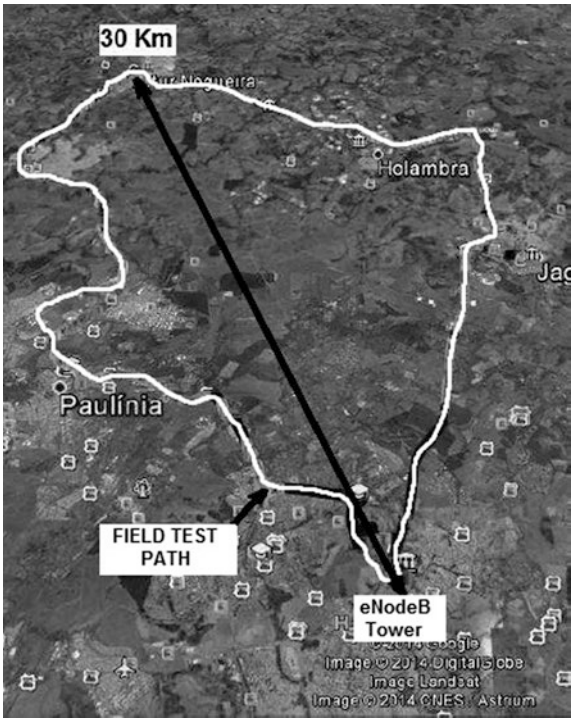

Fig. 7 Field test route, in the city of Campinas (SP), near CPqD premises

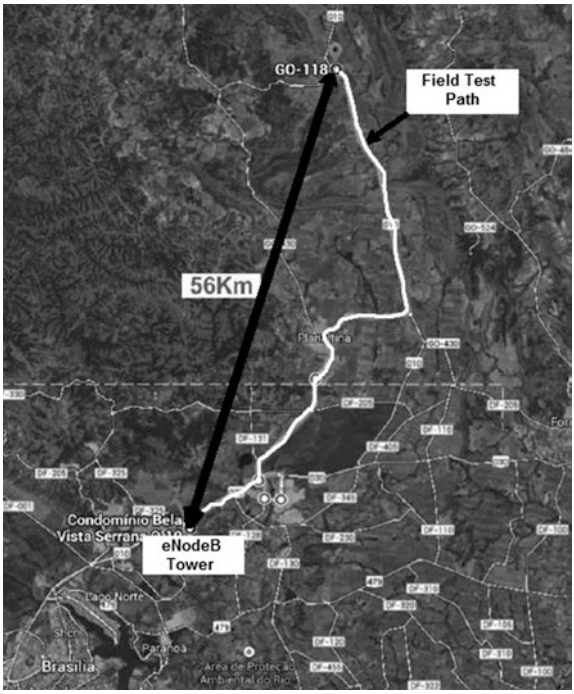

Fig. 8 Field test route, in the city of Sobradinho (DF), near Brasília (DF)

Another important detail to be discussed is related to the characteristics of the area where the field tests were performed, since the results of tests performed at distances of 13, 16, 27, 30, and 36 km were obtained in the city of Campinas (SP), with the eNodeB and its antenna installed in the tower of CPqD (Fig. 7), while the results obtained at distances of 37, 38, 40, and 52 km were collected in the region of Brasilia (DF) with the eNodeB and its antenna installed in the tower in the city of Sobradinho (DF) (Fig. 8), i.e., in different conditions of topography and morphology.

5 Conclusion

In this chapter we presented a method for the validation of the PRACH procedure, which was widely used during the development of LTE 450 MHz at CPqD. This method is particularly useful for this band, because one of the main advantages of the LTE 450 MHz system is to attend to the cells with coverage of the order of tens of kilometers.

The validation of the implementation of PRACH algorithms in the laboratory, i.e., before the field tests, enabled the implementation of the necessary adjustments with a significant reduction in costs, avoiding the costs associated to activities and resources necessary to carry out systemic tests in the field or in real operation environment.

By analyzing the results obtained in the laboratory, including the confrontation with results obtained in the field, it was possible to validate, with a very good accuracy, the distance limit for the UE attach procedure. Even before obtaining the final version of software used in the field tests, tests were performed in the laboratory in several versions. These tests made it possible to anticipate implementation problems and make the necessary adaptations and adjustments. If the field tests would have been necessary to validate the implementation of PRACH algorithms, the cost would be much higher and the impact on the development time would be quite significant.

Other parameter measurements made during the tests, such as RSSI, SNR, and system performance data transmission capacity (the latter is not considered in this chapter because it is not relevant to the analysis of the method described in this chapter), could not be compared because of the difficulty of reproduction in laboratory of all conditions encountered in the field. In fact, in the field, other factors, such as fading, multipath, and presence of interference and influences associated with the type of relief and antennas used, may cause discrepancies between the values obtained in the field and laboratory. It is important to remember that this method enables, in the way it is currently implemented, to emulate only the path loss and the propagation delay (by considering the relative refractive index of the optical fiber).

Therefore, it is important to highlight that the results obtained so far are promising, justifying the use of the method as a development tool of LTE 450 MHz

system. Among the next steps in the development of the system, an increased cell area, which must be of at least 70 km radius, is planned.

Among other improvements planned for the methodology, aiming toward the approach of the test in the laboratory to the scenario found in field tests, the inclusion of interfering signals and the incorporation of fading simulators, considering variations of signals associated with mobility, can be highlighted.

References

1. 3rd Generation Partnership Project (3GPP) (2014) 3GPP Releases. Disponível em: <http://www.3gpp.org/specifications/67-releases>. Acesso em: ago. 2014
2. PNBL—Programa Nacional de Banda Larga (2014) Disponível em: <http://www.mc.gov.br/programa-nacional-de-banda-larga-pnbl>. Acesso em: ago. 2014
3. Agência Nacional de Telecomunicações (ANATEL) (2010) Resolução nº 558. 20 de dezembro de 2010. Disponível em: <http://legislacao.anatel.gov.br/resolucoes/2010/24-resolucao-558>. Acesso em: ago. 2014
4. Rocha A et al (2013) On the adoption of LTE 450 MHz technology as a tool to leverage broadband services in rural and remote areas. ITU News magazine, n. 10., 2013. Disponível em: <https://itunews.itu.int/En/4618-LTE-450MHz-technology-for-broadband-services-in-rural-and-remote-areas-BR-Case-study-of-Brazil.note.aspx>. Acesso em: ago. 2014
5. 3rd Generation Partnership Project (3GPP) (2014) 3GPP TR 36.840: LTE 450 MHz in Brazil work item technical report. Disponível em: <http://www.3gpp.org/DynaReport/36840.htm>. Acesso em: ago. 2014
6. Dahlman E et al (2008) 3G Evolution: HSPA and LTE for mobile broadband. 2nd edn. Academic Press, Oxford
7. 3rd Generation Partnership Project (3GPP) (2009) 3GPP Technical specification 36.211: physical channels and modulation (Release 8). 2009. Disponível em: <www.3gpp.org>. Acesso em: ago. 2014
8. Sesia S, Toufik I, Baker M (2009) LTE—The UMTS long term evolution: from theory to practice. Wiley, Chichester
9. Kim HB et al (2005) A radio over fiber network architecture for road vehicle communication systems. In: IEEE 61st vehicular technology conference, 2005 (VTC 2005-Spring). IEEE, vol 5, pp 2920–2924
10. Lee K (2005) Radio over fiber for beyond 3G. In: Proceedings of the international topical meeting on microware photonics (MWP), 2005, pp 9–10
11. Pereira LCP, Vicente DR (2011) Implementação e Demonstração em Laboratório de Rede de Acesso Híbrida Experimental GPON-WiMAX. PD.33.13.05A.0005A/RT-01-AA. CPqD, jun. 2011. (relatório técnico)
12. Midwinter JE (1991) Optical fibers for transmission. Krieger Pub Co., Malabar

Experimental Assessment of Voice Over IP in LTE Systems Under Different Cell Conditions

Ricardo Takaki, Juliano Joao Bazzo, Flávia M.F. Rocha, Jorge Seki and João Paulo Miranda

Abstract This chapter presents a measurement-based performance assessment of voice over IP in long term evolution (LTE) networks for suburban and rural applications. The behavior of the embedded eNodeB quality of service (QoS) aware scheduler is evaluated when different LTE configurations of QoS and cell conditions are taken into consideration. Our results suggest that the aforementioned scheduler maintains VoIP quality using guaranteed bit rate (GBR) with concurrent traffic over default bearer or even over non-GBR dedicated bearer. The QoS aware algorithm works in such a fashion that the mean opinion score remains constant even in adverse conditions, for instance, under concurrent traffic delay increase conditions, or in the presence of signal reception degradation due to changes in the terminal position within the cell.

R. Takaki (✉) · J.J. Bazzo · F.M.F. Rocha · J. Seki · J.P. Miranda
CPqD Foundation, Campinas, São Paulo, Brazil
e-mail: rtakaki@cpqd.com.br

J.J. Bazzo
e-mail: jbazzo@cpqd.com.br

F.M.F. Rocha
e-mail: flavia@cpqd.com.br

J. Seki
e-mail: jseki@cpqd.com.br

J.P. Miranda
e-mail: jmiranda@cpqd.com.br

A. Paradisi et al. (eds.), *Long Term Evolution*, Telecommunications and Information Technology, DOI 10.1007/978-3-319-23823-4_8

1 Introduction

The long term evolution (LTE) technology has been a hot research topic in wireless communications due to its central role in the standardization of next-generation cellular systems carried out by third generation partnership project (3GPP). In densely populated areas, LTE systems have mostly been deployed in standard 3GPP frequency bands, such as the 700 MHz and 2.6 GHz bands. In order to benefit from the superior propagation characteristics of lower frequencies in a new LTE profile suitable for sparsely populated areas, 3GPP has recently standardized the 450–470 MHz range as 3GPP Band 31 [1].

Since its Release 8, the LTE standard defines different quality of service (QoS) levels for data, video and voice over internet protocol (VoIP) services [2]. Scheduling mechanisms for VoIP calls in LTE systems have been studied via simulation. In [3], for instance, the capacity derived when dynamic schedulers are employed in multi-cell scenarios (low mobility, 5 MHz operation bandwidth) is shown to depend on the control plane resource allocation scheme. It turns out from this study that up to 50–300 simultaneous calls per cell can be supported by dynamic schedulers depending on the number of symbols available to the physical downlink control channel (PDCCH). In contrast, the VoIP traffic that can be accommodated using semi-persistent mechanisms is shown to be fixed and around 175 calls per cell. All in all, the message conveyed by Puttonen et al. [3] is that one has to cope with some capacity constraints when dynamic scheduling packets are used with persistent scheduling mechanisms.

The aforementioned multi-cell scenario is extended in [4] for different operation bandwidths and inter-cell distances. The results shown present the absolute VoIP capacity numbers of the LTE downlink. It is also shown that link adaptation together with packet bundling provides a clear gain in capacity, as more VoIP packets can be scheduled in each transmission time interval (TTI). Limitations in the control channel can also be effectively compensated by packet bundling. End-to-end delays and throughput in the presence of VoIP traffic are assessed in [5] for several scenarios considering stationary and mobile terminals. In the absence of mobility, it is shown via simulation work that the delays are slightly higher for networks congested with VoIP only. In other cases, better performance is derived due to the presence of moving terminals.

Notwithstanding the value of the related work toward a better understanding of VoIP using LTE infrastructure, their results primarily rely on simulation work and exploit various parameters in a multiple cell environment, leading to experiments almost impossible to be performed with real equipment. One alternative to complement such purely theoretical modeling and analysis is practical implementation, as it can be employed to validate the design of algorithms, protocols, software, and hardware under a genuine radio frequency (RF) environment. Motivated by the several ways in which measurement-based experimentation may be rewarding, the performance of VoIP calls on a real LTE system was evaluated in a previous work of the authors [6]. Among the conclusions drawn therein, it was found that

the scheduler provides good quality of VoIP service when the QoS class identifier (QCI) type guaranteed bit rate (GBR) is used. In this chapter, we conduct a measured-based performance assessment of VoIP in LTE systems. Our analysis considers different positions of the terminal inside the cell, i.e., different signal reception conditions for a fixed number of VoIP calls. Concurrent traffic with congestion is also taken into account. These settings differ from those used in [6] in that there the number of calls is allowed to vary but terminal positions are kept fixed, and the concurrent traffic considered is now with and without congestion.

Our results suggest that, among the schedulers available at the eNodeB, only the one with QoS aware weighted priority (WP) and GBR maintains call quality under congestion operation conditions. It is worth mentioning at this point that one distinguishing aspect between VoIP and voice over LTE (VoLTE) is that the latter employs an IP multimedia subsystem (IMS) for call control [7]. VoLTE also calls for eNodeB support for semi-persistent scheduling, TTI bundling, header compression, and the terminal needs to support the AMR-WB codec [8]. The tests presented herein focus on the LTE QoS behavior using the G711u codec encapsulated within a real-time transport protocol (RTP) data packet under data traffic congestion [9]. The data packets are generated using a tool that simulates the G711u RTP payload and simply creates VoIP traffic between two personal computer (PC) endpoints.

The remainder of the chapter is organized as follows. Section 2 overviews the basics of QoS provisioning in LTE networks. Scheduler algorithm and the figures of merit used to evaluate voice quality in our experiments are also described there. We carry on in Sect. 3 with a description of the experimental setup based upon which three test scenarios are considered. Results for these scenarios are then discussed in Sect. 4. Section 5 wraps up the chapter with some remarks and future works.

2 Fundamentals of QoS in LTE Networks

This section describes briefly the fundamentals of QoS in LTE network. Section 2.1 explains about the service bearers used to establish a QoS connection between the devices that communicates in a LTE network. Section 2.2 introduces the QoS parameters and their properties used to define the bearer characteristics for the VoIP data packets' transport and Sect. 2.3 explains a resumed overview of the scheduler algorithm used to optimize the QoS within the network to allow the best VoIP data flow.

The LTE standard has been designed bearing in mind the need to provide appropriate capabilities for different service categories, such as voice, video, messaging, and exchange of data files. This is possible thanks to an implementation of QoS control supported by architectures defined by 3GPP [2, 10]. In evolved packet systems (EPS), QoS control takes place at the level of the service flows, referred to as bearer services in the context of LTE. The traffic mapped onto a specific bearer

service is treated equally with respect to packet forwarding, including the application of policies for scheduling and queue management. Different service flows are available to make the implementation of different packet forwarding treatments possible, namely default bearers and dedicated bearers. Default and dedicated bearers are briefly described in the sequel along with QoS parameters, the scheduling algorithm implemented at the eNodeB, and the metrics used for evaluating voice quality later on in the performance characterization of our experiments.

2.1 Service Bearers

The default service bearer is established whenever the user equipment (UE) connects to the packet data network (PDN). This bearer possesses the basic QoS capacities. For each PDN that the UE connects to, a default bearer is established. Any additional bearer established between the UE and the same PDN connection resulting by demanded services with specific QoS requirements is called a dedicated bearer. In general, a bearer is characterized in terms of the bit rate guarantees it provides. A bearer is then said with GBR when the network resources related to the associated GBR value are permanently allocated in the constitution or the modification of the service flow. Likewise, a bearer characterized as without GBR, i.e., non-GBR, provides no guarantee that a given bit rate is supported for that service flow. In either case, a bearer is associated with a set of IP packet filters that control the user traffic carrying the user service for a specific bearer. Filtering mechanism in the uplink traffic flow template (UL-TFT) and downlink traffic flow template (DL-TFT) is performed according to the pictorial description given in Fig. 1.

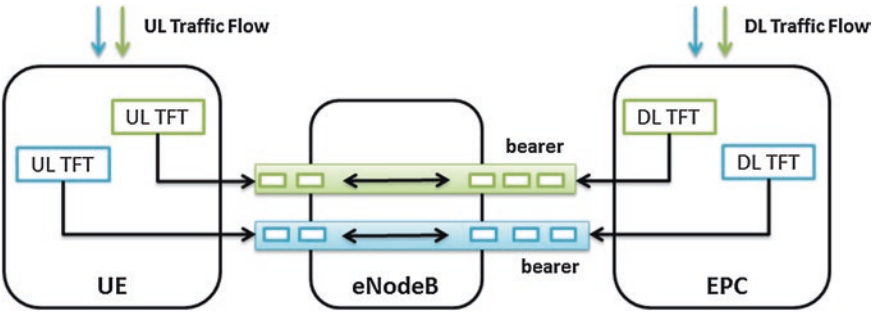

Fig. 1 EPS and TFTs bearer architecture

Table 1 QCI standard characteristics

QCI	Resource type	Priority level	PDB (ms)	PELR	Service samples
1	GBR	2	100	10^{-2}	Conversational voice
2	GBR	4	150	10^{-3}	Live streaming video
3	GBR	3	50	10^{-3}	Real-time games
4	GBR	5	300	10^{-6}	Buffered streaming video
5	non-GBR	1	100	10^{-6}	IMS signaling
6	non-GBR	6	300	10^{-6}	TCP-based services
7	non-GBR	7	100	10^{-3}	Video, voice, and games
8	non-GBR	8	300	10^{-6}	Buffered streaming video
9	non-GBR	9	300	10^{-6}	TCP-based services

2.2 QoS Parameters

The QoS bearer profile includes QCI, GBR, allocation and retention priority (ARP), and maximum bit rate (MBR). For non-GBR bearers, QCI and ARP are the sole parameters specified. For GBR bearers, QCI, ARP, GBR, and MBR parameters are all specified. In this chapter, we consider the QoS parameters that influence the performance analysis of voice calls in 450 MHz LTE network only. The QCI parameter defines the QoS class associated with a bearer, and is used as a reference to specific parameters that control packet forwarding treatment in the bearer, namely packet delay budget (PDB) and packet error loss rate (PELR). The nine QCI values mandated by 3GPP are summarized in Table 1. Voice service flow, video, messaging, and file transfer have different characteristics and are associated with different QCIs. The GBR parameter identifies the bit rate that should be guaranteed for a given GBR bearer, while the MBR parameter sets the MBR allowed for that bearer.

2.3 Scheduler Algorithm

As with the identifiers assigned to dedicated bearers, which ensure the necessary traffic for voice packets in terms of resource type, priority level, PDB, and PELR, the scheduler role is also of utmost importance to ensure the correct scheduling of multiple packets traversing the eNodeB. Here, the QoS aware approach implemented in the eNodeB is based on the WP algorithm [11]. This proprietary algorithm basically computes the WP of each bearer created in accordance with modulation aspects, class of service, delay, and traffic prioritization. Once priorities are assigned to the bearers, all traffic flows are served with resources allocated according to the corresponding bearers, with the priority order set up to the limit of exhausted resources.

One alternative for measuring the resulting voice quality of a scheduler is mean opinion score (MOS), a subjective method defined by the ITU-T P.800 standard

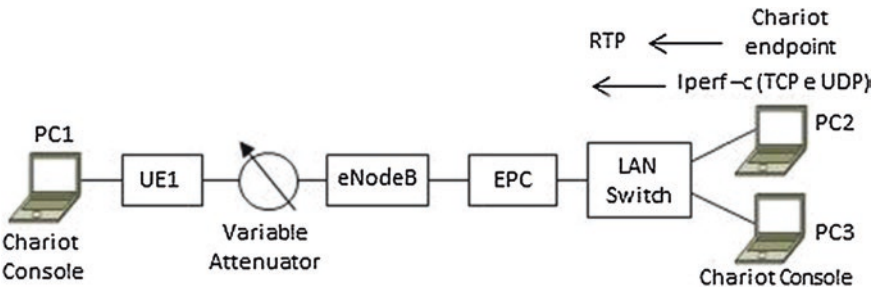

Fig. 2 Setup used in our experiments

Table 2 MOS scores obtained using the E-model algorithm

Inferior limit	Degree of user satisfaction
4,34	Very satisfied
4,03	Satisfied
3,60	Some users unsatisfied
3,10	Many users unsatisfied
2,58	Almost all users unsatisfied

[12]. The transmitted and received voice quality are evaluated according to an algorithm that gives scores on a scale of 1–5, where 1 and 5 correspond to "bad" and "excellent", respectively. The tool used in the VoIP service performance test between PC1 and PC2 (shown in Fig. 2, which will be explained in the next section) uses the E-Model algorithm, defined by the ITU-T G.107 standard [13] as a means to estimate the MOS quality for every pair of endpoints. Table 2 lists the MOS values obtained from the execution of this algorithm. In order to verify the behavior of the scheduler algorithm another metric that can be used in addition to MOS is PDB, as it is among the QCI characteristics in Table 1. In our experiments, we compute delay variations relative to the delay measured at the center of the cell using

$$\Delta_\sigma(\%) = \frac{\sigma_{\text{pos}} - \sigma_{\text{ref}}}{\sigma_{\text{ref}}}, \tag{1}$$

where the subscript pos is the delay at the position of interest (measured in the middle or on the edge of the cell) and subscript ref is the reference delay (measured in the center of the cell).

3 Experiment Setup and Test Scenarios

This section presents the general experiment setup and test scenarios. Section 3.1 describes the real-world experiment setup considering the LTE system equipment and test tools as well as the configuration of these device parameters. Moreover, Sect. 3.2 describes the test scenarios in order to verify the behavior of VoIP calls considered in this chapter.

Table 3 Reception conditions considered in all test scenarios

Terminal position	Reception intensity	SNR (dB)
In the center of the cell	High	22
In the middle of the cell	Medium	13
On the edge of the cell	Low	5

3.1 General Settings

In order to verify the behavior of VoIP calls in a LTE network, consisting of real-world equipment, we set up the experiment shown in Fig. 2. External interference is kept under control by connecting the eNodeB to the UE through an RF cable with a variable attenuator, which allows us to vary the signal-to-noise ratio (SNR) to mimic changes in the UE position within the cell. We consider the frequency range 450–470 MHz (3GPP Band 31), 5 MHz operation bandwidth, and different modulation schemes using 25 physical resource blocks. The test topology comprises two PC endpoints monitored by the testing tool IxChariot [14]. Such PC endpoints are responsible for sending and receiving dedicated RTP traffic [9]. Termination points PC1 and PC2 relate to UE and evolved packet core (EPC), respectively. The network that connects to the EPC includes PC3, with IxChariot tool controlling the two endpoints and generating reports for different traffic parameter configuration, and MOS and delay variation measurements.

The VoIP traffic performance tests were conducted using test scenarios including LTE network devices with QoS parameters appropriately configured, and with the IxChariot tool configured to generate, measure, and report both dedicated RTP traffic and concurrent traffic based on the transmission control protocol (TCP) or the user datagram protocol (UDP). In all tests the RTP traffic generated is always transported through a dedicated bearer, and the concurrent traffic (either TCP or UDP) flows are transported through a default bearer. Both types of concurrent traffic were generated using Iperf [15]. The QoS control behavior was verified for RTP traffic under the cell reception conditions listed in Table 3. These conditions reflect different signal intensities obtained by reception through RF attenuator adjustments. Finally, the system was evaluated under different eNodeB modulation configurations, such as adaptive modulation and fixed modulation, quadrature amplitude modulation (64-QAM), and quadrature phase shift keying (QPSK) used in the uplink and downlink. All tests were performed with 20 pairs of RTP conversation, corresponding to 20 concurrent voice calls with the G.711 codec configured and generated with the IxChariot tool for rate 1.280 kbps.

3.2 Test Scenarios

Table 4 summarizes the test scenarios considered in this chapter. In all scenarios and cases considered, we assume that default bearers are set with QCI = 9 (non-GBR) and adaptive modulation is in use at the eNodeB unless otherwise stated.

Table 4 Specific settings associated with each test scenario

Test scenario	QCI	Bearer type	Concurrent traffic	Modulation scheme	Figure
I	1	Dedicated	None	Adaptive	3a–d
	7	Dedicated			
	1, 7	Dedicated	Without congestion		
	9	Default			
II	1	Dedicated	Without congestion	Adaptive	4a, b
	9	Default			
	1	Dedicated	With congestion		
	9	Default			
III	1	Dedicated	Without congestion	Adaptive	5
	9	Default			
	1	Dedicated		QPSK	
	9	Default			
	1	Dedicated		64-QAM	
	9	Default			

Scenario I consists of passing a RTP traffic flow through a dedicated bearer with QCI = 1 (type GBR), and a second RTP traffic flow through a dedicated bearer with QCI = 7 (type non-GBR). The experiment is repeated for the self-explanatory cases "no concurrent traffic", "TCP concurrent traffic without congestion", and "UDP concurrent traffic without congestion". In scenario II, the test consists of passing a RTP traffic flow through a dedicated bearer with QCI = 1 (type GBR), and a concurrent TCP traffic flow through a default bearer. The cases considered here are "no concurrent traffic", "TCP concurrent traffic with congestion", and "TCP concurrent traffic without congestion". Scenario III augments scenario II by letting the modulation scheme used at the eNodeB vary among the cases "adaptive modulation", "QPSK", and "64-QAM". For quick referencing, the last column of Table 4 links the test scenarios to the figures providing their corresponding results. These will be discussed later on in Sect. 4.

TCP traffic transmitted through the default bearer under concurrent condition corresponds to the maximum throughput supported by the LTE channel under different cell reception conditions and modulation schemes. This ascertains that the default bearer traffic competes with the dedicated bearer traffic in the event of a congestion condition, thus allowing us to check the system behavior using the QoS aware WP scheduler. In the absence of congestion, the traffic transmitted in the default bearer assumes a value below the maximum throughput supported by the LTE channel, enabling RTP traffic through the dedicated bearer below the congestion threshold.

4 Experimental Results

In this section, we present preliminary results aimed at evaluating the implementation of the WP QoS aware algorithm for maintaining quality of VoIP service as mandated by the 3GPP LTE standard. The experimentally driven assessment discussed in what follows considers the test scenarios in Tables 3 and 4.

4.1 Test Scenario I

MOS and delay variation results obtained for scenario I are shown in Fig. 3. According to Fig. 3a, the MOS decreases as the UE moves from the center to the middle of the cell to then increase as the UE further moves toward the cell

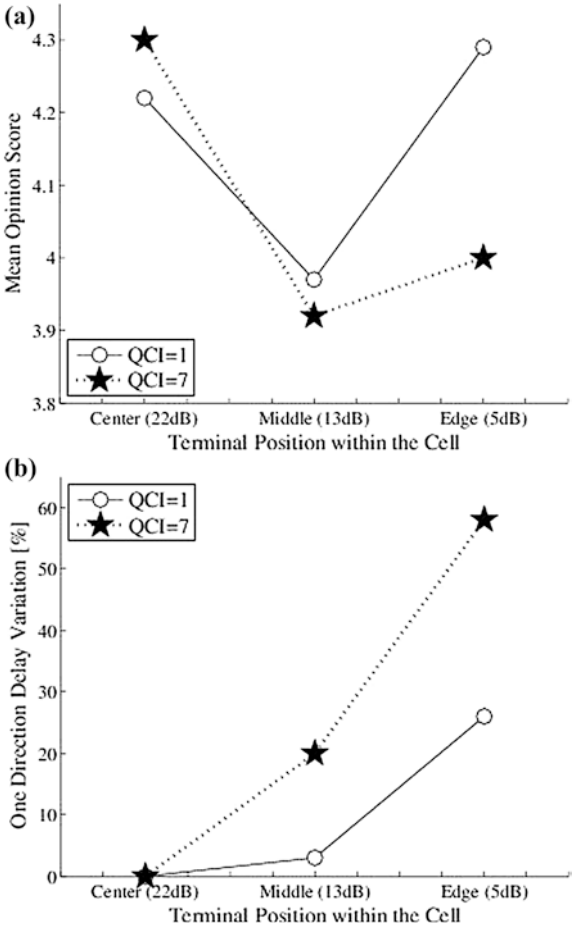

Fig. 3 Test scenario I: MOS and delay variation measured for different QCI settings using RTP traffic in the absence and in the presence of TCP/UDP concurrent traffic without congestion. **a** MOS without concurrent traffic. **b** Delay variation without concurrent traffic. **c** MOS with concurrent traffic (QCI = 1). **d** MOS with concurrent traffic (QCI = 7)

Fig. 3 (continued)

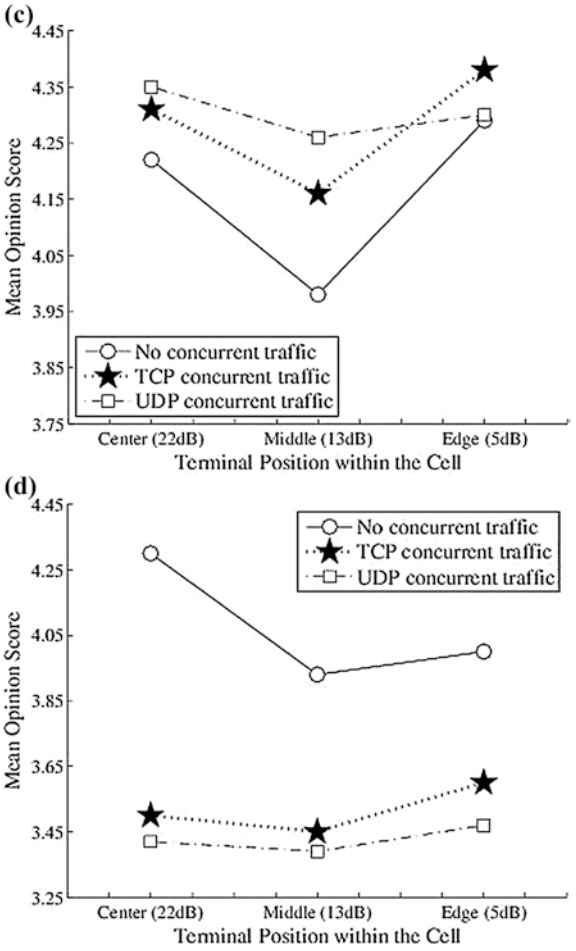

edge. It can also be seen from the figure that regardless of the QCI considered, the MOS assumes values ranging from "some users unsatisfied" to "very satisfied". However, thanks to the QoS aware WP scheduler, which prioritizes GBR flows over non-GBR flows, the MOS degradation perceived as the UE moves toward the cell edge is more significant for QCI = 7 than for QCI = 1. As for the delay variation, a substantial increase is observed in Fig. 3b as the UE departs from the center of the cell and approaches the cell edge. For QCI = 7, the delay variation on the cell edge is roughly three times higher than that measured for QCI = 1 at the same position. If we now move on to the results of MOS with concurrent traffic, shown in Fig. 3c, d for QCI = 1 and QCI = 7, respectively, we see a dramatic MOS degradation for QCI = 7 but not for QCI = 1. While the MOS remains in between "satisfied" and "very satisfied" for QCI = 1, it undergoes a big drop from "very satisfied" to "many users un satisfied". This is in good agreement with our

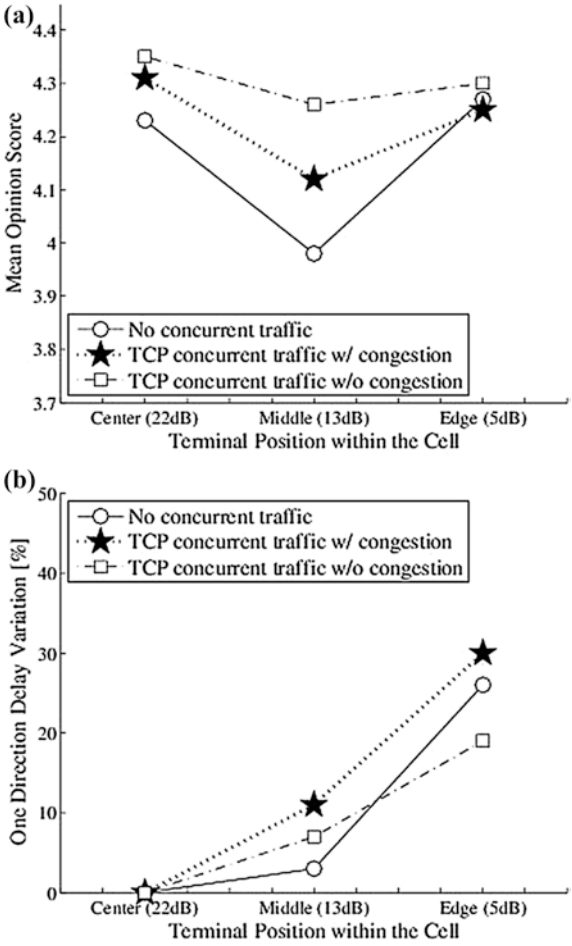

Fig. 4 Test scenario II: MOS and delay variation measurements obtained using RTP traffic under TCP concurrent traffic with and without congestion. **a** MOS (QCI = 1 for RTP, QCI = 9 for TCP). **b** Delay variation (QCI = 1 for RTP, QCI = 9 for TCP)

expectations, as the QoS aware WP scheduler again prioritizes QoS with QCI = 1 (even under unfavorable concurrent traffic conditions). When it comes to the type of concurrent traffic, the variations in MOS observed for TCP and UDP traffic are minimal for both QCIs.

4.2 Test Scenario II

MOS and delay variation results obtained for scenario II are shown in Fig. 4. Under different traffic conditions, it is shown in Fig. 4a that the MOS once again decreases as the UE moves from the center to the middle of the cell to then increase when the UE further moves toward the cell edge. However, the careful

reader will see that the overall MOS score without concurrent traffic is lower than with concurrent traffic. While this finding may sound somewhat counterintuitive, it is indeed related to the QoS aware WP scheduler (which prioritizes the GBR traffic flow so as to maximize the system performance under concurrent non-GBR traffic flows). MOS variations due to both type of concurrent traffic and changes in the UE position within the cell are not that significant, as a result of QoS aware WP scheduling working alongside with adaptive modulation.

Figure 4b shows that the increase in delay variation in one direction varies from 20 to 30 % as the UE moves from the cell of the center toward the cell edge. This suggests that the QoS aware WP scheduler is prioritizing the GBR traffic flow so as to maximize its performance in the presence of a concurrent non-GBR traffic flow.

4.3 Test Scenario III

MOS results obtained for scenario III are shown in Fig. 5. When 64-QAM is in use, the MOS decreases as the distance between the UE position and the center of the cell increases. In contrast, when adaptive modulation or QPSK is employed, the MOS decreases as the UE moves from the center to the middle of the cell to then increase as the UE further moves toward the cell edge. Regarding the adaptive modulation, the message conveyed by the MOS behavior observed here is that the modulation order does not change as the UE moves from the center to middle of the cell, but does change as the UE moves from the middle to the edge of the cell.

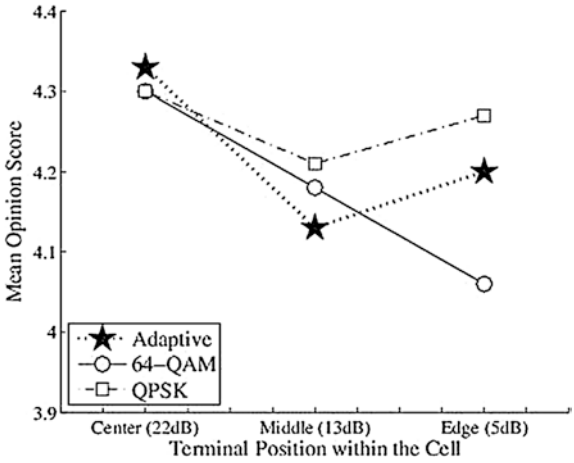

Fig. 5 Test scenario III: MOS measurements obtained for different modulations using RTP traffic under TCP concurrent traffic without congestion

5 Concluding Remarks

This chapter has presented a measurement-based performance assessment of VoIP in LTE networks for suburban and rural applications. The behavior of the embedded eNodeB QoS aware scheduler is evaluated when different LTE configurations of QoS and cell conditions are taken into consideration. Our results suggest that the aforementioned scheduler is capable of maintaining VoIP quality using QCI = 1 with concurrent traffic over default bearer or even over the non-GBR dedicated bearer.

The QoS aware algorithm works in such a way that the MOS parameter remains constant even in adverse conditions, for instance, under concurrent traffic delay increase conditions, or in the presence of signal reception degradation due to the UE position within the cell. Regarding adaptive modulation, our results suggest that the modulation order decreases as the UE moves from the middle to the edge of the cell. However, the same does not happen as the UE moves from the center to the middle of the cell. Despite the preliminary nature of our results, this is a clear indication that the adaptive modulation is not working properly on the eNodeB software version used in our test scenarios. Apart from that, the results obtained in our tests demonstrate accordance with the QoS standards mandated by 3GPP. As future work, new tests will be carried out to augment the present work with other important variables, such as, new codecs used by the LTE technology, other QCI comparisons, different LTE VoIP QoS control mechanisms, and different modulation schemes, with the aim of verifying the technology robustness in application scenarios with UE mobility and interference presence. We also plan to repeat the tests after having corrected the adaptive modulation software, and consider over-the-air test scenarios focusing on QoS tests for performance of VoIP calls over LTE.

Acknowledgment This material is based upon the work supported by FUNTTEL/FINEP 01.12.0481.00.

References

1. 3GPP TR 36.840, LTE 450 MHz in Brazil Work Item Technical Report. Sept 2013
2. 3GPP TS 23.401, LTE—general packet radio service enhancements for evolved universal terrestrial radio access (release 8), Sept 2010
3. Puttonen J, Kolehmainen N, Henttonen T, Moisio M (2008) Persistent packet scheduling performance for voice-over-IP in evolved UTRAN downlink. In: Proceedings of the IEEE PIMRC, pp. 1–6
4. Puttonen J et al (2008) Voice-over-IP performance in UTRA long term evolution downlink. In: Proceedings of the IEEE VTC (Spring), pp. 2502–2506
5. Masum E and Babu J (2011) End-to-end delay performance evaluation for VoIP in the LTE network. M.Sc. thesis, Blekinge Institute of Technology
6. Takaki R et al (2013) VoIP performance evaluation under a LTE 450 MHz network. In: Proceedings of the Brazilian symposium on telecommunications

7. GSM Association IR.92, IMS profile for voice and SMS, Mar 2013
8. 3GPP TS 26.204, Speech codec speech processing functions; adaptive multi-rate—wideband (AMR-WB) speech codec; ANSI-C code, Sept 2012
9. Schulzrinne H, Casner S, Frederick R, Jacobson V (2013) RTP: a transport protocol for real-time applications. In: RFC 3550 of the IETF internet society
10. 3GPP TS 23.203, Policy and charging control architecture (release 8), Mar 2010
11. Rastogi MK, Developing a QoS aware framework for LTE 4G (Online). Available: http://www.telecomlead.com/whitepaper/developing-aqos-aware-framework-for-lte-4g-aricent-group-8790
12. ITU-T Recommendation P.800, Methods for subjective determination of transmission quality, Aug 1996
13. ITU-T Recommendation G.107, The E-model: a computational model for use in transmission planning, Feb 2014
14. IXIA, IxChariot User Guide (Online). Available: http://www.netcor.de/download.php?file=1966
15. Iperf (Online). Available: http://iperf.sourceforge.net/

Integration Between LTE and Satellite Networks

Ricardo Takaki, Luis Cláudio Palma Pereira, Ivan Lucio Junqueira, Jorge Seki and João Paulo Miranda

Abstract Long Term Evolution (LTE) technology is the evolution to 3G technology providing improvements for delivered services, such as voice calls with high-quality user experience characterized by higher throughput, low latency, and quality of service. This chapter evaluates the LTE network system composed by radio access and core network with impairments to LTE technology characteristics, introduced by geostationary satellite link as backhaul connectivity to the system. The study is carried out including tests of throughput, latency, and voice service that are provided through the satellite link. Two distinct environments, namely a simulated satellite link and a real-world satellite link, are taken into consideration. The first one is carefully assembled in the laboratory to reflect the typical effects of satellite link delay on the LTE protocol and its consequent impacts on data transmission and real-time services. The second environment features a real-world satellite link, made available to CPqD by a geostationary satellite network operator. The LTE network system used in both environments consists of practical devices and prototypes developed by CPqD for operation in the 450 MHz band, and targeting application in sparsely populated areas. Presented results show that satellite-based backhaul is a technically feasible option for LTE networks, and the introduced impairments are not a real limitation for provided services, thus leveraging the deployment of such networks in rural and sparsely populated remote areas.

R. Takaki (✉) · L.C.P. Pereira · I.L. Junqueira · J. Seki · J.P. Miranda
CPqD Foundation, Campinas, São Paulo, Brazil
e-mail: rtakaki@cpqd.com.br

L.C.P. Pereira
e-mail: lclaudio@cpqd.com.br

A. Paradisi et al. (eds.), *Long Term Evolution*, Telecommunications and Information Technology, DOI 10.1007/978-3-319-23823-4_9

1 Introduction

Satellite access links for services like voice, video, and Internet access have been widely used over the past years, providing access to these services at remote and sparsely populated regions. However, until recently, the use of satellite access link for these scenarios was considered a challenge due to the results of low attractiveness of investment returns for telecommunication operators. This low return of investment was caused by reduced local users' traffic demand per coverage area and high cost for deployment and operation of this type of access link.

The adoption of low-cost satellite equipment stations, such as geostationary satellite orbit (GSO) very small aperture terminals (VSATs) [1], in a large number in remote areas (typically countryside areas), does not totally solve commercial issues, maintaining, as a challenge, the expansion and provision of these services to the population of these areas. However, with the possibility of using this low-cost equipment station to provide satellite system as backhaul for a local wireless access system, it becomes very interesting and capable of boosting the expansion in areas lacking infrastructure. In that solution, the interface between the core network and remote end user network, or last mile, is an open field for different technologies to provide services to these remote areas even considering impairments introduced by the satellite communication [2], this is a very interesting option.

After standardization of the band 31 (range of 450 MHz) for the 3GPP LTE [3], one of the most viable possibilities began to be the integration of LTE network with the satellite backhaul. Besides the positive economic aspects resulting from standardization, other important factors are the 450 MHz range suitability to obtain extensive cell coverage, appropriate to the application in rural and sparsely populated remote areas, and the availability of entitlement usage of this range through auctions coordinated by ANATEL [4]. The reference model for this network solution integrating the LTE and satellite backhaul is shown in Fig. 1 in which different network services for users (voice and public Internet access) are centralized and connected to the concentrating station (HUB) subnetwork and the LTE radio access network is connected to a VSAT station located at a strategic remote area.

In tests conducted in real-world satellite link provided by satellite system operator, two Evolved Packet Core (EPC) [5] integration scenarios were considered. In one of them, the EPC is collocated in the VSAT remote station subnetwork, together with the base station or Evolved Node B (eNodeB) [6]. In another scenario, the EPC is collocated in the HUB station subnetwork far away from the

I.L. Junqueira
e-mail: ivanj@cpqd.com.br

J. Seki
e-mail: jseki@cpqd.com.br

J.P. Miranda
e-mail: jmiranda@cpqd.com.br

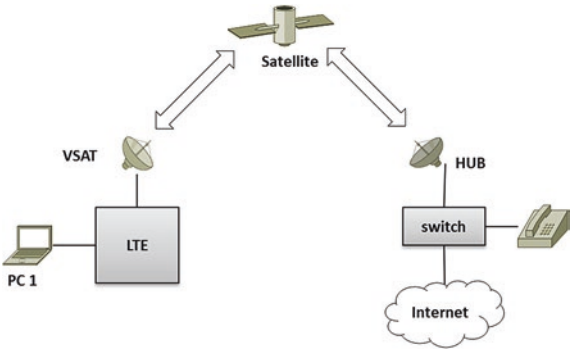

Fig. 1 Satellite-LTE integration

base station collocated at the VSAT remote station subnetwork. For these scenarios, tests were performed including latency, data throughput, and public Internet connection speedtest. To determine the quality of voice services, tests included voice over Internet Protocol (VoIP) calls along with latency, throughput, jitter, and MOS measurements.

The remainder of this chapter is structured as follows: Sect. 2 contains a brief description about Satellite VSATs; information about the LTE technology; some considerations about the metric used to evaluate voice transmission; Perceptual Evaluation of Speech Quality (PESQ) [7]; and commercial tool used in the tests, the IxChariot [8] descriptions. Sect. 3 provides information about the test environments used. Sect. 4 examines the obtained test results, and finally, Sect. 5 presents conclusions and offers possibilities for future work associated with the topic covered in this chapter.

2 Technical Aspects of the Components Used

This section shows relevant aspects of the elements used on the created setups to build the testing scenario.

2.1 Satellite VSATs

VSATs are devices formed by antennas with limited diameters, usually to 2.4 m (may reach 5 m exceptionally, depending on the operational circumstances) and fixed satellite services, implemented in shared or private networks and in dedicated applications, regulated by Recommendation ITU-R S.725 [1]. The VSAT stations operate at Ku band and are usually part of a network star topology, which incorporates a central station called HUB, responsible for controlling and monitoring various VSAT remote stations. However, some networks can operate establishing point-to-point linkage or mesh configuration, without a central station HUB.

2.2 The LTE Architecture

LTE is a wireless technology that has been standardized by 3GPP [9] to provide all IP-based services, in order to replace, gradually, the previous wireless technologies (such as 2G and 3G) used to provide distinctive circuit switched based network for voice services, and packet switched based network for data services.

LTE technology uses resources that enable Quality of Service (QoS) deployment, configuration, and the definition of priority services flows for data, voice, and video in real time. This ensures the necessary band for such services to operate properly, even at the expense of bandwidth used by other services which do not require priority for their usage, such as Internet access. The LTE architecture is basically composed by the User Equipment (UE), the eNodeB, and the EPC [5]. In the LTE architecture, the EPC is the entity responsible for default or dedicated service flows creation, whereby, respectively, flowing best-effort traffic services, such as Internet access, and the priority real-time traffic, such as voice and video. Either the default or the dedicated service flows (bearers) are created taking into account QoS parameters classified according to the traffic type. Generally the default bearers are created using not guaranteed bit rate traffic (Non-Granted Bit Rate—non-GBR) parameter values, with QoS class indicator (QoS Class Indicator—QCI) including values from 5 to 9 and with low prioritization (best-effort strategy). The dedicated bearers are created using parameter values used to guarantee guaranteed bit rate services (Granted Bit Rate—GBR) that include QCI values from 1 to 4 and with top prioritization. Figure 2 and Table 1 show typical LTE architecture and QoS-related QCI parameters, respectively.

2.3 Mean Opinion Score

The mean opinion score (MOS) is a subjective method of measurement voice quality, defined by Recommendation ITU-T P.800 [10]. The voice quality transmitted by one device and received by another is evaluated according to an algorithm that scores according to a scale of 1- 5, in which Value 1 corresponds to a bad voice quality and Value 5 corresponds to excellent voice quality. The IxChariot tool used to test the VoIP service performance employs the E-model

Fig. 2 LTE architecture

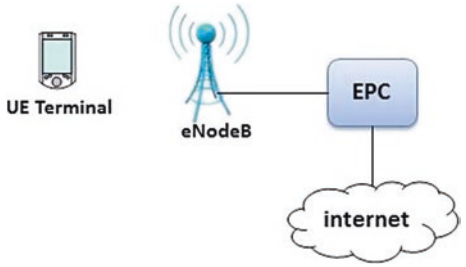

Table 1 QCI standard characteristics

QCI	Resource type	Priority level	PDB (ms)	PELR	Services
1	GBR	2	100	10^{-2}	Conversational voice
2		4	150	10^{-3}	Conversational video (live streaming)
3		3	50	10^{-3}	Real-Time games
4		5	300	10^{-6}	Non-conversational video (buffered streaming)
5	Non-GBR	1	100	10^{-6}	IMS signaling
6		6	300	10^{-6}	Video (buffered streaming), TCP-based services
7		7	100	10^{-3}	Voice, video (live streaming), interactive games
8		8	300	10^{-6}	Video (buffered streaming), TCP-based services
9		9	300	10^{-6}	

Table 2 MOS scores

Inferior limit	User satisfaction
4.34	Very satisfied
4.03	Satisfied
3.60	Some users unsatisfied
3.10	Many users unsatisfied
2.58	Almost all users unsatisfied

algorithm defined by Recommendation ITU-T G.107 [11], whose objective is to estimate the MOS quality for each connection endpoints' pair. Table 2 shows the MOS values achieved from the E-model algorithm and used as a reference.

2.4 Perceptual Evaluation of Speech Quality

PESQ is a method standardized by the ITU-T [7], by Recommendation P.862 for voice quality measures, and it can be used during installation, commissioning, and possible problems' solution, in real networks that use telephony devices. PESQ tool that incorporates PESQ algorithm is usually installed in test equipment, but can also be integrated into routers, telephone exchanges, voice quality enhancers, and other network devices. The PESQ measurement is considered intrusive since it compares the quality of real voice message transmitted through the system with a reference obtained from the original signal. Among the tool features, it may include:

(a) Possibility of listening quality measures in intrusive applications;
(b) Quality of accurate prediction in a wide variety of applications;

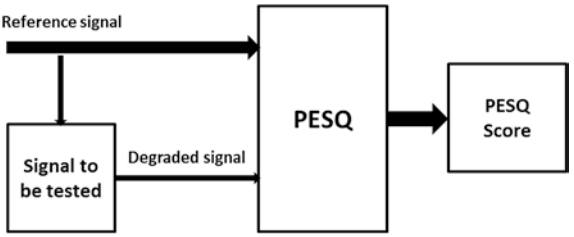

Fig. 3 PESQ algorithm (adapted from [12])

(c) Implementation of Chat Stimulated Artificial Test (Artificial Speech Test Stimulus—ASTS). Test signal designated specifically for use with PESQ, with shorter speech duration than the original speech.

The PESQ makes speech quality or voice measurements, in point to point and in one direction. It is suitable to be used in intrusion test. A signal is transmitted through the system to be tested and the degraded output is compared to the input reference signal. Figure 3 illustrates the use of the simplified PESQ algorithm, a PESQ score in the range of 1–4.5 is generated and a function is used to convert these ITU-T P.800 PESQ values into the MOS scale.

2.5 IxChariot

IxChariot is an assessment network tool for troubleshooting and pre-assessment of networks and applications. This tool simulates real-world applications, aiming to predict the performance of devices, systems, and networks when subjected to real traffic conditions. The IxChariot consists of:

(a) A server or console, where test performances are configured and, later, the data collection and reports generation are performed;
(b) At least two Performance Endpoints installed in devices included in the test scenario. The endpoints are responsible for initiating traffic, receiving traffic, and sending data to the IxChariot console.

Thus, there are three essential elements required for a test environment which uses the IxChariot:

(a) Console tool responsible for endpoints' monitoring and responsible for generation of the measures' results;
(b) The device has endpoint 1 which communicates directly with the IxChariot console and with Termination point 2, located at another device;
(c) Termination point 2 that communicates only with the device which has endpoint 1.

Endpoint 1, after receiving the test scripts and data from the IxChariot console, coordinates the VoIP test actions with the second endpoint, performs the test instructions generating simulated VoIP calls, and returns all test results to the

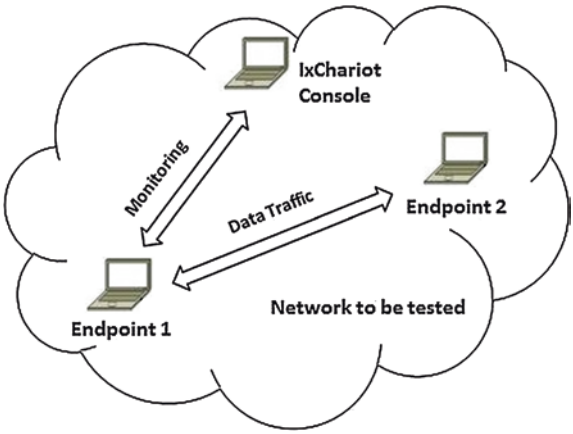

Fig. 4 Basic test using the IxChariot tool

IxChariot console. Termination point 2 receives the script test and generated simulated VoIP calls from endpoint 1 and returns to this device the results of tests performed. Figure 4 shows a basic test environment using the IxChariot tool components and contains the IxChariot console and endpoints 1 and 2, necessary for carrying out performance tests.

3 Description of Test Environment

Tests using the network integrated VSAT satellite link and LTE system were performed in two environments:

(a) Simulated environment, from which the satellite network presence was simulated through a computer that implemented the delay characteristics of a real satellite link scenario;
(b) Real environment, wherein the satellite link used and the real operating environment were provided by a carrier satellite system.

3.1 Simulated Scenario

In this environment, a computer with a delay simulator, a Linux application was used in order to obtain in a controlled way, the delay characteristic value found in a real satellite link. The simulator was configured to insert, in both downlink and uplink channels, a 300 ms delay, thus obtaining a 600 ms Round Trip Time (RTT) for the traffic between VSAT and HUB stations. The connections' configurations were made taking into account the location of the EPC on the satellite-LTE architecture as illustrated in Fig. 5. In this figure, the test environment was formed

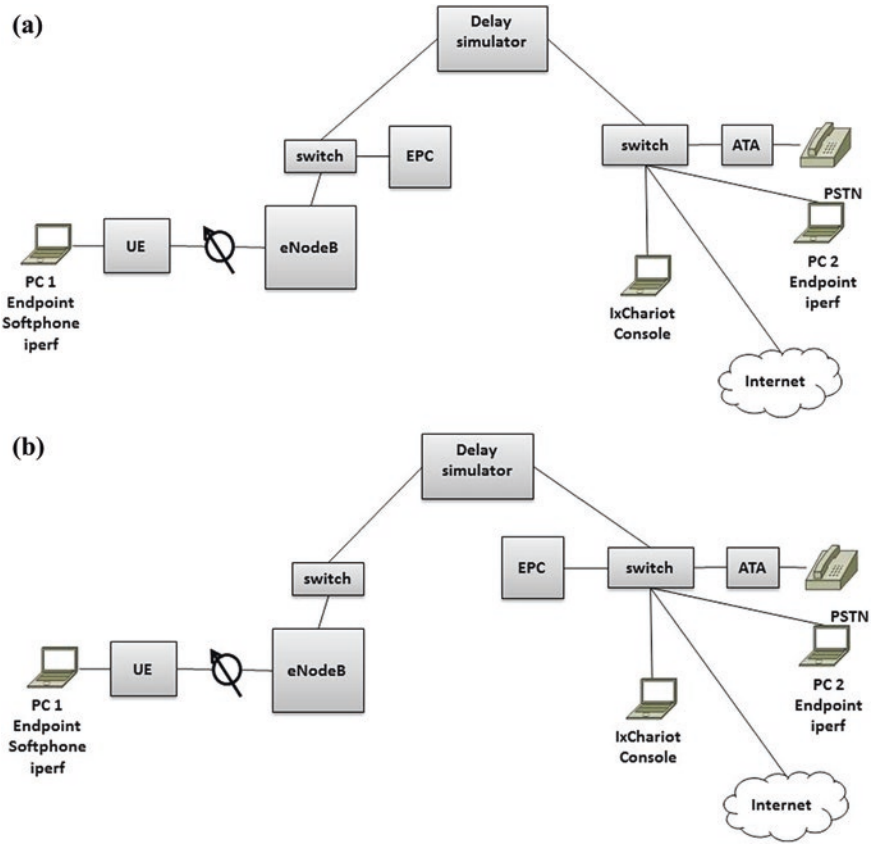

Fig. 5 Test scenarios used in the simulated LTE-satellite environment (laboratory). **a** Test scenario 1—simulation of EPC next to the eNodeB and UE terminal. **b** Test scenario 2—EPC simulation next to IxChariot and PC2 (HUB subnetwork)

Table 3 Description of test scenarios on the simulated environment

Scenario	Description	Figure
Test 1	EPC next to the eNodeB and UE terminal	5a
Test 2	EPC simulation next to IxChariot and PC2	5b

by the subnetwork which comprises the fixed components: PC1, UE terminal, and the eNodeB. The EPC could be located on this subnetwork for the test scenario shown in Fig. 5a or alternatively, in the HUB subnetwork where the operator Public Internet access is located, including PC2 with IxChariot endpoint and IxChariot console tool, as shown in Fig. 5b. For PESQ measurement, real VoIP conversational call was performed using the softphone installed in PC1 and the Analog Terminal Adapter (ATA) connected to the same subnetwork at the EPC side. Table 3 summarizes the test scenarios used in the simulated environment.

3.1.1 LTE Configuration

The eNodeB was configured to operate with central frequency equal to 450 MHz, 64-QAM modulation in the downlink and 16-QAM in the uplink, maximum power of 30 dBm, 8 Mbps flow in the downlink, and 1 Mbps in the uplink. The EPC has been configured with two bearers, one dedicated bearer with QCI = 1 and UDP filter (User Datagram Protocol) for voice traffic, and another default bearer with QCI = 7 for non-priority concurrent data traffic. VoIP calls were originated and received through IxChariot endpoints, and for this, two PCs were used as endpoints. Endpoint 1 was performed on PC1, connected into the UE terminal. Endpoint 2 was performed on PC2, connected to the same subnetwork of the EPC, as well as the IxChariot console tool. The real VoIP conversational calls were performed using the softphone installed in PC1 and the ATA connected to the subnetwork at the EPC side.

3.1.2 Performance Tests

Performance tests on the satellite simulated environment consisted in performing real voice calls between PC1 and ATA and simulated calls between IxChariot endpoints at PC1 and PC2. For both voice tests, traffic was generated with a concurrent TCP traffic between PC1 and PC2, routed through default. Table 4 lists the main tests made for performance evaluation. For latency and rate measurements, the speedtest [13], ping and iperf (version 2014) [14] tools were used. The test which used the speedtest tool consisted of latency verification by sending Internet Control Message Protocol (ICMP) from PC1 terminal to a server located on the public Internet network.

The higher the distance between PCI and server, or the higher the network congestion, the higher was the latency. Another important measure, taken by speedtest, was the UDP packets flow measurement from the server at downlink direction to the terminal and from the terminal at uplink direction to the server.

The ping tool, unlike speedtest tool, performed the latency measurement between PC1 and PC2, the latter one located after the delay simulator. The iperf tool was used to flow UDP data packets, with a fixed rate, in download direction between PC2 and PC1 and in upload direction between PC1 and PC2. The tool generated a concurrent traffic for voice traffic and provided the network latency evaluated during the network traffic generated presence. The VoIP test was

Table 4 Tests realized and their respective used tools

Tests	Used tools
Latency and throughput	speedtest
Latency	ping
Latency and concurrent traffic	iperf
VoIP	IxChariot
VoIP	wireshark, pesq

performed in two steps: first by getting MOS through the IxChariot tool that generated a RTP traffic encoded using G.711 codec between PC1 and PC2, and containing the endpoints monitored by IxChariot console. The tests were performed in both directions (download and upload). The second step was to conduct a real voice call between PC1 and PC2 using the application PortGo [15] and to save the generated RTP packets during the call flow, through the wireshark tool [16], for data extraction and processing, to finally get the voice quality metrics using the PESQ application.

3.2 Real Scenario

In this environment, the operational devices: VSAT station, satellite and HUB station, available under operational conditions by a satellite system operator, were used. The connection settings were made taking into account the EPC location in the LTE-satellite architecture, as shown in Fig. 6. The test environment was formed by the subnetwork consisting of the fixed components: PC1, UE terminal and eNodeB, and the VSAT station which was responsible for connecting the LTE network components to the geostationary satellite. In this scenario, the EPC was located in VSAT subnetwork, for the test case shown in Fig. 6a or located at the HUB station subnetwork that interconnects the public Internet access, PC2, PC with IxChariot console and PC2 with xChariot endpoint, as shown in Fig. 6b. Table 5 summarizes the test scenarios used in the real environment.

3.2.1 LTE Configuration and Description of Performance Tests

As in the simulated scenario, the eNodeB was configured to operate in the frequency of 450 MHz, 64-QAM modulation on the downlink and 16-QAM in the uplink, maximum power of 30 dBm, 8 Mbps of throughput on the downlink, and 1 Mbps on the uplink.

The EPC was configured with two bearers, one dedicated bearer using QCI = 1 and UDP filter for voice traffic, and other default bearer with QCI = 7 for concurrent data traffic.

The satellite link in this scenario was provided with TCP acceleration feature, using the ports 20,000–20,004 to the RTP protocol and port 80 to the TCP protocol. In addition, the SIP protocol prioritization was applied on port 5060 and configured in the satellite platform.

For the VoIP calls realization through IxChariot tool, two PCs were used as endpoints, from where the voice call was originated and received. Endpoint 1 was performed on PC1, connected to the UE terminal and Endpoint 2 was executed in PC2 and connected to the EPC and IxChariot console subnetwork. The VoIP call

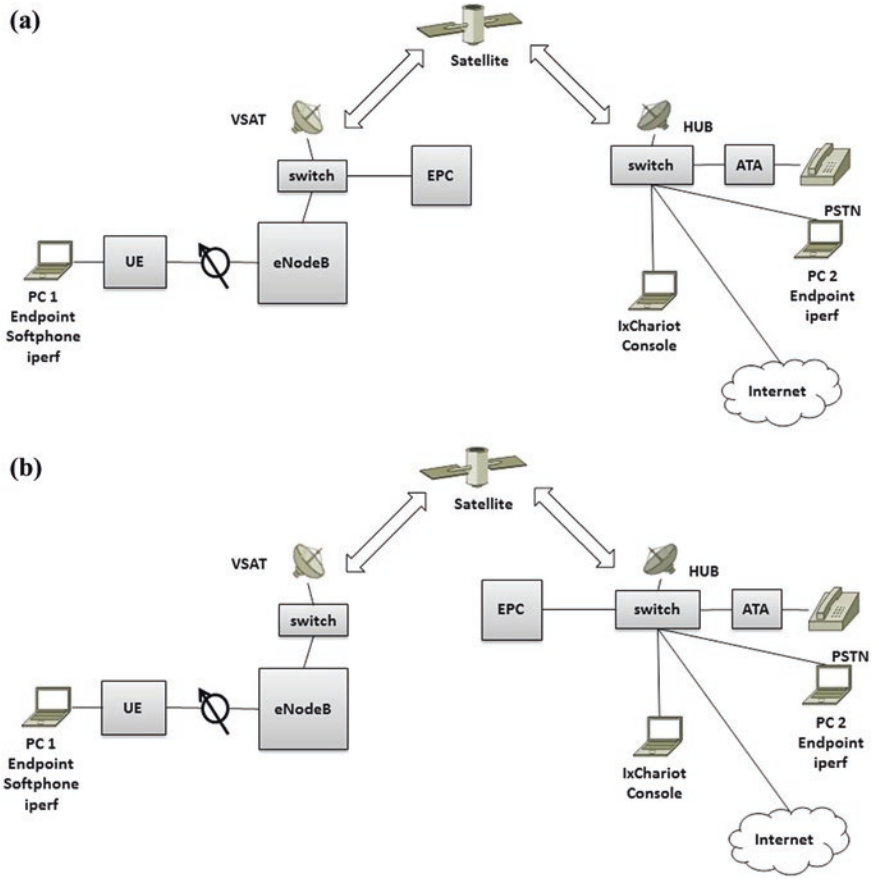

Fig. 6 Test scenarios used in the real LTE-satellite environment. **a** Test scenario 3—validation with the EPC next to the VSAT station. **b** Test scenario 4—validation with the EPC next to the HUB station

Table 5 Description of test scenarios on a real environment

Scenario	Description	Figure
Test 3	The EPC next to the VSAT station	6a
Test 4	EPC next to the HUB station	6b

conversation has been performed using a softphone installed on PC1 and a terminal ATA connected to the network where the EPC was found.

The latency measurements, concurrent traffic rate, and VoIP quality measurements were all performed using the same procedure described in a simulated test scenario.

4 Results Analysis and Discussion

Through test realization, according to the two scenarios, the simulated and real environments, described in the previous section, measurements were performed and results obtained for tests of latency, throughput, MOS, and PESQ. The following subsections show the obtained results.

4.1 Latency (Round Trip Time—RTT)

The results of the latency tests between the PC1 and PC2 are shown in Figs. 7 and 8. These average results were obtained through the ping and speedtest tools, respectively. The ping tool used between PC1 and PC2 generating ICMP traffic and providing RTT or latency results.

Comparing the graphs in Fig. 7a, b, it was found that there were no latency changes in the simulated environment, being indifferent, in this case, whether the EPC is at VSAT station side or HUB station side and indifferent also with traffic direction if it is downlink or uplink. The same happens to the values obtained on the VSAT side in the real environment, where a latency increase of 108 ms comparing to the simulated environment is verified. On the other hand, in the case the EPC was

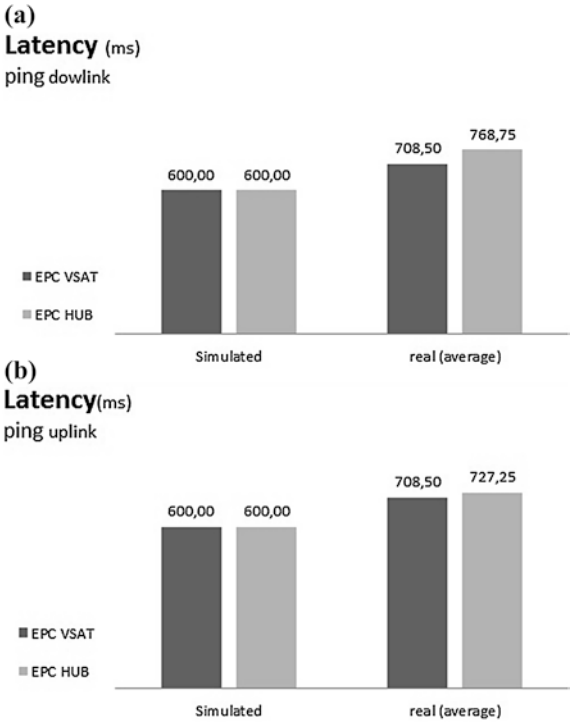

Fig. 7 Downlink and uplink latency obtained by ping tool. **a** Downlink latency values; **b** uplink latency values

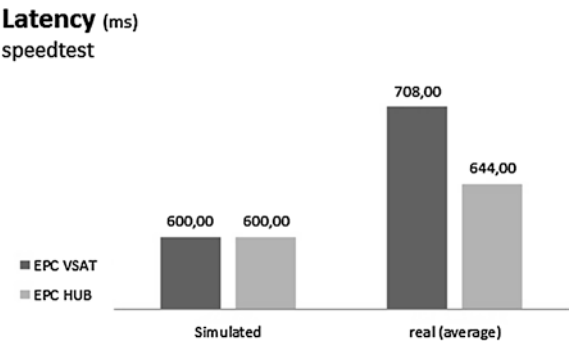

Fig. 8 Latency downlink obtained by speedtest tool

Table 6 Real scenario results with the satellite system integration

Configuration	Satellite system optimization	Latency—RTT (ms)
EPC next VSAT station	No	700
	Yes	700
EPC next HUB station	No	750
	Yes	650

located on the HUB station side, a latency decrease of about approximately 5.3 % in uplink compared to the value obtained in downlink was observed. The comparison between values obtained in simulated and real scenarios resulted in latency increases of 169 and 127 ms, in the uplink and downlink, respectively, for the real scenarios. Finally, when comparing the results obtained with different tools (ping and speedtest), it was found that the values of latency on the downlink, in the real environment, obtained with the two tools and shown in Figs. 7a and 8, showed the greatest difference of approximately 11.4 % when the EPC was located on the HUB station side. A comparison is made with the case wherein the EPC was located on the VSAT station side, when the difference was reduced to 0.07 %. It is noteworthy that the evaluation of latency through speedtest, for the EPC located in the VSAT station side, is performed without the use of optimizations on the satellite link. On the other hand, as this optimization was performed as part of the process of latency measurements for the EPC located next to the HUB station, the difference between the measured values using the different tools in this configuration can be justified.

Finally, we also emphasize that, in the conditions under which the real satellite link test evaluations were made, the comparison between the real environment scenario and the simulated scenario highlights, in any situation, a latency increase by 15 % when the EPC is on the VSAT side, and a latency increase from 7 to 17 % when the EPC is on the HUB side. Regardless of the optimizations in the satellite system, these higher latency results are due to many factors over which you cannot have control in the real scenario of integration, such as: weather conditions that affect the satellite link and the dynamics of suitable band shared among different VSAT stations found in the satellite link. These factors are not present in the controlled environment laboratory, when using the simulator delay. Table 6 summarizes the main results for real scenario of satellite system integration.

4.2 Throughput

The results (averages) of throughput tests between PC1 and PC2 are shown in Figs. 9 and 10. These results were obtained through iperf and speedtest tools, respectively. The iperf was used to generate UDP data traffic with a fixed rate on the downlink direction, i.e., traffic generated from PC2 to PC1 and the uplink direction, from PC1 to PC2. The speedtest tool was used through Web browser by accessing the server webpage. The Internet connection was set on the side of

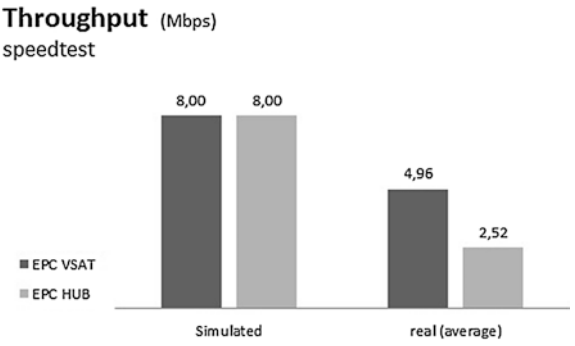

Fig. 9 Throughput obtained through the speedtest tool (downlink)

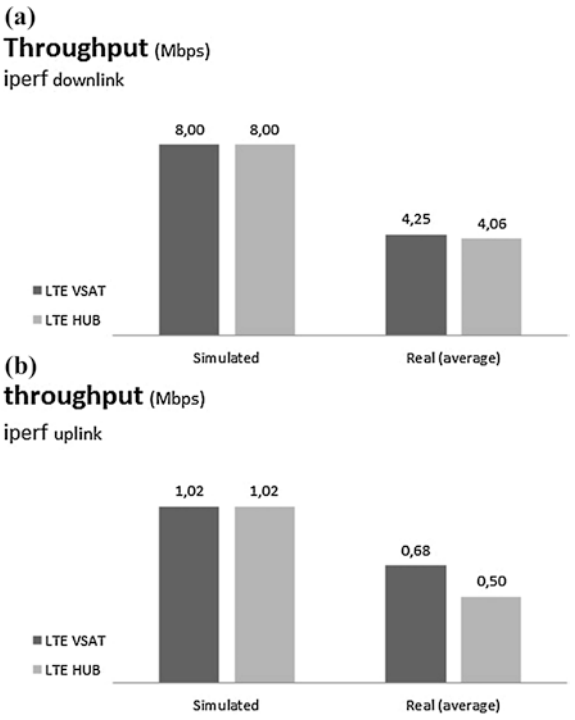

Fig. 10 Throughput obtained through the iperf tool. **a** Downlink throughput values. **b** Uplink throughput values

Table 7 Throughput efficiency loss in a real scenario

Configuration	Efficiency (download) (%)	Efficiency (upload) (%)
EPC next VSAT station	58	67
EPC next HUB station	41	49

the carrier or through the HUB station. For the test implementation, maximum throughput values were set to the satellite link: 8 Mbps downlink and 1 Mbps in the uplink.

The flow results through the speedtest and iperf tools for the downlink (download) are shown in Figs. 9 and 10a, respectively. A throughput decrease was observed in the UDP traffic in the real environment (Fig. 9) compared with the simulated environment. This decrease was approximately 38 % for the case wherein the EPC was located on the VSAT side, and 68.5 % when the EPC was located on the HUB station side. In the case where the EPC was on the VSAT side and using the iperf tool, a drop in the downlink throughput value of the order of 46.9 % was observed and for the uplink (upload), a drop value of the order of 32 %. For the configuration in which the EPC was on the HUB station side, there was a throughput value drop around 49.2 % for downlink and 51 % for uplink. For both throughputs obtained, there was the sharpest drop in the scenario in which EPC was located on the HUB station side. This can be explained by the fact that the real environment incorporates variable influences not controlled, such as weather conditions and satellite link sharing as previously mentioned, during the measurements performed, by other VSAT stations. These variables are not present in the controlled laboratory environment, when using the latency simulator. Likewise the network sharing may explain the variation of the verified and obtained results using the two tools. Table 7 shows the efficiency drop for the throughput verified in the real satellite system integration scenario with EPC located at HUB station, with bandwidth upload and download limiting.

4.3 MOS Score

Figure 11 shows obtaining the MOS through the IxChariot tool resulted in MOS scores ratings equivalent to “Some dissatisfied users” and “Many users dissatisfied” (see Table 2) for the simulated test environment, and MOS scores equivalent to the ratings “Many users dissatisfied” and “Almost all users dissatisfied” in the real environment.

The results of the simulated environment were obtained for EPC located on both the VSAT station side and HUB station side. These results showed only 0.6 % of difference between these two cases. The results obtained in real environment, using the same tool, showed a 53.8 % MOS score increase related to the measurement obtained for the EPC located on the VSAT station side when comparing to the MOS score for the EPC located on the HUB station side. Both score ratings match “Almost all users dissatisfied” MOS classification.

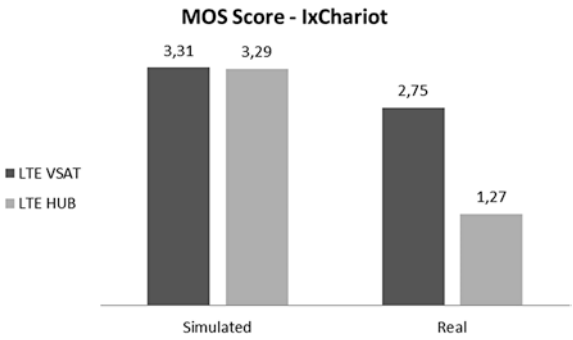

Fig. 11 MOS obtained by IxChariot tool

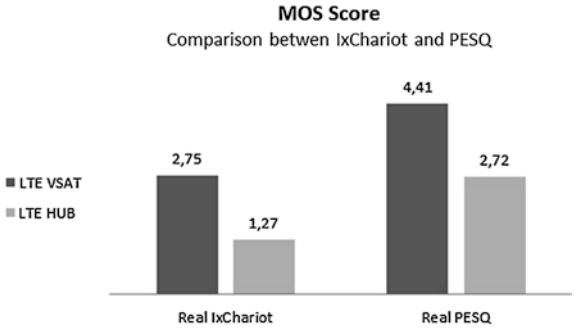

Fig. 12 MOS obtained in real scenario with the IxChariot tool and PESQ algorithm

Figure 12 compares the MOS and PESQ results in the real scenario. The variation in MOS values obtained by IxChariot tool and the PESQ algorithm when the EPC was located next to the VSAT station and when it was part of the hub station are, respectively, 37.6 and 53.6 %. The lower values were obtained with the MOS results. The tests results analysis of the various situations indicate greater PESQ algorithm reliability for the real environment evaluation. Note that all evaluated audio files, regardless of the delay considered in a simulated environment between 0 and 300 ms, showed excellent audio quality. In the real environment an excellent MOS result evaluated by this algorithm in the case EPC was located in the VSAT station side was also observed. This result is consistent with the excellent recording audio quality experienced. In the scenario where the EPC was located on the HUB station side, a significant occurrence of jitter and delay in voice traffic due to the control signaling presence and data traveling on the bus satellite, which may explain the MOS values drop measured in this configuration, was registered. The MOS results' comparison between the IxChariot tool measurement for the perceived audio quality, and the PESQ algorithm used to evaluate recorded calls, indicated that the first tool (IxChariot) was not properly prepared for voice quality measurements in systems where the delay is the predominant factor in the degradation of real-time services.

5 Conclusion

This chapter presented the results of performance measurements in a LTE wireless communication network that integrates a GSO system that provides the backhaul for the LTE system, as an access segment to the EPC or an access segment to an operator services network provider. The measurements were performed in two steps, the first one simulating the delay caused by the satellite system in the laboratory, and the second one, in a real satellite link environment, in real operating conditions. In both steps, LTE radio access (RAN) network components were used, that is, base station and terminals prototypes were connected to the laboratory environment. Results presented in this chapter show the real possibility of using the LTE system integrated with satellite backhaul, also indicating the importance of optimizations on the satellite segment for this integration to be performed most efficiently, exploiting the full potential of access segment provided by the LTE system, constituted by the RAN and the EPC. Those optimizations should cover aspects related to both configuration parameters of the LTE system as with acceleration mechanisms used in satellite networks and the available capacity for backhaul reserved link. The presented results show the possibility through these optimizations and band reservations with appropriate Committed Information Rate (CIR), to achieve latencies in one way, download or upload below 350 ms, and efficiencies greater than 50 and 60 % for the configuration where the EPC is next to the HUB station or next to the VSAT station and there is provided a dedicated link. The results showed also the necessity to use tools available to evaluate voice calls' quality performance subject to excessive delays, such as those typically found in geostationary satellite systems. However, even with these limitations, as reported, it was possible to prove the feasibility, as well as the good quality voice service to the LTE assessed network integration with the GSO system segment.

References

1. ITU Radiocommunication SECTOR (ITUR) S.725 (1992) Technical characteristics for very small aperture terminals (VSATs). Available at https://www.itu.int/rec/R-RECS.725-0-199203-I/en. Accessed on 05 Sept 2014
2. Thompson L, Enga B (2013) Analysis of satellite-based telecommunications and broadband services, Vantage Point Paper, Nov 2013
3. 24 Resolution-558. Access: May 6, 2013. RESEARCH CENTRE DEVELOPING TELECOMMUNICATIONS (CPqD) et al. TP on frequency band arrangement, 3GPP TSG-RAN WG4 Meeting # 67, R4-133076. Fukuoka, Japan, 20–24 May 2013
4. User Equipment (UE) radio transmission and reception (Release 8), v8.24.0, June 2014. NATIONAL AGENCYTELECOMMUNICATIONS (ANATEL). Resolution at 558: Approves the Regulation on Plumbing and Terms of Use Radio frequencies in the range of 450 MHz to 470 MHz Brasilia, 2010. Available in http://legislacao.anatel.gov.br/resolucoes/2010/

5. 3GPP TS 23.401: Technical specification group services and system aspects; general packet radio service (GPRS) enhancements evolved universal terrestrial radio for access network (eUTRAN) access (Release 8), v8.18.0, March 2013
6. 3GPP TS 36.104: Technical specification group radio access network; evolved universal terrestrial radio access (E-UTRA); base station (BS) radio transmission and reception (Release 8), v8.13.0, July 2012
7. P.862 (2007) Perceptual evaluation of speech quality (PESQ): an objective method for end-toend speech quality assessment of narrow-band telephone networks and speech codecs
8. IXIA (2013) IxChariot® user guide release 10.7913-0949-04 Rev. A. Available in http://www.netcor.de/download.php?file=1966. Accessed on 09 Sept 2014
9. 3rd Generation Partnership Project (3GPP). TS 36.300: technical specification group radio access network; evolved universal terrestrial radio access 9E-UTRA) and evolved terrestrial radio access network (E-UTRAN); overall description; Stage 2 (Release 8), v8.12.0, March 2010
10. INTERNATIONAL TELECOMMUNICATION STANDARDIZATION SECTOR (ITU-T) (1996) P.800 subjective methods for determination of transmission quality. Available at http://www.itu.int/rec/T-REC-P.800-199608-I. Accessed on 11 May 2013
11. G.107 (2012) The E-model: a computational model for use in transmission planning. Available at https://www.itu.int/rec/TRECG.107-201112-I/en. Accessed on 09 Sept 2014
12. P.862.1 (2003) Mapping functions for transforming P.862 raw scores to MOSLQO results
13. Ookla. Speedtest. Available in http://www.speedtest.net/. Accessed on 27 Aug 2014
14. Iperf. Available at https://iperf.fr/. Accessed on 27 Aug 2014
15. PORTSIP SOLUTIONS. PortGo. Available in http://www.portsip.com/softphone.html. Accessed on 27 Aug 2014
16. WIRESHARK FOUNDATION. Wireshark. Available at https://www.wireshark.org. Accessed on 27 Aug 2014